THE

LONDON, EDINBURGH, AND DUBLIN

PHILOSOPHICAL MAGAZINE

AND

JOURNAL OF SCIENCE.

[SEVENTH SERIES.]

FEBRUARY 1935.

XV. *Matrices applied to the Motions of Damped Systems.*

By W. J. DUNCAN, *D.Sc., A.M.I.Mech.E., Wakefield Lecturer in Aeronautics at University College, Hull, and* A. R. COLLAR, *B.A., B.Sc., of the Aerodynamics Department, National Physical Laboratory* *.

CONTENTS.

	Page
§ 1. Introduction and Summary	197
§ 2. The Reduced Equations of Motion	198
§ 3. Determination of the "Dominant" Mode of Motion.	202
§ 4. Completion of the Solution	207
§ 5. Transformation of the Equations of Motion and Normal Coordinates	211
§ 6. Extension of Rayleigh's Principle	211
§ 7. Remarks on Arithmetical Methods	212
§ 8. Numerical Example	213

§ 1. *Introduction and Summary* †.

A METHOD is given in the previous paper (Ref. 1) for the solution of a large class of problems concerning the oscillations of dynamical systems. This method depends on the use of matrices, and one of its principal characteristics is that the solution is obtained

* Communicated by E. F. Relf, A.R.C.Sc.

† The writers are indebted to the Aeronautical Research Committee for permission to publish the paper.

without expansion of the Lagrangian determinant; but its application is limited to systems where damping or "motional" forces are absent. In the present paper this restriction is removed.

As a preliminary to the application of the process of solution by matrices it is necessary to obtain the equations of motion in the "reduced" form in which the dependent variables are so chosen that the time-rate of change of each such variable is equal to a homogeneous linear function of the variables. This usually involves the introduction of a set of auxiliary variables, which, in the classical example of the Hamiltonian canonical equations, are the generalized momenta. In another scheme, which has been largely used by Mr. R. A. Frazer, the auxiliary variables are simply the generalized velocities. The matrix of the coefficients in the reduced equations of motion is called the dynamical matrix, and the problem of determining the modes of motion of the system is solved exclusively by operations with or upon this matrix. These modes are obtained successively in the order of ascending or descending moduli of the corresponding roots of the determinantal equation (latent roots of the dynamical matrix).

The language of the dynamics of material systems is employed throughout the paper, but it is scarcely necessary to add that the method given here is also applicable to electrical or mixed electrical and mechanical systems.

§ 2. *The Reduced Equations of Motion.*

The method, which will be explained in succeeding sections, is applicable to the solution of equations of motion which can be written in the form

$$\left.\begin{aligned} \dot{x}_1 &= u_{11}x_1 + u_{12}x_2 + \ldots u_{1n}x_n, \\ \dot{x}_2 &= u_{21}x_1 + u_{22}x_2 + \ldots u_{2n}x_n, \\ &\cdots\cdots\cdots\cdots \\ \dot{x}_n &= u_{n1}x_1 + u_{n2}x_2 + \ldots u_{nn}x_n, \end{aligned}\right\} \quad . \quad . \quad . \quad (2.1)$$

where the coefficients u are constants. As a rule the dynamical equations for the free motions of a system are not originally obtained in this form, but can very frequently be transformed into it by the introduction of auxiliary variables. This can always be done when the

coefficients in the ordinary Lagrangian dynamical equations of a holonomous system are constants.

The classical example of equations of the type (2.1) is provided by the Hamiltonian canonical equations for a system with constant dynamical coefficients, in which case the auxiliary variables are the generalized components of momentum. Suppose that the Lagrangian equations of motion of the system are

$$\left.\begin{aligned} &f_{11}(q_1)+f_{12}(q_2)+\ldots+f_{1m}(q_m)=0,\\ &f_{21}(q_1)+f_{22}(q_2)+\ldots+f_{2m}(q_m)=0,\\ &\cdots\cdots\cdots\cdots\\ &f_{m1}(q_1)+f_{m2}(q_2)+\ldots+f_{mm}(q_m)=0, \end{aligned}\right\} \quad . \quad . \quad (2.2)$$

where f_{ij} stands for the following linear differential operator with constant coefficients

$$\mathrm{A}_{ij}\frac{d^2}{dt^2}+\mathrm{B}_{ij}\frac{d}{dt}+\mathrm{C}_{ij}. \quad . \quad . \quad . \quad . \quad . \quad (2.3)$$

The m scalar equations (2.2) can be represented very concisely by the single matrix equation

$$[\mathrm{A}]\{\ddot{q}\}+[\mathrm{B}]\{\dot{q}\}+[\mathrm{C}]\{q\}=0, \quad . \quad . \quad . \quad (2.4)$$

where

$$\{q\}=\begin{Bmatrix} q_1\\ q_2\\ \cdot\cdot\\ \cdot\cdot\\ \cdot\cdot\\ \cdot\cdot\\ q_m \end{Bmatrix}, \quad . \quad . \quad . \quad . \quad . \quad . \quad . \quad . \quad . \quad (2.5)$$

$$[\mathrm{A}]=\begin{bmatrix} \mathrm{A}_{11} & \mathrm{A}_{12} & \ldots & \mathrm{A}_{1m}\\ \mathrm{A}_{21} & \mathrm{A}_{22} & \ldots & \mathrm{A}_{2m}\\ \cdot & \cdot & \cdot & \cdot\\ \mathrm{A}_{m1} & \mathrm{A}_{m2} & \ldots & \mathrm{A}_{mm} \end{bmatrix}, \quad . \quad . \quad (2.6)$$

and the other matrices are similarly defined. The matrices [A], [B], and [C] will be called the inertia, damping, and stiffness matrices respectively. The typical component of momentum is

$$p_r=\mathrm{A}_{r1}\dot{q}_1+\mathrm{A}_{r2}\dot{q}_2+\ldots+\mathrm{A}_{rm}\dot{q}_m. \quad . \quad . \quad (2.7)$$

Hence
$$\{p\} = [A]\{\dot{q}\}, \quad . \quad . \quad . \quad . \quad . \quad . \quad . \quad (2.8)$$

or *
$$\{\dot{q}\} = [A]^{-1}\{p\}. \quad . \quad . \quad . \quad . \quad . \quad . \quad (2.9)$$

The complete set of Hamiltonian equations consists of (2.8) together with the equations of motion (2.4) re-written as

$$\{\dot{p}\} + [B][A]^{-1}\{p\} + [C]\{q\} = 0, \quad . \quad . \quad (2.10)$$

in virtue of (2.8) and (2.9). Now let

$$\{\xi\} = \begin{Bmatrix} q_1 \\ \cdot\cdot \\ \cdot\cdot \\ q_m \\ p_1 \\ \cdot\cdot \\ \cdot\cdot \\ p_m \end{Bmatrix} \quad . \quad . \quad . \quad . \quad . \quad . \quad , \quad (2.11)$$

Then (2·9) and (2.10) can be combined in the single equation

$$\{\dot{\xi}\} = [v]\{\xi\}, \quad . \quad . \quad . \quad . \quad . \quad . \quad (2.12)$$

where $[v]$ is a square matrix of order $2m(=n)$, which, when partitioned into four square matrices of order m, is conveniently represented as

$$\begin{bmatrix} 0 & A^{-1} \\ -C & -BA^{-1} \end{bmatrix} \quad . \quad . \quad . \quad . \quad . \quad . \quad (2.13)$$

A rather more convenient form, which has been extensively employed by Mr. R. A. Frazer in the course of investigations on the stability of dynamical systems, is obtained by taking the generalized velocities as auxiliary variables, so that the complete set of dependent variables is

$$\{x\} = \begin{Bmatrix} q_1 \\ \cdot\cdot \\ \cdot\cdot \\ q_m \\ \dot{q}_1 \\ \cdot\cdot \\ \cdot\cdot \\ \dot{q}_m \end{Bmatrix} \quad . \quad . \quad . \quad . \quad . \quad . \quad . \quad (2.14)$$

* It may be remarked that [A] cannot be singular unless the system is such that all its particles can be at rest while some of the generalized velocities are not zero.

After premultiplication by $[A]^{-1}$, equation (2.4) becomes

$$\{\ddot{q}\}+[A]^{-1}[B]\{\dot{q}\}+[A]^{-1}[C]\{q\}=0,$$

and this is equivalent to

$$\{\dot{x}\}=[u]\{x\}, \quad . \quad . \quad . \quad . \quad . \quad (2.15)$$

where $[u]$ is a square matrix of order n which can be represented as

$$\begin{bmatrix} 0 & I \\ -A^{-1}C & -A^{-1}B \end{bmatrix} . \quad . \quad . \quad . \quad (2.16)$$

Here I is the unit matrix of order m. It is easy to see that

$$\{\xi\} = \begin{bmatrix} I & 0 \\ 0 & A \end{bmatrix} \{x\}, \quad . \quad . \quad . \quad . \quad (2.17)$$

and by substitution (2.12) becomes

$$\begin{bmatrix} I & 0 \\ 0 & A \end{bmatrix} \{\dot{x}\} = \begin{bmatrix} 0 & A^{-1} \\ -C & -BA^{-1} \end{bmatrix} \begin{bmatrix} I & 0 \\ 0 & A \end{bmatrix} \{x\}.$$

Premultiply by $\begin{bmatrix} I & 0 \\ 0 & A^{-1} \end{bmatrix}$, which is the reciprocal of $\begin{bmatrix} I & 0 \\ 0 & A \end{bmatrix}$. The equation becomes

$$\{\dot{x}\} = \begin{bmatrix} I & 0 \\ 0 & A^{-1} \end{bmatrix} \begin{bmatrix} 0 & A^{-1} \\ -C & -BA^{-1} \end{bmatrix} \begin{bmatrix} I & 0 \\ 0 & A \end{bmatrix} \{x\}$$

$$= \begin{bmatrix} 0 & I \\ -A^{-1}C & -A^{-1}B \end{bmatrix} \{x\}, \quad . \quad . \quad . \quad . \quad . \quad (2.18)$$

in accordance with (2.15) and (2.16).

Equation (2.18) can be conveniently illustrated by the case of a binary system. Let

$$\left.\begin{aligned} \dot{q}_1 &= r_1, \\ \text{and} \qquad \dot{q}_2 &= r_2. \end{aligned}\right\} \quad . \quad . \quad . \quad . \quad . \quad . \quad (2.19)$$

Then the two equations of motion corresponding to (2.4) can be written

$$A_{11}\dot{r}_1+A_{12}\dot{r}_2+B_{11}r_1+B_{12}r_2+C_{11}q_1+C_{12}q_2=0,$$

and

$$A_{21}\dot{r}_1+A_{22}\dot{r}_2+B_{21}r_1+B_{22}r_2+C_{21}q_1+C_{22}r_2=0.$$

Solution of these for $\dot{r}_1$ yields

$$\dot{r}_1 = -\Delta^{-1}\Big(\begin{vmatrix} A_{22} & B_{21} \\ A_{12} & B_{11} \end{vmatrix} r_1 + \begin{vmatrix} A_{22} & B_{22} \\ A_{12} & B_{12} \end{vmatrix} r_2 + \begin{vmatrix} A_{22} & C_{21} \\ A_{12} & C_{11} \end{vmatrix} q_1 + \begin{vmatrix} A_{22} & C_{22} \\ A_{12} & C_{12} \end{vmatrix} q_2 \Big), \quad (2.20)$$

where

$$\Delta = (A_{11}\ A_{22} - A_{12}\ A_{21}),$$

and there is a similar expression for $\dot{r}_2$. It will be seen that equations (2.19) and (2.20) taken together constitute a system of the type (2.1), and the set of four equations can be represented as

$$\begin{bmatrix} \dot{q}_1 \\ \dot{q}_2 \\ \dot{r}_1 \\ \dot{r}_2 \end{bmatrix} = \begin{bmatrix} 0 & 0 & 1 & 0 \\ 0 & 0 & 0 & 1 \\ -\gamma_{11} & -\gamma_{12} & -\beta_{11} & -\beta_{12} \\ -\gamma_{21} & -\gamma_{22} & -\beta_{21} & -\beta_{22} \end{bmatrix} \begin{bmatrix} q_1 \\ q_2 \\ r_1 \\ r_2 \end{bmatrix}, \quad (2.21)$$

where

$$\beta_{11} = \Delta^{-1} \begin{bmatrix} A_{22} & B_{21} \\ A_{12} & B_{11} \end{bmatrix}, \text{ etc.}$$

This agrees with equation (2.18).

For some purposes it is convenient to use equations (2.12) and (2.15) in the forms

$$\{\xi\} = [v]^{-1}\{\dot{\xi}\} \quad . \quad . \quad . \quad . \quad . \quad (2.22)$$

and

$$\{x\} = [u]^{-1}\{\dot{x}\} \quad . \quad . \quad . \quad . \quad . \quad (2.23)$$

It can readily be verified that

$$[v]^{-1} = \begin{bmatrix} -C^{-1}B & -C^{-1} \\ A & 0 \end{bmatrix} \quad . \quad . \quad . \quad (2.24)$$

and

$$[u]^{-1} = \begin{bmatrix} -C^{-1}B & -C^{-1}A \\ I & 0 \end{bmatrix} \quad . \quad . \quad . \quad (2.25)$$

§ 3. *Determination of the "Dominant" Mode of Motion.*

The equations to be solved are (2.1), which are equivalent to

$$\{\dot{x}\} = [u]\{x\}. \quad . \quad . \quad . \quad . \quad . \quad (3.1)$$

In accordance with the usual method, put

$$\{x\} = e^{\lambda t}\{K\}, \quad . \quad . \quad . \quad . \quad . \quad . \quad (3.2)$$

where $\{K\}$ is a columnar matrix of constants (usually complex). On substitution of this expression in (3.1) and cancellation of the exponential factor that equation becomes

$$\lambda\{K\} = [u]\{K\}, \quad . \quad . \quad . \quad . \quad . \quad (3.3)$$

which is also equivalent to

$$\lambda'\{K\} = [u]^{-1}\{K\}, \quad . \quad . \quad . \quad . \quad . \quad (3.4)$$

where

$$\lambda' = 1/\lambda. \quad . \quad . \quad . \quad . \quad . \quad . \quad . \quad (3.5)$$

It is worthy of note that (3.3) and (3.4) imply that

$$\lambda^s\{K\} = [u]^s\{K\}, \quad . \quad . \quad . \quad . \quad . \quad (3.6)$$

where s is any positive or negative integer. It will be made clear later that equation (3.6) may have advantages over (3.3) in numerical applications.

Equation (3.3) is equivalent to n scalar equations which are homogenous and linear in the n numbers K. These equations will only be compatible if

$$| \lambda I - u | = 0, \quad . \quad . \quad . \quad . \quad . \quad (3.7)$$

so that λ must be one of the latent roots of $[u]$. Associated with a particular latent root λ_r there is a corresponding " modal matrix,"

$$\{K_r\} = \begin{pmatrix} K_{1r} \\ K_{2r} \\ \cdot\cdot \\ \cdot\cdot \\ \cdot\cdot \\ \cdot\cdot \\ K_{nr} \end{pmatrix}, \quad . \quad . \quad . \quad . \quad . \quad (3.8)$$

and the n modal matrices may be combined into a single square matrix,

$$[K] = \begin{pmatrix} K_{11} & K_{12} & \cdots & K_{1n} \\ K_{21} & K_{22} & \cdots & K_{2n} \\ \cdot & \cdot & \cdot & \cdot \\ K_{n1} & K_{n2} & \cdots & K_{nn} \end{pmatrix} \quad . \quad . \quad . \quad (3.9)$$

It may be well to emphasize that the first suffix of K_{rs} specifies the coordinate and the second the mode of motion. Provided that the latent roots are all distinct

(as will be assumed in the present exposition), [K] is not singular. Let

$$[\mathrm{K}]^{-1} = [k]. \quad . \quad . \quad . \quad . \quad . \quad . \quad (3.10)$$

Then, by an important theorem of the matrix calculus,

$$[u]^s = [\mathrm{K}] \begin{bmatrix} \lambda_1^s & 0 & \dots & 0 \\ 0 & \lambda_2^s & \dots & 0 \\ . & . & . & . \\ 0 & 0 & \dots & \lambda_n^s \end{bmatrix} [k] \quad . \quad (3.11)$$

$$= \sum_{r=1}^{r=n} \lambda_r^s [\mathrm{Z}_r], \quad . \quad . \quad . \quad . \quad . \quad . \quad . \quad . \quad . \quad (3.12)$$

where

$$[\mathrm{Z}_r] = \begin{bmatrix} \mathrm{K}_{1r}k_{r1} & \mathrm{K}_{1r}k_{r2} & \dots & \mathrm{K}_{1r}k_{rn} \\ \mathrm{K}_{2r}k_{r1} & \mathrm{K}_{2r}k_{r2} & \dots & \mathrm{K}_{2r}k_{rn} \\ . & . & . & . \\ \mathrm{K}_{nr}k_{r1} & \mathrm{K}_{nr}k_{r2} & \dots & \mathrm{K}_{nr}k_{rn} \end{bmatrix}. \quad (3.13)$$

For convenience the latent roots are supposed arranged in order of decreasing modulus,

$$|\lambda_1| \geq |\lambda_2| \geq |\lambda_3| \dots \geq |\lambda_n|, \quad . \quad (3.14)$$

and the latent root or roots possessing the greatest modulus will be called *dominant*. Now when s is large it is clear that only the terms in (3.12) corresponding to the dominant latent root or roots need be retained. The following two important cases arise, and these must be considered separately :

(a) Single dominant real root.
(b) Conjugate pair of dominant complex roots.

Case (a). *Single dominant real root.*—Here only the first term of (3.12) need be retained, so that when s is sufficiently large

$$[u]^s = \lambda_1^s [\mathrm{Z}_1]. \quad . \quad . \quad . \quad . \quad . \quad (3.15)$$

Now let $\{x\}_0$ be an arbitrary columnar matrix of order n. By the last equation

$$[u]^s\{x\}_0 = \lambda_1^s [\mathrm{Z}_1]\{x\}_0$$
$$= \lambda_1^s \Phi_1 \{\mathrm{K}_1\}, \quad . \quad . \quad . \quad . \quad (3.16)$$

where

$$\Phi_1 = \sum_{r=1}^{r=n} k_{1r}x_{r0}. \quad . \quad . \quad . \quad . \quad (3.17)$$

Provided then that $\{x\}_0$ is not so selected that Φ_1 vanishes, the result of repeated premultiplication of $\{x\}_0$ by $[u]$ is a columnar matrix whose elements are proportional to the corresponding elements of the dominant modal matrix $\{K_1\}$. Further, if E_s is the element occupying any arbitrary fixed position in $[u]^s\{x\}_0$, then it follows from (3.16) that

$$\lambda_1 = \frac{E_{s+1}}{E_s}. \quad . \quad . \quad . \quad . \quad . \quad (3.18)$$

Hence the dominant latent root, and the corresponding mode of motion can be obtained by the method of repeated substitution. The process is exactly the same as that given in the earlier paper (ref. 1).

Next, let $[y]_0$ be an arbitrary line matrix of order n. By (3.15)

$$[y]_0[u]^s = \lambda_1^s[y]_0[Z_1]$$

$$= \lambda_1^s \Psi_1[k_1], \quad . \quad . \quad . \quad . \quad (3.19)$$

where

$$\Psi_1 = \sum_{r=1}^{r=n} y_{0r}K_{r1}. \quad . \quad . \quad . \quad . \quad (3.20)$$

Hence $[k_1]$ can be found by repeated postmultiplication of $[y]_0$ by $[u]$.

Case (*b*). *Conjugate pair of dominant complex roots.*—The dominant pair of complex roots are

$$\lambda_1 = \mu_1 + i\omega_1 \quad . \quad . \quad . \quad . \quad . \quad . \quad (3.21)$$

and

$$\lambda_2 = \bar{\lambda}_1 = \mu_1 - i\omega_1. \quad . \quad . \quad . \quad . \quad (3.22)$$

Hence when s is large (3.12) gives

$$[u]^s = \lambda_1^s[Z_1] + \bar{\lambda}_1^s[\bar{Z}_1]$$

$$= R.2\lambda_1^s[Z_1], \quad . \quad . \quad . \quad . \quad . \quad (3.23)$$

where the R prefixed to the expression means that the real part of the complex quantity is to be taken. Suppose now that $\{x\}_0$ is a *real* columnar matrix. Then

$$[u]^s\{x\}_0 = R.2\lambda_1^s[Z_1]\{x\}_0$$

$$= R.2\lambda_1^s\Phi_1\{K_1\}, \quad . \quad . \quad . \quad (3.24)$$

where Φ_1 is as defined in equation (3.17). Let E_{rs} be the

rth element in the columnar matrix $[u]^s\{x\}_0$. Then by equation (3.24)

$$\left.\begin{aligned} \mathrm{E}_{r,\,s} &= \mathrm{R}.2\lambda_1{}^s\Phi_1\mathrm{K}_{r1}, \\ \mathrm{E}_{r,\,s+1} &= \mathrm{R}.2\lambda_1{}^{s+1}\Phi_1\mathrm{K}_{r1}, \\ \mathrm{E}_{r,\,s+2} &= \mathrm{R}.2\lambda_1{}^{s+2}\Phi_1\mathrm{K}_{r1}. \end{aligned}\right\} \quad . \quad . \quad . \quad (3.25)$$

and

But $\{\mathrm{K}_1\}$ is arbitrary to a complex scalar multiplier. Hence there is no real loss of generality in substituting the following equations for (3.25) :

$$\left.\begin{aligned} \mathrm{E}_{r,\,s} &= \mathrm{R}.\mathrm{K}_{r1}, \\ \mathrm{E}_{r,\,s+1} &= \mathrm{R}.\lambda_1\mathrm{K}_{r1}, \\ \mathrm{E}_{r,\,s+2} &= \mathrm{R}.\lambda_1{}^2\mathrm{K}_{r1}. \end{aligned}\right\} \quad . \quad . \quad . \quad . \quad (3.26)$$

If

$$\mathrm{K}_{r1} = \mathrm{G}_{r1} + i\mathrm{H}_{r1}, \quad . \quad . \quad . \quad . \quad . \quad (3.27)$$

then by (3.21) the equations (3.26) become

$$\mathrm{E}_{r,\,s} = \mathrm{G}_{r1}, \quad . \quad . \quad . \quad . \quad . \quad . \quad . \quad . \quad . \quad (3.28)$$

$$\mathrm{E}_{r,\,s+1} = \mu_1\mathrm{G}_{r1} - \omega_1\mathrm{H}_{r1}, \quad . \quad . \quad . \quad . \quad . \quad (3.29)$$

and

$$\mathrm{E}_{r,\,s+2} = (\mu_1{}^2 - \omega_1{}^2)\mathrm{G}_{r1} - 2\mu_1\omega_1\mathrm{H}_{r1}. \quad . \quad . \quad (3.30)$$

Multiply (3.28) by $(\mu_1{}^2+\omega_1{}^2)$, (3.29) by $-2\mu_1$, and add to (3.30). The result is

$$(\mu_1{}^2+\omega_1{}^2)\mathrm{E}_{r,\,s} - 2\mu_1\mathrm{E}_{r,\,s+1} + \mathrm{E}_{r,\,s+2} = 0, \quad . \quad (3.31)$$

and similarly the pth elements in the sequence of matrices satisfy the equation

$$(\mu_1{}^2+\omega_1{}^2)\mathrm{E}_{p,\,s} - 2\mu_1\mathrm{E}_{p,\,s+1} + \mathrm{E}_{p,\,s+2} = 0. \quad . \quad (3.32)$$

These equations can be solved for μ_1 and ω_1, and then (3.28) and (3.29) yield G_{r1} and H_{r1}. Thus the frequency, damping factor, amplitude ratios, and phase differences of the dominant mode can be found by the method of successive substitution.

In order to obtain $[k_1]$ it is only necessary to post-multiply an arbitrary line matrix $[y]_0$ repeatedly by $[u]$. The elements in the resulting sequence of matrices satisfy equations of exactly the same type as (3.28) to (3.30), and the real and imaginary parts of the elements of $[k_1]$ can

be found from any two of the equations, since μ_1 and ω_1 will now be known.

§ 4. *Completion of the Solution.*

The remaining modes of motion of the system can be found by a method which is the same in principle as that used in Ref. 1 for systems without damping forces. The method depends on the fact that, when the matrix $[k_1]$ is known, it becomes possible to derive a modified dynamical system which possesses all the modes of the original system with the exception of its dominant mode. In Ref. 1 the legitimacy of this method was inferred from physical ideas, but a mathematical proof will be given here

On account of the reciprocity of $[k]$ and [K] it follows that

$$\left.\begin{aligned}[k_r]\{\mathrm{K}_s\} &= 1 \text{ if } r=s,\\ &= 0 \text{ if } r\neq s.\end{aligned}\right\} \quad . \quad . \quad . \quad . \quad (4.1)$$

Now the general solution of the dynamical equation (3.1) is

$$\{x\} = \sum_{s=1}^{n} \alpha_s e^{\lambda_s t}\{\mathrm{K}_s\}. \quad . \quad . \quad . \quad . \quad (4.2)$$

Hence

$$[k_r]\{x\} = \alpha_r e^{\lambda_r t} \quad . \quad . \quad . \quad . \quad . \quad (4.3)$$

by equations (4.1). Thus, if the mode corresponding to λ_r is absent (*i. e.*, if $\alpha_r=0$), then

$$[k_r]\{x\} = 0 \quad . \quad . \quad . \quad . \quad . \quad . \quad (4.4)$$

at all instants. Thus, if the dominant mode is absent, the coordinates must satisfy the homogeneous linear scalar equation

$$[k_1]\{x\} = 0. \quad . \quad . \quad . \quad . \quad . \quad . \quad (4.5)$$

Consequently one of the coordinates may be eliminated, and one of the equations of motion can be discarded as redundant. The order of the system is thus reduced by 1, and the dominant mode of the modified system (*i. e.*, the sub-dominant mode of the original system) can be found by the same process as before. In this way all the modes of the system can be obtained in succession. It may be remarked that, when it is only desired to obtain the frequencies and damping factors of the system, the

whole solution can be obtained by the method of post-multiplying an arbitrary line matrix by $[u]$ or by the corresponding modified matrices (see end of § 3).

When λ_1 is real there will be a single equation (4.5) with real coefficients. When, however, λ_1 is complex, the pair of modes corresponding to λ_1 and $\bar{\lambda}_1$ will both be absent when

$$[k_1]\{x\} = 0,$$

and

$$[\bar{k}_1]\{x\} = 0.$$

If

$$k_{1r} = g_{1r} + ih_{1r}, \quad . \quad . \quad . \quad . \quad . \quad . \quad (4.6)$$

then the last equations require that

$$\left.\begin{aligned} &[g_1]\{x\} = 0, \\ \text{and} \quad &[h_1]\{x\} = 0. \end{aligned}\right\} \quad . \quad . \quad . \quad . \quad . \quad (4.7)$$

Hence two coordinates can be eliminated *, and the order of the matrix of the modified system is $(n-2)$. The elements of the modified matrix can be obtained directly by use of (4.5) or (4.7).

When interest is confined to the latent roots there is an alternative procedure in which successive reduction of the dynamical matrix is not employed. The process in question consists in an adaptation of Aitken's extension of Bernoulli's method for the solution of algebraic equations (Ref. 2). Suppose that the equation to be solved is

$$\lambda^n + p_1\lambda^{n-1} + p_2\lambda^{n-2} + \ldots + p_{n-1}\lambda + p_n = 0. \quad . \quad (4.8)$$

Then there is an associated finite difference equation

$$Z_{n+s} + p_1 Z_{n-1+s} + p_2 Z_{n-2+s} + \ldots + p_{n-1} Z_{1+s} + p_n Z_s = 0, \quad (4.9)$$

whose solution is easily proved to be

$$Z_{n+s} = \Sigma a_r \lambda_r^{n+s}, \quad . \quad . \quad . \quad . \quad . \quad (4.10)$$

where $\lambda_1 \ldots \lambda_n$ are the roots of (4.8). If $Z_0 \ldots Z_{n-1}$ are arbitrarily assigned, equation (4.9) gives Z_n explicitly, and Z_{n+1}, Z_{n+2}, etc., can be obtained successively. When s becomes large, the terms in (4.10) corresponding to the root or roots with largest modulus become dominant, and the roots in question can then be determined as explained

* See further in § 7.

in Aitken's paper. Now if (4.8) is the characteristic equation of a matrix $[u]$, the Cayley–Hamilton theorem states that $[u]$ satisfies

$$[u]^n+p_1[u]^{n-1}+\ldots+p_{n-1}[u]+p_n\mathrm{I}=0. \quad (4.11)$$

On multiplication by $[u]^s$ it becomes apparent that the sequence of the powers of $[u]$ satisfies the difference equation (4.9), and it of course follows that a sequence formed by homologous elements in the successive powers of $[u]$ also satisfies (4.9). Hence Aitken's methods for finding the roots of (4.8) can be applied *in toto* to the determination of the latent roots of the dynamical matrix. The most useful of the formulæ which can be borrowed in this way is

$$\lambda_1\lambda_2\lambda_3\ldots\lambda_p=\frac{\begin{vmatrix} \mathrm{E}_{r,s+1} & \mathrm{E}_{r,s+2} & \ldots & \mathrm{E}_{r,s+p} \\ \mathrm{E}_{r,s+2} & \mathrm{E}_{r,s+3} & \ldots & \mathrm{E}_{r,s+p+1} \\ \ldots & \ldots & \ldots & \ldots \\ \mathrm{E}_{r,s+p} & \mathrm{E}_{r,s+p+1} & \ldots & \mathrm{E}_{r,s+2p-1} \end{vmatrix}}{\begin{vmatrix} \mathrm{E}_{r,s} & \mathrm{E}_{r,s+1} & \ldots & \mathrm{E}_{r,s+p-1} \\ \mathrm{E}_{r,s+1} & \mathrm{E}_{r,s+2} & \ldots & \mathrm{E}_{r,s+p} \\ \ldots & \ldots & \ldots & \ldots \\ \mathrm{E}_{r,s+p-1} & \mathrm{E}_{r,s+p} & \ldots & \mathrm{E}_{r,s+2p-2} \end{vmatrix}}, \quad (4.12)$$

where $\mathrm{E}_{r,s}$ is as defined in § 3. This can be easily deduced as follows. It is evident from (3.12) and (3.16) that

$$\mathrm{E}_{r,s}=\sum_{q=1}^{q=p} e_{rq}\lambda_q^{\,s}, \quad (4.13)$$

when s is large, for the neglected terms will be very small compared with those retained. Hence

$$\begin{bmatrix} \mathrm{E}_{r,s+1} & \mathrm{E}_{r,s+2} & \ldots & \mathrm{E}_{r,s+p} \\ \mathrm{E}_{r,s+2} & \ldots & \ldots & \ldots \\ \ldots & \ldots & \ldots & \ldots \\ \mathrm{E}_{r,s+p} & \ldots & \ldots & \mathrm{E}_{r,s+2p-1} \end{bmatrix} = \begin{bmatrix} \lambda_1^{s+1} & \lambda_2^{s+1} & \ldots & \lambda_p^{s+1} \\ \lambda_1^{s+2} & \lambda_2^{s+2} & \ldots & \lambda_p^{s+2} \\ \ldots & \ldots & \ldots & \ldots \\ \lambda_1^{s+p} & \lambda_2^{s+p} & \ldots & \lambda_p^{s+p} \end{bmatrix} \begin{bmatrix} e_{r1} & \lambda_1 e_{r1} & \ldots & \lambda_1^{p-1}e_{r1} \\ e_{r2} & \lambda_2 e_{r2} & \ldots & \lambda_2^{p-1}e_{r2} \\ \ldots & \ldots & \ldots & \ldots \\ e_{rp} & \lambda_p e_{rp} & \ldots & \lambda_p^{p-1}e_{rp} \end{bmatrix} \quad (4.14)$$

and

$$\begin{pmatrix} \mathrm{E}_{r,s} & \mathrm{E}_{r,s+1} & \dots & \mathrm{E}_{r,s+p-1} \\ \mathrm{E}_{r,s+1} & \cdot & \cdot & \cdot \\ \cdot & \cdot & \cdot & \cdot \\ \mathrm{E}_{r,s+p-1} & \dots & \dots & \mathrm{E}_{r,s+2p-2} \end{pmatrix}$$

$$= \begin{pmatrix} \lambda_1^{s} & \lambda_2^{s} & \dots & \lambda_p^{s} \\ \lambda_1^{s+1} & \dots & \dots & \lambda_p^{s+1} \\ \cdot & \cdot & \cdot & \cdot \\ \lambda_1^{s+-1} & \dots & \dots & \lambda_p^{s+p-1} \end{pmatrix} \begin{pmatrix} e_{r1} & \lambda_1 e_{r1} & \dots & \lambda_1^{p-1} e_{r1} \\ e_{r2} & \cdot & \cdot & \cdot \\ \cdot & \cdot & \cdot & \cdot \\ e_{rp} & \lambda_p e_{rp} & \dots & \lambda_p^{p-1} e_{rp} \end{pmatrix}. \quad \dots \quad (4.15)$$

Thus the expression on the right-hand side of (4.12)

$$= \frac{\begin{vmatrix} \lambda_1^{s+1} & \lambda_2^{s+1} & \dots & \lambda_p^{s+1} \\ \lambda_1^{s+2} & \dots & \dots & \lambda_p^{s+2} \\ \cdot & \cdot & \cdot & \cdot \\ \lambda_1^{s+p} & \dots & \dots & \lambda_p^{s+p} \end{vmatrix}}{\begin{vmatrix} \lambda_1^{s} & \lambda_2^{s} & \dots & \lambda_p^{s} \\ \lambda_1^{s+1} & \lambda_2^{s+1} & \dots & \lambda_p^{s+1} \\ \cdot & \cdot & \cdot & \cdot \\ \lambda_1^{s+p-1} & \dots & \dots & \lambda_p^{s+p-1} \end{vmatrix}} = \lambda_1 \lambda_2 \dots \lambda_p. \quad (4.16)$$

The special case of (4.12) when $p=2$ is important. When λ_1 and λ_2 are conjugate complexes the equation becomes

$$\lambda_1 \lambda_2 = \mu_1^2 + \omega_1^2 = \frac{\begin{vmatrix} \mathrm{E}_{r,s+1} & \mathrm{E}_{r,s+2} \\ \mathrm{E}_{r,s+2} & \mathrm{E}_{r,s+3} \end{vmatrix}}{\begin{vmatrix} \mathrm{E}_{r,s} & \mathrm{E}_{r,s+1} \\ \mathrm{E}_{r,s+1} & \mathrm{E}_{r,s+2} \end{vmatrix}}, \quad \dots \quad (4.17)$$

which can also be deduced from (3.31) and the consecutive equation obtained by substituting $(s+1)$ for s. Another useful formula which can be obtained at once from (4.13), in the manner already indicated, is

$$\lambda_1 + \lambda_2 = \frac{\begin{vmatrix} \mathrm{E}_{r,s} & \mathrm{E}_{s,s+2} \\ \mathrm{E}_{r,s+1} & \mathrm{E}_{r,s+3} \end{vmatrix}}{\begin{vmatrix} \mathrm{E}_{r,s} & \mathrm{E}_{r,s+1} \\ \mathrm{E}_{r,s+1} & \mathrm{E}_{r,s+2} \end{vmatrix}}, \quad \dots \quad (4.18)$$

and this agrees with the expression for $2\mu_1$ yielded by (3.31) and the consecutive equation of the sequence.

§ 5. *Transformation of the Equations of Motion and Normal Coordinates.*

Suppose that

$$\{x\} = [\mathrm{H}]\{\phi\}, \quad . \quad . \quad . \quad . \quad (5.1)$$

where [H] is a non-singular matrix, and let

$$[\mathrm{H}]^{-1} = [h]. \quad . \quad . \quad . \quad . \quad . \quad . \quad (5.2)$$

Then the dynamical equation (3.1) becomes

$$[\mathrm{H}]\{\dot{\phi}\} = [u][\mathrm{H}]\{\phi\}$$

or

$$\{\dot{\phi}\} = [u']\{\phi\}, \quad . \quad . \quad . \quad . \quad . \quad (5.3)$$

where

$$[u'] = [h][u][\mathrm{H}]. \quad . \quad . \quad . \quad . \quad (5.4)$$

In equation (3.11) put $s=1$, premultiply by $[k]$, and post-multiply by [K]. The result is

$$[k][u][\mathrm{K}] = \begin{bmatrix} \lambda_1 & 0 & \dots & 0 \\ 0 & \lambda_2 & \dots & 0 \\ \dots & \dots & \dots & \dots \\ 0 & 0 & \dots & \lambda_n \end{bmatrix} . \quad . \quad (5.5)$$

Hence, if

$$[\mathrm{H}] = [\mathrm{K}], \quad . \quad . \quad . \quad . \quad . \quad . \quad (5.6)$$

the expression for the transformed dynamical matrix is, by (5.4),

$$[u'] = \begin{bmatrix} \lambda_1 & 0 & \dots & 0 \\ 0 & \lambda_2 & \dots & 0 \\ \dots & \dots & \dots & \dots \\ 0 & 0 & \dots & \lambda_n \end{bmatrix} . \quad . \quad . \quad . \quad (5.7)$$

Thus the coordinate system given by

$$\{\phi\} = [k]\{x\} \quad . \quad . \quad . \quad . \quad . \quad . \quad (5.8)$$

is such that the dynamical matrix assumes the diagonal form. Accordingly such coordinates may be described as *normal*, although in general they will be linear functions of the velocities as well as of the displacements of the system, and the coefficients will in general be complex.

§ 6. *Extension of Rayleigh's Principle.*

Suppose that

$$\{q\} = \{\mathrm{Q}\}e^{\lambda t} \quad . \quad . \quad . \quad . \quad . \quad . \quad (6.1)$$

is a solution of the equation (2.4), so that

$$\lambda^2[\mathrm{A}]\{\mathrm{Q}\} + \lambda[\mathrm{B}]\{\mathrm{Q}\} + [\mathrm{C}]\{\mathrm{Q}\} = 0. \quad . \quad . \quad (6.2)$$

Premultiply by [Q] (*i. e.*, the line matrix of the complex amplitudes Q). Then

$$\lambda^2[Q][A]\{Q\}+\lambda[Q][B]\{Q\}+[Q][C]\{Q\}=0. \quad (6.3)$$

This is a scalar quadratic equation for λ, and the coefficients are quadratic forms in the variables Q. For conciseness put

$$\left.\begin{aligned} &[Q][A]\{Q\}=A(Q),\\ &[Q][B]\{Q\}=B(Q),\\ \text{and}\quad &[Q][C]\{Q\}=C(Q). \end{aligned}\right\} \quad . \quad . \quad . \quad . \quad (6.4)$$

Then, if Q_r alone is varied, equation (6.3) gives

$$-\frac{\partial\lambda}{\partial Q_r}\{2\lambda A(Q)+B(Q)\}=\lambda^2\frac{\partial A(Q)}{\partial Q_r}+\lambda\frac{\partial B(Q)}{\partial Q_r}+\frac{\partial C(Q)}{\partial Q_r}. \quad . \quad . \quad . \quad (6.5)$$

But if [A], [B], and [C] are all *symmetrical* matrices, then the right-hand side of this equation vanishes by (6.2), and consequently

$$\frac{\partial\lambda}{\partial Q_r}=0. \quad . \quad . \quad . \quad . \quad . \quad . \quad (6.6)$$

It must be remarked, however, that the matrices [B] and [C] are not as a rule symmetrical for systems in which aerodynamical forces play a part.

§ 7. *Remarks on Arithmetical Methods.*

A numerical example of the application of the process explained in this paper is given in § 8, but as a preliminary some general remarks on arithmetical methods will be made.

In the first place it is evident that the rapidity of the convergence in the process of successive substitution depends acutely on the separation of the moduli of the latent roots. This can be increased by using some power of the dynamical matrix in place of the dynamical matrix itself (see equation (3.6)), but this does not always lead to a saving of labour, as the advantage of the simple form of the dynamical matrix is lost. The latent root obtained by the process of successive substitution will be the corresponding power of $(\mu_1+i\omega_1)$. The true value of this

quantity can be obtained without ambiguity by substitution in one of the equations of motion *, since the mode will now be known. If interest happens to be confined to the latent roots having the smallest modulus, it will be convenient to use the reciprocal of the dynamical matrix, or some power of this (see equations (2.24) and (2.25)).

If two roots, while distinct, have equal or nearly equal moduli, they can be found from equations (4.17) and (4.18). This covers the case of a conjugate complex pair.

It may be well to emphasize that when the chief object is to obtain the frequencies and damping factors of the system it is better to employ the equation

$$\lambda_1[k_1] = [k_1][u] \quad . \quad . \quad . \quad . \quad . \quad (7.1)$$

rather than

$$\lambda_1\{\mathrm{K}_1\} = [u]\{\mathrm{K}_1\} \quad . \quad . \quad . \quad . \quad . \quad (7.2)$$

in the process of successive substitution, for (7.1) yields the matrix $[k_1]$ required for the determination of the next latent root (see § 4). When the latent roots are known, the modes can be found by solving a set of homogeneous linear equations, but this may be laborious when the system has many degrees of freedom. In such a case labour may be saved by obtaining the modes directly by successive substitution.

When the dominant roots consist of a conjugate complex pair, two coordinates are eliminated by means of equations (4.7). It is not, however, necessary to obtain $[g_1]$ and $[h_1]$ separately, and it suffices to use in their place a consecutive pair of matrices obtained by repeated substitution in (7.1), for (*cp.* equations (3.28) and (3.29)) corresponding elements in the consecutive matrices can be represented as g_{r1} and $(\mu_1 g_{r1} - \omega_1 h_{r1})$.

With regard to the application of Aitken's methods (see end of § 4), it should be pointed out that these will fail to give more than the first one or two of the latent roots unless an excessively high order of accuracy is maintained in the calculations.

§ 8. *Numerical Example.*

The dynamical system consists of a model aeroplane wing placed at a small angle of incidence in a uniform

* Or equally well from one of the scalar equations represented by $\lambda_1[k_1] = [k_1][u]$, if $[k_1]$ has been found.

air-stream. This system possesses three degrees of freedom, namely, (1) wing-flexure, (2) wing-twist, and (3) aileron angle measured relative to the wing-chord at the wing-tip. When the wind-speed is 12 ft. per second, the matrices of the dynamical coefficients * are as follows :—

$$\text{Inertia matrix} = [A] = \begin{bmatrix} 17{\cdot}6 & 0{\cdot}128 & 2{\cdot}89 \\ 0{\cdot}128 & 0{\cdot}00824125 & 0{\cdot}0413 \\ 2{\cdot}89 & 0{\cdot}0413 & 0{\cdot}725 \end{bmatrix}$$

$$\text{Damping matrix} = [B] = \begin{bmatrix} 7{\cdot}65833 & 0{\cdot}245 & 2{\cdot}10 \\ 0{\cdot}023 & 0{\cdot}0104 & 0{\cdot}0223 \\ 0{\cdot}60 & 0{\cdot}0756 & 0{\cdot}658333 \end{bmatrix}$$

$$\text{Stiffness matrix} = [C] = \begin{bmatrix} 121{\cdot}042 & 1{\cdot}89 & 15{\cdot}9497 \\ 0 & 0{\cdot}027 & 0{\cdot}0145 \\ 11{\cdot}9097 & 0{\cdot}364 & 15{\cdot}4722 \end{bmatrix}$$

It is found that

$$[A]^{-1} = \begin{bmatrix} 0{\cdot}170883 & 1{\cdot}06301 & -0{\cdot}741731 \\ 1{\cdot}06301 & 176{\cdot}433 & -14{\cdot}2880 \\ -0{\cdot}741731 & -14{\cdot}2880 & 5{\cdot}14994 \end{bmatrix}$$

Hence equation (2.16) gives

$$[u] = \begin{bmatrix} 0 & 0 & 0 \\ 0 & 0 & 0 \\ 0 & 0 & 0 \\ -11{\cdot}8502 & -0{\cdot}08168 & 8{\cdot}73526 \\ 41{\cdot}4969 & -1{\cdot}57195 & 201{\cdot}554 \\ 28{\cdot}4464 & -0{\cdot}086931 & -67{\cdot}6433 \end{bmatrix} \begin{bmatrix} 1 & 0 & 0 \\ 0 & 1 & 0 \\ 0 & 0 & 1 \\ -0{\cdot}888089 & 0{\cdot}003153 & 0{\cdot}105747 \\ -3{\cdot}62604 & -1{\cdot}01517 & 3{\cdot}23949 \\ 2{\cdot}91908 & -0{\cdot}059016 & -1{\cdot}51412 \end{bmatrix}$$

The results of successive premultiplication of an arbitrary columnar matrix by $[u]$ are given in Table I., where the early products are omitted. Since the numders in successive columns are not in a constant ratio, it is evident that the dominant roots are a complex pair. In order to test the convergence it will be

* The coefficients are obtained from §49 of Ref. 3, and the lower value of D_2, namely, $8{\cdot}24125 \times 10^{-6}$ is adopted.

TABLE I.

Arbitrary Columnar Matrix repeatedly premultiplied by the Dynamical Matrix.

The first three numbers in any column are the same as the last three in the previous column.

Initial matrix.	Result of number of multiplications stated. (All numbers divided by 10^6.)			
	9.	10.	11.	12.
0	−2·387034	26·36482	124·8462	−2115·576
0	−38·62270	523·3891	1848·175	−40880·255
0	15·36335	−179·9971	−785·1628	14324·28
0	26·36482	124·8462	−2115·576	− 5224·339
0	523·3891	1848·175	−40880·255	−60402·28
1·0	−179·9971	−785·1628	14324·28	31050·14

The last element in the result of 13 multiplications is −1084268.

convenient to use the formula (4.17). The following table gives the values of the last element in the sequence of columnar matrices, together with the successive approximations to $\lambda_1\lambda_2=\mu_1^2+\omega_1^2$ deduced therefrom.

TABLE II.

Successive Approximations to the Square of the Modulus of the Dominant Roots.

Last element in columnar matrix.	Value of $(\mu_1^2+\omega_1^2)$.
1·0	—
−1·5	—
$-6{\cdot}53\times10$	—
$2{\cdot}163\times10^2$	67·93
$4{\cdot}2755\times10^3$	71·04
$-2{\cdot}3038\times10^4$	71·35
$-2{\cdot}662306\times10^5$	71·76
$2{\cdot}126375\times10^6$	71·82
$1{\cdot}536335\times10^7$	71·844
$-1{\cdot}799971\times10^8$	71·853
$-7{\cdot}851623\times10^8$	71·8545
$1{\cdot}432428\times10^{10}$	71·8553
$3{\cdot}105014\times10^{10}$	71·8554
$-1{\cdot}084268\times10^{12}$	71·8555

When the last four values given in the first column of Table II. are substituted in equation (4.18), the result is

$$2\mu_1 = -1{\cdot}77099.$$

Hence the dominant pair of latent roots are the roots of the quadratic equation

$$\lambda^2 - 1{\cdot}77099\,\lambda + 71{\cdot}8555 = 0,$$

namely, $$-0{\cdot}885495 \pm 8{\cdot}43039\,i.$$

Also the dominant mode as deduced from the last two columns of Table I. by means of equations (3.28) and (3.29) is

$$\{q\} = \begin{Bmatrix} -2115{\cdot}576 + 841{\cdot}9153\,i \\ -40880{\cdot}255 + 11458{\cdot}73\,i \\ 14324{\cdot}28 - 5187{\cdot}689\,i \end{Bmatrix},$$

which, since $\{q\}$ is arbitrary to a complex scalar multiplier, is equivalent to

$$\{q\} = \begin{Bmatrix} 1{\cdot}0 \\ 18{\cdot}5424 + 1{\cdot}96276\,i \\ -6{\cdot}68759 - 0{\cdot}209256\,i \end{Bmatrix}.$$

This solution has been checked by substitution in the equation

$$\lambda^2[\mathrm{A}]\{q\} + \lambda[\mathrm{B}]\{q\} + [\mathrm{C}]\{q\} = 0.$$

The alternative procedure of repeated postmultiplication of an arbitrary line matrix by $[u]$ is exhibited in Table III., where the initial matrix is [0 0 0 0 0 1], and the convergence of the approximations to $(\lambda_1^2 + \omega_1^2)$ given by equation (4 17) is shown in Table IV. On substitution from Table IV. in equation (4.18) it is found that

$$2\mu_1 = -1{\cdot}77099.$$

Hence the dominant latent roots are

$$-0{\cdot}885495 \pm 8{\cdot}43039\,i,$$

in agreement with the values already obtained by the other method.

The remaining latent roots can be obtained by eliminating two coordinates in the manner explained at the end of § 7. Thus the dominant modes will be absent if

$$-20210{\cdot}44\,x_1 + 68{\cdot}19841\,x_2 + 54860{\cdot}72\,x_3$$
$$-8823{\cdot}726\,x_4 + 42{\cdot}39843\,x^5 + 14204{\cdot}82\,x_6 = 0,$$

TABLE III.

Arbitrary Line Matrix repeatedly postmultiplied by the Dynamical Matrix.

	Initial matrix.	0.	0.	0.	0.	0.	1.
Result of number of multiplications stated (all entries in Table divided by 10^6).	7	−0·9255568	0·0004434	1·6761397	0·0509419	0·0013998	−0·2681778
	8	−8·17428	0·0169516	18·867557	−1·758706	0·0150094	2·092115
	9	90·9770	−0·061813	−153·855	−0·559766	−0·127299	15·562489
	10	444·0476	−1·107033	−1083·245	127·3639	−0·852784	−177·8901
	11	−6605·009	6·401615	12973·75	−185·2461	10·65863	−803·1927
	12	−20210·44	68·19841	54860·72	−8823·726	42·39843	14204·82
	13	510398·3	−580·7654	−1029393·	28937·08	−840·976	32557·18

The value of the element in the last column for 14 multiplications is −1078353·0.

and

$$510398{\cdot}3\,x_1 - 580{\cdot}7654\,x_2 - 1029393{\cdot}0\,x_3 + 28937{\cdot}08\,x_4 - 840{\cdot}976\,x_5 + 32557{\cdot}18\,x_6 = 0,$$

where the coefficients are obtained from the last two

TABLE IV.

Successive Approximations to the Square of the Modulus of the Dominant Roots.

Last element in line matrix.	Value of $(\mu_1^2+\omega_1^2)$.
1·0	—
−1·5	—
−6·53 × 10	—
2·081 × 10^2	67·75
4·291 × 10^3	70·69
−2·25074 × 10^4	71·39
−2·681778 × 10^5	71·76
2·092115 × 10^6	71·81
1·5562489 × 10^7	71·85
−1·778901 × 10^8	71·851
−8·031927 × 10^8	71·855
1·420482 × 10^{10}	71·8551
−3·255718 × 10^{10}	71·8555
−1·078353 × 10^{12}	71·8555

lines of Table III. It will be convenient to eliminate x_1 and $x_4(=\dot{x}_1)$. The foregoing equations yield

$$x_1 = 0{\cdot}000804089\,x_2 + 1{\cdot}9127294\,x_3 + 0{\cdot}001580505\,x_5 - 0{\cdot}17819858\,x_6$$

and

$$x_4 = 0{\cdot}005887241\,x_2 + 1{\cdot}836369\,x_3 + 0{\cdot}001184957\,x_5 + 2{\cdot}0180013\,x_6.$$

The modified dynamical matrix of the 4th order will be of the standard form if the 1st and 4th equations of motion are rejected as redundant. On substitution of the foregoing values for x_1 and x_4 in the remaining

equations of motion it is found that the new dynamical matrix is

$$[u'] = \begin{bmatrix} 0 & 0 & 1 & 0 \\ 0 & 0 & 0 & 1 \\ -1{\cdot}55993 & 274{\cdot}267 & -0{\cdot}95388 & -11{\cdot}47255 \\ -0{\cdot}046873 & -7{\cdot}8725 & -0{\cdot}010597 & -0{\cdot}69252 \end{bmatrix}.$$

This can be treated in the same manner as the original 6th order matrix, or its characteristic equation can be obtained by direct expansion and solved by the usual methods.

List of References.

(1) W. J. Duncan and A. R. Collar, "A Method for the Solution of Oscillation Problems by Matrices," Phil. Mag., May 1934.
(2) A. C. Aitken, "On Bernoulli's Numerical Solution of Algebraic Equations," Proc. Roy. Soc. Edinburgh, xlvi. p. 289 (1926).
(3) R. A. Frazer and W. J. Duncan, "The Flutter of Aeroplane Wings," 'Reports and Memoranda of the Aeronautical Research Committee,' No. 1155 (August 1928).

XVI. *Hardness and Lattice-distortion of cold-rolled α-brass.*

By W. A. Wood, *M.Sc., Physics Department, National Physical Laboratory, Teddington, Middlesex* *.

[Plate VII.]

THE work described in this paper is an investigation into the differences between the X-ray spectra of samples of cold-worked α-brass of which the composition was the same but the hardness different. The object was to determine to what extent the changes in microstructure, indicated by the changes in the X-ray spectra, were associated with the variations in hardness.

That the X-ray spectrum of a normal and of a cold-worked metal is different is now well established. The differences may be grouped into two classes: the first includes those due to the disturbance of atoms in any given grain; the second, those associated with changes in the distribution and size of the separate grains.

In the first class come modifications in the electron configuration of the atoms and in the placing of the atoms

* Communicated by Dr. G. W. C. Kaye, O.B.E., M.A.

in the crystal lattice ; both will be included in the term lattice-distortion. The disturbance of the electrons causes an abnormal weakening of the high order lines in the X-ray spectrum. It is comparable with altering the distribution of intensity of the light energy across the slits of an optical diffraction grating. The effect has been observed repeatedly. The work of Hengstenberg may be instanced * ; he found that the high order reflexions from aluminium, as a result of cold-working the metal, could be reduced from the normal value by as much as 50 per cent. The other aspect of lattice-distortion, that due to an irregular displacement of atoms from their normal positions, is even more marked. This effect is equivalent to introducing irregularities into the spacing of the lines of a diffraction grating ; it produces a broadening of the X-ray spectral lines. From numerous investigations the fact emerges that there are very few metals or alloys which, as a result of cold-working, do not give this diffuse form of spectrum. The known exceptions, like lead or aluminium, are usually metals which are soft and tend to recrystallize during deformation. There is no evidence as yet to suggest that a cold-worked metal does not exhibit either one or the other form of distortion ; most metals and alloys show both.

The second class of changes, involving the crystallites as a whole, includes the effects of departure from a random orientation of grains, and of changes in grain-size. The selective orientation effect is portrayed in the X-ray spectra by the formation of maxima and minima of intensity along the lines. Numerous metals have been examined in this connexion. But, in respect of strain-hardening, the orientation may be dismissed as a very secondary factor. This conclusion is based upon observations which showed that the orientation, unlike the lattice-distortion, becomes appreciable only after a high degree of cold-work has been imposed on the metal † ; whereas the increase in hardness, or the contrary, is evident most in the early stages of working. The effect of decrease in grain-size is discussed below.

The physical interpretation of the line-broadening in terms of the associated structure of the metal is complicated by the fact that the broadening may be due not

* Hengstenberg, Fortschr. der Röntgenstrahl. p. 139 (1931).
† W. A. Wood, Phil. Mag. vol. vii. p. 656 (1932).

only to distortion of the lattice, but also to the presence of a very fine grain. The latter factor operates because the resolving power of the reflecting planes in a grain depends, as in the analogous case of an optical grating, on the number of planes, and, therefore, on the size of the grain. It is suggested that the fine grain can be considered, in its effect on physical properties, the equivalent of lattice-distortion. For the boundaries of the grains, whatever the interior may be like, must possess an arrangement of atoms and electrons which is different from the ideal structure. Also the smaller the grains the larger will be the ratio of the distorted surface-layer to the volume of the whole. Thus, taking a case from work on electroplated chromium *, it is found the mean grain-size of the deposit was usually of the order of 10^{-6} cm. If now a surface, only one unit-cell in depth, were distorted, then such a disturbed layer would represent 20 per cent. of the whole volume of the grain. A surface-layer which was two unit-cells thick would represent an affected volume 30 per cent. of the whole. This means that an excessive broadening of the X-ray lines, though due essentially to fine grain, indicates the presence of a high proportion of distorted lattice. The broadening can be taken, therefore, as an overall measure of disturbance in the lattice, although, in actual fact, it may arise primarily because of a fine-grained structure. The problem of dissociating the diffusion due to fine grain from that due to pure lattice distortion has been discussed in a previous paper †. For the present purpose it is sufficient to point out that the big difference between the X-ray spectra of a normal and cold-worked metal lies in the definition of the diffraction lines, and that this decrease in definition is a measure of a distorted structure.

Now results obtained during the last few years suggest that when a metal or alloy, with a given structure and composition, is much harder than normal, then it gives an X-ray spectrum which is diffuse or weak in the manner described above. If the change in hardness is large, then the effect may be very pronounced. Thus, in the case of the electro-deposited chromium, the same line which was about 1 mm. broad, from the soft annealed metal, would diffuse into a band 1 cm. wide when obtained

* W. A. Wood, Phil. Mag. xii. p. 853 (1931).
† W. A. Wood, Phil. Mag. xv. p. 553 (1933).

from the hard electroplate. Also, in an examination of alloy steels hardened by nitriding, it was found that the (220) lines of iron, though obtainable strong and sharp from the soft core, could not be detected at all from the case-hardened surface *. Other cases published include tungsten steels †, stainless steels ‡ and cold-rolled metals. The effects are too striking to be overlooked and the examples too numerous to be fortuitous. Therefore there is a need for quantitative experiments to test definitely whether the distortion is related in a regular way to the degree of strain-hardening.

X-ray Photographs of α-brass.

That the cold-rolling of α-brass obeys the above generalization is shown by the diffraction photographs reproduced in Pl. VII.

The specimens were obtained from the same material, which had a cell-size of 3·70 Å. It was used in the form of a strip approximately $\frac{1}{4}$ in. by $\frac{1}{8}$ in. This was cleaned and annealed *in vacuo* until free from distortion, as shown by the sharpness of the spectral lines. The strip was then etched and divided into portions, each of which was cold-rolled to give a range of samples reduced in thickness by 0, $2\frac{1}{2}$, 5, 10, 15, 30, and 50 per cent.

The photographs were secured with an X-ray camera designed to give high dispersion and precision. The object was to photograph each specimen under exactly similar conditions so that variations in the spectra could be due only to changes in the microstructure of the specimen, and could not be caused by any variations in the geometry of the apparatus. With this end in view, the flat surface of each specimen was pressed by screws against a fixed plate at the centre of the camera; the plate contained an aperture to allow the entry of the incident beam and exit of the diffracted beams. Any personal errors in placing the specimens were then obviated. With the same object, the recording photographic plate was held by springs in close contact with a metal frame which contained an opening large enough for the required reflected rays to enter. Both plate and specimen-holder were screwed to a metal base-plate, which could be

* W. A. Wood, Phil. Mag. xvi. p. 719 (1933).
† W. A. Wood, Phil. Mag. vii. p. 355 (1932).
‡ W. A. Wood, Phil. Mag. x. p. 1073 (1930).

maintained at a steady temperature by water-cooling. A high dispersion of the diffracted beams was secured by using a large separation, 11·5 cm., between specimen and photographic plate. The distance of the slit-system from the specimen, and the angle made by the specimen-holder with the incident beam, were adjusted to give the (331) and (420) lines of the α-brass in sharp focus on the photographic plate.

These are the lines shown in the photographs of Pl. VII., and the changes in intensity and width apparent in the various photographs are, therefore, the result of changes in the structure of the brass. In the first photograph (*a*), obtained from the initial specimen with a Brinell hardness of 119, the (331) and (420) lines are each sharp enough to show the separate α_1 and α_2 components. The lines are as sharp as can be secured under the experimental conditions used. But in the case of the specimen which has undergone 50 per cent. reduction, shown by photograph (*f*), the spectrum lines are definitely broadened; the α_1 and α_2 components of each line are no longer resolved, and the (420) line resembles rather a diffuse band. Also the lines are weakened relative to the background. The hardness of the material at the same time has increased to 186 Brinell.

Now the point is made that the changes in definition of the lines are so marked, and the corresponding distortion in the microstructure so large, that it is inconceivable that such modifications can take place without causing associated modifications in the physical properties of the brass. This view is upheld by the fact that the photographs of the brass reduced by intermediate amounts, photographs (*b*) to (*e*), which represent specimens of increasing hardness values, show at the same time increasing changes in line-breadth. The hardness values are indicated underneath the photographs.

The next step was to measure as accurately as possible the actual breadths, so as to compare them quantitatively.

Measurement of Line-breadths.

The breadths of the lines and the distribution of intensity inside the boundaries of the lines were obtained with the aid of a Moll self-recording microphotometer. The first measurement made was that of the difference in breadth of the (331) line reflected from each specimen

and the same line from the standard annealed material, so that for each specimen a quantity was determined which represented an increase in breadth caused solely by the cold-working.

It was necessary to ensure that the measurements were not influenced by the changes in size of the bromide paper (used on the recording-drum of the microphotometer), which are brought about by the developing and subsequent treatment of the paper. Such changes were

Fig. 1.

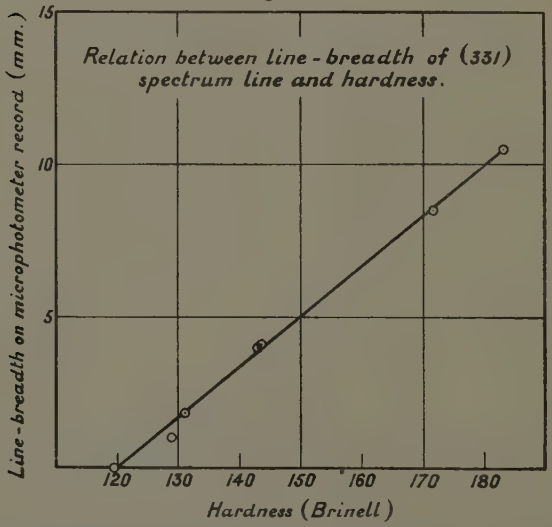

nullified by securing on each record two traces, one from the negative to be studied and one from a standard negative from the normal material. By this method the subtraction of the breadths of the corresponding lines on each trace automatically allowed for possible changes in size of the paper. It was also necessary to measure the breadth of the lines at corresponding points on the peaks. The point taken in each case was that where the intensity of the line was a half of the intensity at the peak. This gives the " half-breadth." Also the galvonometer deflexion corresponding to the trace of the base-line, or background, on each side of a peak was adjusted

to be approximately the same for both cold-worked and standard specimen on each record. The comparison was therefore made in the same region of sensitivity of the microphotometer, and made as if the two negatives to be compared had received similar exposures to the diffracted X-ray beams, as measured by the density of the background.

The increase in breadth of the (331) lines thus obtained were then compared with the hardness values. The results

Fig. 2.

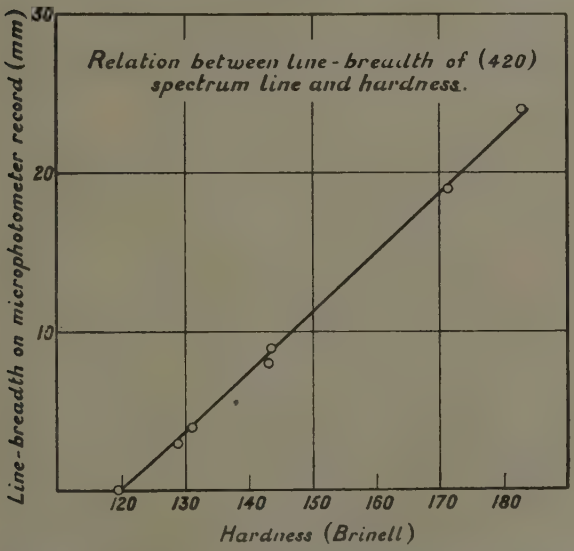

are shown in fig. 1; the hardness Brinell numbers are plotted against the change in line-breadth measured in mm. on the microphotometer records. The point brought out by the graph is that there is a continuous curve connecting the two quantities; the hardness is connected with the change in breadth of the diffraction line by a relation which, to a first approximation, appears to be linear. This, therefore, confirms quantitatively the relation suggested by the X-ray photographs in Pl. VII.

The measurements were then extended to include the (420) line. These were made in the same way, and the results are shown in fig. 2. Again a smooth curve is obtained.

The conclusion is made that, in view of the evidence of the X-ray photographs (Pl. VII.) and of figs. 1 and 2, there is a relation between the increase in hardness due to cold-rolling and the increase in diffusion of the X-ray lines, whatever the physical cause of that diffusion may be.

Physical Interpretation of the Broadening of the Lines.

As mentioned previously, the broadening may be the result of lattice-distortion, or of the breaking down of the grains to ultra-microscopic size, or of a combination of both factors. The first step is deciding which of the two predominates. The experimental evidence available may be divided into two types. The first has been discussed in a previous paper * ; it is based upon observations regarding the way the broadening increases with the degree of deformation imposed on the metal. It is found that the broadening begins almost at once, grows rapidly at first, and then more slowly rises towards a limiting value. This limiting value is small compared with the breadths which can be obtained in finely divided metals, in electro-deposited chromium for instance. Therefore, when the observed broadening is very large, the effect must be due rather to grain-size, and the contribution due to distortion can be neglected. But in the case of rolled metals the broadening is relatively small and, in view of the tendency to a limiting value, is probably due to lattice-distortion only. The second type of evidence is more direct. It approaches from the standpoint that in the case of the true fine-grain effect there should be no change in the shape and size of the unit-cell †. A line should broaden symmetrically about the position of the normal sharp line. But X-ray examination of certain rolled metals shows that this is not the case ; the lines tend usually to diffuse in one direction rather than the other. Also different lines have been found to broaden at different rates in a way not compatible with the fine-grain effect‡. For these, and similar reasons, the broadening of the lines due to cold-working is to be attributed to the lattice-distortion effect.

The asymmetrical type of broadening characterizes also the spectrum of the cold-rolled brass. This is shown

* W. A. Wood, Phil. Mag. xv. p. 553 (1933),
† V. Laue, *Zeit. für Krist.* lxiv. p. 115 (1926).
‡ W. A. Wood, Nature, cxxix. p. 760 (1932).

in fig. 3. There are reproduced microphotometer traces of two negatives on the same record. The upper one, marked N, is from the normal undistorted material, and the lower one, marked D, from the brass after 10 per cent. reduction. Each trace shows the (331) and (420) lines. (The small peak to the left of the (420) line is due to a scratch placed on the negative to identify the trace of the standard specimen.) Now the negatives were placed in the microphotometer in such a way that the (331) lines from the normal and cold-worked specimen coincide as nearly as possible. Since the experimental conditions used to obtain each negative were standardized, one would expect that if the (331) lines coincide,

Fig. 3.

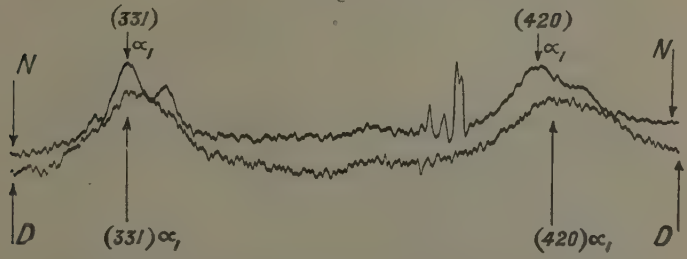

Displacement of (420)α_1 spectrum lines of cold-worked (D) and normal (N) brass.

then the (420) lines would also coincide. But reference to the figure shows that this is not so. The (420) lines are asymmetrically displaced with respect to each other. Conversely, if the (420) lines are made to coincide, then the (331) lines fall out of register. The effect was found common to each cold-rolled specimen. It means that the (331) and (420) planes are distorted by different amounts ; that the unit-cell, which in the normal material is face-centred cubic, can no longer be considered as strictly cubic after deformation. It means, also, that the latent energy of the lattice is not the same after the cold-rolling as before.

Estimation of the Degree of Distortion.

If a family of parallel planes of spacing d undergoes disturbance in such a way that the spacing is made

to vary between the limits d and $d+\delta d$, then the fractional change in spacing can be measured from the diffusing of the X-ray line reflected from those planes. Instead of the reflexion occurring at the angle θ given by the Bragg law, $2d \sin\theta = \lambda$, where λ is the wave-length used, it will be spread between the angles θ and $\theta - \delta\theta$, where $\delta\theta$ is given by

$$\frac{\delta d}{d} = \cot\theta \ \delta\theta.$$

A change δx mm. in the breadth of a line measured on the microphotometer record corresponds to a change in θ given by

$$\delta\theta = 6{\cdot}18 \times 10^{-4} \times \delta x \text{ for the (331) line}$$

and

$$\delta\theta = 6{\cdot}20 \times 10^{-4} \times \delta x \text{ for the (420) line.}$$

These values are calculated from the dimensions of the X-ray camera in the usual way, taking the distance of the specimen to the photographic plate as 11·5 cm., the plate set at 135° to the direction of the incident beam, and a magnification of seven times introduced by the gear-ratio of the microphotometer.

Therefore, for the (331) planes where θ is 65·2° we have

$$\frac{\delta d}{d} = 2{\cdot}85 \times \delta x \times 10^{-4}$$

and for the (420) planes

$$\frac{\delta d}{d} = 2{\cdot}43 \times \delta x \times 10^{-4}.$$

If we now take the specimen rolled down by 50 per cent., the one showing the maximum change in breadth, as given in figs. 1 and 2, we have to substitute for δx a value of 10·5 mm. in the case of the (331) and 24 mm. in the case of the (420) line. We then obtain for the fractional change in spacing

$$\frac{\delta d}{d} = 3 \times 10^{-3} \text{ reckoned from the (331) line}$$

and

$$\frac{\delta d}{d} = 6 \times 10^{-3} \text{ reckoned from the (420) line.}$$

Therefore the (420) planes vary from the correct spacing by twice the variation shown by the (331)—0·6 as against 0·3 per cent.

It is important to note that if the unit-cell, cubic before deformation, were cubic also after cold-working, then the fractional changes in the various spacings would be the same. The fact that experimental measurement shows that this is not the case confirms the view that, after lattice-distortion has occurred, the cell ceases to be cubic. It is possible, by taking tentative shapes which might be assumed by the cell after distortion, to find one which satisfies the observations. But this would be outside the purpose of the present paper, which, in this connexion, is to show that the differential broadening of the lines is direct evidence that, in the case of brass, the observed broadening, and the associated changes in hardness, must be put down to the effect of lattice-distortion.

Connexion with Theories of Strain-hardening.

The presence of lattice-distortion means that at certain points in a crystallite is a disturbance of the lattice which is equivalent to a fault in the structure. The fact that the distortion grows with the applied stress means that the number of these faults, or the intensity of each, must also increase. Since the intensity of one can hardly exceed the limit compatible with the stability of the lattice, it is probable that the increase in distortion is associated with an increase in number rather than the intensification of any one fault. If a centre of distortion is regarded as a region of stress concentration, then as their number increases the imposed stress is distributed more widely. The material is in a condition to withstand further stress before the maximum permissible at any one point of the lattice is exceeded—the metal is hardened. This view would fall in line with the theories elaborated by G. I. Taylor and others *, provided that the dislocations, in those theories hypothetical, were identified with the centres of lattice-distortion. These centres need not be associated with the boundaries of the crystallites until the grain-size of the material is small, when, as shown earlier in the paper, the volume affected by the

* G. I. Taylor, Proc. Roy. Soc. A, 1934, p. 388.

surface distortion becomes a large proportion of the whole. Nor need they be associated entirely with the aspect of distortion treated above. There is also the other factor, that which affects the intensity of the spectra, presumably by disturbing the electron configuration, as in aluminium ; the arguments applying to one form of distortion would apply equally to the other.

Summing up, the experiments demonstrate a relation between the effect of strain-hardening on the one hand and the diffusing or weakening of the X-ray spectral lines on the other—the line-broadening is due to distortion of the crystal lattice. If the experimental evidence is to be interpreted in terms of the recent theories of strain-hardening, then the flaws or dislocations assumed by those theories would be associated with the centres of distortion observed by the X-ray method.

Summary.

The differences in the X-ray spectra of samples of α-brass hardened to different degrees by cold-rolling are determined. Particular attention is paid to the increase in breadth of the diffraction lines. The increase in breadth is found to be proportional to the increase in hardness of the brass, and a relation between the two quantities is suggested. The broadening of the lines is attributed to lattice-distortion as a result of measurements which show that the unit-cell of the brass ceases to be cubic after the material has been cold-worked.

XVII. *Bessel Functions of nearly equal Order and Argument.* *By* J. R. Airey, *D.Sc., Sc.D.**

BESSEL functions of nearly equal order and argument were independently investigated by J. W. Nicholson and P. Debye. The former derived the first two or three terms of the expansion for $J_\nu(x)$, when x is nearly equal to ν, from the consideration of the relationship of this function to Airy's integral and to Bessel functions of fractional order [1], $\pm\frac{1}{3}$; the latter, from Sommerfeld's integral, by the Saddle point or Pass method of contour integration [2]. An interesting paper by Fritz Emde and Rudolf Rühle has recently appeared on Debye's

* Communicated by the Author.

asymptotic series, with particular reference to their use in numerical calculations.

Tables of Bessel and Neumann functions, where the order and argument are equal or differ by unity, were first published nearly twenty years ago, followed by similar and more extensive tables of $J_\nu(x)$, $Y_\nu(x)$, Schläfli's integral,

$$\int_0^\infty e^{-x\sinh\theta}\, e^{-\nu\theta}.\, d\theta\,,$$

and the Lommel-Weber function,

$$\Omega_\nu(x)=\frac{1}{\pi}\int_0^\pi \sin(\nu\phi - x\sin\phi)\, d\phi,$$

the variable 4ν ranging from 0 to 40 by unit intervals. The tables of $J_\nu(\nu)$ and $J_{\nu-1}(\nu)$ were calculated from the formulæ, λ is written for $\left(\frac{6}{\nu}\right)^{\frac{1}{3}}$,

$$J_\nu(\nu)=\frac{1}{2\pi\sqrt{3}}\left[\lambda\,.\,\Gamma\left(\tfrac{1}{3}\right)-\frac{1}{420}\lambda^5\Gamma\left(\tfrac{2}{3}\right)-\frac{1}{8100}\lambda^7\Gamma\left(\tfrac{1}{3}\right)\right.$$
$$\left.+\frac{1}{182300}\lambda^{11}\,.\,\Gamma\left(\tfrac{2}{3}\right)\ldots\right]$$

and

$$J_{\nu-1}(\nu)=\frac{1}{2\pi\sqrt{3}}\left[\lambda\,.\,\Gamma\left(\tfrac{1}{3}\right)+\lambda^2\Gamma\left(\tfrac{2}{3}\right)\right.$$
$$-\frac{1}{30}\lambda^4\Gamma\left(\tfrac{1}{3}\right)-\frac{1}{420}\lambda^5\Gamma\left(\tfrac{2}{3}\right)-\frac{1}{8100}\lambda^7\Gamma\left(\tfrac{1}{3}\right)$$
$$\left.+\frac{23}{113400}\lambda^8\Gamma\left(\tfrac{2}{3}\right)+\frac{947}{74844000}\lambda^{10}\Gamma\left(\tfrac{1}{3}\right)\ldots\right].$$

The coefficient of λ^{11} in the $J_\nu(\nu)$ series is approximate, but so near the correct value, $\frac{1213}{221130000}$, that the sixth significant figure in this term is not affected. In the general case, if $x=\nu+\kappa$, κ small compared with ν,

$$J_\nu(x)=\frac{1}{2\pi\sqrt{3}}\left[\lambda\,.\,\Gamma\left(\tfrac{1}{3}\right)+B_1\lambda^2\Gamma\left(\tfrac{2}{3}\right)-\frac{1}{3}B_3\lambda^4\Gamma\left(\tfrac{1}{3}\right)\right.$$
$$\left.-\frac{2}{3}B_4\lambda^5\Gamma\left(\tfrac{2}{3}\right)+\frac{4}{9}B_6\lambda^7\Gamma\left(\tfrac{1}{3}\right)+\frac{10}{9}B_7\lambda^8\Gamma\left(\tfrac{2}{3}\right)\right.$$

$$-\frac{28}{27}B_9\lambda^{10}\Gamma\left(\frac{1}{3}\right)\ldots\Big], \quad \ldots\ldots\ldots \quad (1)$$

where

$$B_1(\kappa)=\kappa,\ B_3(\kappa)=\frac{\kappa^3}{6}-\frac{\kappa}{15},\ B_4(\kappa)=\frac{\kappa^4}{24}-\frac{\kappa^2}{24}+\frac{1}{280},\ \text{etc.}$$

The polynomials B_m have been computed as far as B_{19} from the expansion

$$(1+a_1\omega^2+a_2\omega^4+a_3\omega^6+\ldots)^s$$
$$=1+sa_1\omega^2+(sa_2+s_2a_1^2)\omega^4+(sa_3+2s_2a_1a_2+s_3a_1^3)\omega^6+\ldots$$
$$=1+r_1\omega^2+r_2\omega^4+r_3\omega^6+\ldots$$

Then

$$B_{2m}=\frac{\kappa_{2m}}{2m\,!}+r_1\frac{\kappa^{2m-2}}{(2m-2)\,!}+r_2\frac{\kappa^{2m-4}}{(2m-4)\,!}$$
$$+\ldots+r_{m-1}\frac{\kappa^2}{2\,!}+r_m$$

and

$$B_{2m+1}=\frac{\kappa^{2m+1}}{(2m+1)\,!}+r_1\frac{\kappa^{2m-1}}{(2m-1)\,!}+r_2\frac{\kappa^{2m-3}}{(2m-3)\,!}$$
$$+\ldots+r_{m-1}\frac{\kappa^3}{3\,!}+r_m\kappa,$$

where

$$s=-\frac{1}{3}(m+1), \quad s_2=\frac{s(s-1)}{2\,!}, \quad s_3=\frac{s(s-1)(s-2)}{3\,!},\ \ldots$$

and

$$a_1=\frac{3\,!}{5\,!}, \quad a_2=\frac{3\,!}{7\,!}, \quad \text{etc.}$$

The series (1) was used as a check on the values of $J_\nu(\nu+\kappa)$ computed by interpolation from tables [6] of $J_n(x)$, and [7] $J_{2n+\frac{1}{2}}(x)$, for $x=1$ to $x=20$. Eight decimal places were retained, differenced and interpolated to halves, giving values of $J_p(x)$, $p=\frac{4n\pm1}{4}$.

A further interpolation to fifths completed the tables of $J_\nu(x)$, with the argument ν varying by twentieths of a unit between the values $x-1$ and $x+1$. The colon represents approximately a half unit in the last place of decimals.

ν.	$J_\nu(1)$	ν.	$J_\nu(2)$.	ν.	$J_\nu(3)$.	ν.	$J_\nu(4)$.
0·0	0·765197 :	1·0	0·576725	2·0	0·486091	3·0	0·430171 :
·1	·770765	·1	·568251	·1	·476162 :	·1	·420428
·2	·761544 :	·2	·554639 :	·2	·463422 :	·2	·408841
·3	·740222 :	·3	·536739 :	·3	·448317 :	·3	·395696
·4	·709377	·4	·515368	·4	·431278	·4	·381269
0·5	0·671396 :	1·5	0·491294	2·5	0·412710	3·5	0·365820 :
·6	·628428 :	·6	·465227	·6	·392991 :	·6	·349594
·7	·582349	·7	·437811 :	·7	·372470	·7	·332815 :
·8	·534755 :	·8	·409619	·8	·351460	·8	·315691
·9	·486969 :	·9	·381150 :	·9	·330242	·9	·298406 :
1·0	0·440050 :	2·0	0·352834	3·0	0·309062 :	4·0	0·281129
·1	·394820	·1	·325028 :	·1	·288135 :	·1	·264004
·2	·351884	·2	·298028 :	·2	·267642	·2	·247159
·3	·311664	·3	·272067	·3	·247733	·3	·230702 :
·4	·274424	·4	·247322 :	·4	·228530 :	·4	·214725
1·5	0·240298	2·5	0·223924 :	3·5	0·210132	4·5	0·199300 :
·6	·209313 :	·6	·201958 :	·6	·192609	·6	·184488 :
·7	·181417 :	·7	·181473	·7	·176013 :	·7	·170334 :
·8	·156495 :	·8	·162485 :	·8	·160378	·8	·156870 :
·9	·134387	·9	·144986	·9	·145717 :	·9	·144117 :
2·0	0·114903 :	3·0	0·128943	4·0	0·132034	5·0	0·132086 :

ν.	$J_\nu(5)$.	ν.	$J_\nu(6)$.	ν.	$J_\nu(7)$.	ν.	$J_\nu(8)$.
4·0	0·391232 :	5·0	0·362087	6·0	0·339196 :	7·0	0·320589
·1	·381986	·1	·353372	·1	·330978 :	·1	·312818 :
·2	·371406	·2	·343632	·2	·321939	·2	·304370
·3	·359697	·3	·333022	·3	·312201	·3	·295344
·4	·347054	·4	·321690 :	·4	·301883	·4	·285836 :
4·5	0·333662 :	5·5	0·309779	6·5	0·291096	7·5	0·275940
·6	·319697 :	·6	·297419	·6	·279946 :	·6	·265740 :
·7	·305320 :	·7	·284735 :	·7	·268532 :	·7	·255319 :
·8	·290680 :	·8	·271842 :	·8	·256945 :	·8	·244752 :
·9	·275913	·9	·258844 :	·9	·245270 :	·9	·234110
5·0	0·261140 :	6·0	0·245837	7·0	0·233583 :	8·0	0·223455
·1	·246472	·1	·232905	·1	·221955	·1	·212846 :
·2	·232003	·2	·220124 :	·2	·210446 :	·2	·202336
·3	·217816 :	·3	·207562 :	·3	·199113 :	·3	·191971
·4	·203983 :	·4	·195276 :	·4	·188004 :	·4	·181792 :
5·5	0·190564 :	6·5	0·183316	7·5	0·177161	8·5	0·171837
·6	·177607 :	·6	·171722	·6	·166618 :	·6	·162134 :
·7	·165151 :	·7	·160528 :	·7	·156406 :	·7	·152712 :
·8	·153227	·8	·149762	·8	·146549 :	·8	·143591 :
·9	·141854 :	·9	·139443 :	·9	·137066	·9	·134790
6·0	0·131048 :	7·0	0·129586 :	8·0	0·127970 :	9·0	0·126321

ν.	$J_\nu(9)$.	ν.	$J_\nu(10)$.	ν.	$J_\nu(11)$.	ν.	$J_\nu(12)$.
8·0	0·305067	9·0	0·291855 :	10·0	0·280428	11·0	0·270412 :
·1	·297696 :	·1	·284841 :	·1	·273732 :	·1	·264002 :
·2	·289752 :	·2	·277333 :	·2	·266605 :	·2	·257212
·3	·281319 :	·3	·269404 :	·3	·259110 :	·3	·250096
·4	·272479	·4	·261123 :	·4	·251307 :	·4	·242706 :
8·5	0·263307 :	9·5	0·252556 :	10·5	0·243254	11·5	0·235095
·6	·253878	·6	·243766	·6	·235003 :	·6	·227309
·7	·244259	·7	·234810 :	·7	·226608	·7	·219393 :
·8	·234514 :	·8	·225745 :	·8	·218115 :	·8	·211391
·9	·224703 :	·9	·216621 :	·9	·209570 :	·9	·203341
9·0	0·214880 :	10·0	0·207486	11·0	0·201014	12·0	0·195280
·1	·205095 :	·1	·198382	·1	·192484 :	·1	·187242 :
·2	·195392 :	·2	·189348 :	·2	·184016	·2	·179259
·3	·185813	·3	·180421	·3	·175640 :	·3	·171357 :
·4	·176392 :	·4	·171631 :	·4	·167385 :	·4	·163563
9·5	0·167162	10·5	0·163007 :	11·5	0·159277	12·5	0·155899
·6	·158150	·6	·154573 :	·6	·151336 :	·6	·148385
·7	·149379	·7	·146351	·7	·143583	·7	·141039
·8	·140869	·8	·138358	·8	·136033 :	·8	·133875 :
·9	·132636 :	·9	·130609	·9	·128702	·9	·126908 :
10·0	0·124694	11·0	0·123116 :	12·0	0·121600	13·0	0·120148

ν.	$J_\nu(13)$.	ν.	$J_\nu(14)$.	ν.	$J_\nu(15)$.	ν.	$J_\nu(16)$.
12·0	0·261537	13·0	0·253598	14·0	0·246440	15·0	0·239941
·1	·255385 :	·1	247680 :	·1	·240736	·1	·234432 :
·2	·248894	·2	·241457	·2	·234754 :	·2	·228670
·3	·242111	·3	·234971	·3	·228534 :	·3	·222690 :
·4	·235084 :	·4	·228265	·4	·222114 :	·4	·216527 :
12·5	0·227858 :	13·5	0·221379 :	14·5	0·215531	15·5	0·210215 :
·6	·220476	·6	·214352	·6	·208818 :	·6	·203784 :
·7	·212977 :	·7	·207219	·7	·202010	·7	·197266
·8	·205400	·8	·200014 :	·8	·195136	·8	·190687
·9	·197779 :	·9	·192771	·9	·188226	·9	·184074 :
13·0	0·190149	14·0	0·185517 :	15·0	0·181306 :	16·0	0·177453
·1	·182538 :	·1	·178281 :	·1	·174402 :	·1	·170846
·2	·174975 :	·2	·171089	·2	·167537 :	·2	·164274
·3	·167486 :	·3	·163962	·3	·160732 :	·3	·157757
·4	·160093 :	·4	·156922 :	·4	·154007	·4	·151312 :
13·5	0·152817 :	14·5	0·149989	15·5	0·147378	16·5	0·144957
·6	·145677	·6	·143178	·6	·140861 :	·6	·138704 :
·7	·138688	·7	·136505 :	·7	·134471 :	·7	·132568 :
·8	·131864 :	·8	·129983 :	·8	·128219 :	·8	·126560
·9	·125218 :	·9	·123624	·9	·122117	·9	·120689 :
14·0	0·118761	15·0	0·117437	16·0	0·116173	17·0	0·114965 :

ν.	$J_\nu(17)$.	ν.	$J_\nu(18)$.	ν.	$J_\nu(19)$.	ν.	$J_\nu(20)$.
16·0	0·234005	17·0	0·228553 :	18·0	0·223523	19·0	0·218862
·1	·228675 :	·1	·223390	·1	·218513	·1	·213994
·2	·223113 :	·2	·218011 :	·2	·213303 :	·2	·208941
·3	·217352	·3	·212448 :	·3	·207923	·3	·203728 :
·4	·211422	·4	·206730	·4	·202398 :	·4	·198382
16·5	0·205354	17·5	0·200884 :	18·5	0·196755 :	19·5	0·192925
·6	·199177 :	·6	·194938	·6	·191019	·6	·187380 :
·7	·192919 :	·7	·188916 :	·7	·185212 :	·7	·181771
·8	·186606	·8	·182843	·8	·179357 :	·8	·176116
·9	·180261	·9	·176740 :	·9	·173475 :	·9	·170435 :
17·0	0·173908	18·0	0·170630	19·0	0·167586	20·0	0·164748
·1	·167567 :	·1	·164531	·1	·161706 :	·1	·159069 :
·2	·161259 :	·2	·158461 :	·2	·155855	·2	·153417
·3	·155001 :	·3	·152438 :	·3	·150046	·3	·147804 :
·4	·148810 :	·4	·146478	·4	·144295	·4	·142245 :
17·5	0·142701 :	18·5	0·140593	19·5	0·138614 :	20·5	0·136752 :
·6	·136688	·6	·134796 :	·6	·133016 :	·6	·131337
·7	·130782	·7	·129100	·7	·127512	·7	·126008 :
·8	·124994 :	·8	·123513 :	·8	·122110	·8	·120776 :
·9	·119334 :	·9	·118046 :	·9	·116820	·9	·115649 :
18·0	0·113811	19·0	0·112706 :	20·0	0·111648 :	21·0	0·110633 :

References.

(1) J. W. Nicholson, "On Bessel Functions of Equal Order and Argument," Phil. Mag. xvi. (August 1908).
——, "On the Relation of Airy's Integral to Bessel Functions," Phil. Mag. xviii. (July 1909); xxv. (January 1913).

(2) P. Debye, "Näherungsformeln für die Zylinderfunktionen," *Math. Annalen*, xvii. (1909).
——, "Semikonvergente Entwickelungen für die Zylinderfunktionen und ihre Ausdehnung ins Komplexe," *Sitz. der k.-bayerischen Akademie*, Jahrgang 1910.

(3) Fritz Emde u. Rudolf Rühle, "Die Debyesche halb konvergenten Reihen für die Zylinderfunktionen im Komplexen," *Jahresbericht der Deutschen Math. Verein*, 43 Band (1934).

(4) J. R. Airey, "Bessel and Neumann Functions of Equal Order and Argument," Report of the Math. Tables Comm., British Association, 1916; and Phil. Mag. xxxi. (June 1916).

(5) ——, "Bessel and other related Functions of Equal Order and Argument," Report of the Math. Tables Comm., British Association, 1923.

(6) E. Meissel, 'Tables of Bessel Functions of Integral Order $J_n(x)$ to eighteen places of decimals. Gray and Mathews, 'Bessel Functions.' First and second editions. Macmillan & Co., 1922.

(7) J. R. Airey, "Tables of Bessel Function of Half Odd Integral Order, $J_{\frac{2n+1}{2}}(x)$, n positive and negative to twelve places of decimals," Report of the Math. Tables Comm., British Association, 1925.

XVIII. *The Bessel Function Derivatives* $\frac{\partial}{\partial \nu} . J_\nu(x)$ *and* $\frac{\partial^2}{\partial \nu^2} . J_\nu(x)$. *By* J. R. Airey, *D.Sc., Sc.D.**

THE derivatives of $J_\nu(x)$, with respect to the variable x have a simple expression in terms of the Bessel functions themselves: the derivatives with respect to ν, the order of the function, assume a more complicated form, especially when ν is not an integer.

When ν is an integer,

$$\left[\frac{\partial}{\partial \nu} . J_\nu(x)\right]_{\nu=0} = -G_0(x),$$

$$\left[\frac{\partial}{\partial \nu} . J_\nu(x)\right]_{\nu=1} = -G_1(x) + \frac{J_0(x)}{x},$$

and generally,

$$\left[\frac{\partial}{\partial \nu} . J_\nu(x)\right]_{\nu=n} = -G_n(x) + \frac{n!}{2} \sum_{p=0}^{n-1} \left(\frac{2}{x}\right)^{n-p} \frac{J_p(x)}{(n+p).p!}.$$

Tables of $G_0(x)$ and $G_1(x)$ [1] correct to six decimal places were published in the British Association Reports. From the derivatives of the zero- and unit-order functions, those of functions of higher order can be calculated by means of the recurrence formula found by differentiating

$$J_{\nu+1}(x) = \frac{2\nu}{x} J_\nu(x) - J_{\nu-1}(x)$$

with respect to ν, viz.:

$$\frac{\partial}{\partial \nu} . J_{\nu+1}(x) = \frac{2\nu}{x} . \frac{\partial}{\partial \nu} . J_\nu(x) - \frac{\partial}{\partial \nu} . J_{\nu-1}(x) + \frac{2}{x} . J_\nu(x).$$

The derivatives of Bessel functions of half-odd integral order can be expressed in terms of the sine and cosine integrals [2]

$$\left[\frac{\partial}{\partial \nu} . J_\nu(x)\right]_{\nu=\frac{1}{2}} = J_{\frac{1}{2}}(x)\,\mathrm{Ci}(2x) - J_{-\frac{1}{2}}(x)\,\mathrm{Si}(2x)$$

and

$$\left[\frac{\partial}{\partial \nu} . J_\nu(x)\right]_{\nu=-\frac{1}{2}} = J_{-\frac{1}{2}}(x)\,\mathrm{Ci}(2x) + J_{\frac{1}{2}}(x)\,\mathrm{Si}(2x).$$

* Communicated by the Author.

Schafheitlin [3] had previously shown the close relationship between these derivatives and the sine and cosine integrals, viz.,

$$\mathrm{si}(2x) = -\frac{\pi}{2}\cos 2x - \sqrt{\frac{\pi x}{2}}\,[\cos x.\mathrm{V}_{\frac{1}{2}}(x) - \sin x.\mathrm{W}_{\frac{1}{2}}(x)],$$

$$\mathrm{ci}(2x) = \frac{\pi}{2}\sin 2x + \sqrt{\frac{\pi x}{2}}\,[\sin x.\mathrm{V}_{\frac{1}{2}}(x) - \cos x.\mathrm{W}_{\frac{1}{2}}(x)],$$

and

$$\mathrm{ci}(2x) - i\,\mathrm{Si}(2x) = \frac{i\pi}{2}e^{-2ix} + \sqrt{\frac{\pi x}{2}}.e^{-ix}[i\mathrm{V}_{\frac{1}{2}}(x) - \mathrm{W}_{\frac{1}{2}}(x)],$$

where

$$\mathrm{si}(x) = \mathrm{Si}(x) - \frac{\pi}{2} \quad \text{and} \quad \mathrm{ci}(x) = \mathrm{Ci}(x),$$

$$\mathrm{V}_{\frac{1}{2}} = \left[\frac{\partial}{\partial\nu}.J_\nu(x)\right]_{\nu=\frac{1}{2}}, \quad \mathrm{W}_{\frac{1}{2}} = \left[\frac{\partial}{\partial\nu}.J_\nu(x)\right]_{\nu=-\frac{1}{2}}.$$

Extensive tables [4] of $J_{\pm\frac{1}{3}}(x)$ and $\mathrm{Si}(x)$ and $\mathrm{Ci}(x)$ were published in the Reports of the British Association. No tables of $\frac{\partial}{\partial\nu}.J_\nu(x)$, $\nu = \pm\frac{1}{2}$, $\pm\frac{3}{2}$ appear to have been constructed before those given in the B.A. Report, 1928. The functions $\mathrm{V}_{\frac{1}{2}}(x)$ and $\mathrm{W}_{\frac{1}{2}}(x)$ can be developed in series of Bessel functions [3] of half-odd integral order

$$\mathrm{V}_{\frac{1}{2}}(x) = \{\log 2x + \gamma\}.J_{\frac{1}{2}}(x) + \sum_1^\infty (-1)^{\lambda-1}\frac{1}{\lambda}.J_{2\lambda+\frac{1}{2}}(x) - \sum_0^\infty (-1)^\lambda \frac{2}{2\lambda+1}.J_{2\lambda+\frac{1}{2}}(x)$$

and

$$\mathrm{W}_{\frac{1}{2}}(x) = \{\log 2x + \gamma\}J_{-\frac{1}{2}}(x) + \pi J_{\frac{1}{2}}(x) - \sum_1^\infty (-1)^{\lambda-1}\left(\frac{1}{\lambda} + \frac{2}{2\lambda+1}\right)J_{2\lambda-\frac{1}{2}}(x)$$

where γ is Euler's constant.

The first and second derivatives of $J_\nu(x)$ with respect to ν were calculated from the tables given in the previous paper, using the usual formulæ for the differential coefficients in terms of the central differences of the Bessel functions.

ν.	$\frac{\partial}{\partial\nu}\cdot J_\nu(1)$.	$\frac{\partial^2}{\partial\nu^2}\cdot J_\nu(1)$.	ν.	$\frac{\partial}{\partial\nu}\cdot J_\nu(2)$.	$\frac{\partial^2}{\partial\nu^2}\cdot J_\nu(2)$.
0·0	+0·13863 :	−1·7484 :	1·0	−0·05618	−0·5999 :
·1	−0·02278 :	1·4788	·1	·11186	·5136 :
·2	·15713 :	1·2091 :	·2	·15895	·4285 :
·3	·26499 :	0·9507 :	·3	·19768 :	·3468
·4	·34792	0·7115	·4	·22846 :	·2697 :
0·5	−0·40810 :	−0·4965 :	1·5	−0·25183 :	−0·1987
·6	·44813 :	·3087 :	·6	·26842 :	·1343
·7	·47079	·1491	·7	·27893 :	·0770 :
·8	·47887 :	−0·0171	·8	·28408	−0·0270 :
·9	·47508 :	+0·0887 :	·9	·28458	+0·0158
1·0	−0·46193	+0·1705 :	2·0	−0·28115	+0·0516 :
·1	·44168	·2310 :	·1	·27446 :	·0810 :
·2	·41634	·2729 :	·2	·26515	·1042
·3	·38762	·2991	·3	·25378 :	·1221
·4	·35696	·3122	·4	·24089	·1350
1·5	−0·32552 :	+0·3149	2·5	−0·22693	+0·1435 :
·6	·29425 :	·3094	·6	·21231	·1483
·7	·26385 :	·2977	·7	·19737	·1500
·8	·23486	·2816 :	·8	·18240	·1490
·9	·20762 :	·2626 :	·9	·16764 :	·1458 :
2·0	−0·18239	+0·2419	3·0	−0·15329	+0·1410

ν.	$\frac{\partial}{\partial\nu}\cdot J_\nu(3)$.	$\frac{\partial^2}{\partial\nu^2}\cdot J_\nu(3)$.	ν.	$\frac{\partial}{\partial\nu}\cdot J_\nu(4)$.	$\frac{\partial^2}{\partial\nu^2}\cdot J_\nu(4)$.
2·0	−0·08370 :	−0·3269 :	3·0	−0·08723 :	−0·2138 :
·1	·11410	·2811	·1	·10714	·1843 .
·2	·13996	·2363	·2	·12413	·1556 :
·3	·16142	·1933	·3	·13830 :	·1281
·4	·17869 :	·1526 :	·4	·14980	·1020
2·5	−0·19204	−0·1148	3·5	−0·15876 :	−0·0776
·6	·20175	·0800	·6	·16538 :	·0550 :
·7	·20815 :	·0485 :	·7	·16984	·0344 :
·8	·21158	−0·0205	·8	·17233 :	−0·0158
·9	·21237	+0·0041 :	·9	·17307	+0·0008
3·0	−0·21086	+0·0255	4·0	−0·17224	+0·0154 :
·1	·20738	·0436	·1	·17004 :	·0281 :
·2	·20224	·0587	·2	·16667 :	·0390
·3	·19574	·0709	·3	·16231	·0480 :
·4	·18814 :	·0805 :	·4	·15712	·0554 :
3·5	−0·17971	+0·0878	4·5	−0·15126 :	+0·0613 :
·6	·17066	·0929	·6	·14489 :	·0658 :
·7	·16119 :	·0961	·7	·13813 :	·0691
·8	·15149 :	·0976 :	·8	·13111 :	·0712
·9	·14171	·0978	·9	·12393	·0723
4·0	−0·13197 :	+0·0967 :	5·0	−0·11668	+0·0725

ν.	$\frac{\partial}{\partial\nu}.J_\nu(5)$.	$\frac{\partial^2}{\partial\nu^2}.J_\nu(5)$.	ν.	$\frac{\partial}{\partial\nu}.J_\nu(6)$.	$\frac{\partial^2}{\partial^2}.J_\nu(6)$.
4·0	−0·08510	−0·1543 :	5·0	−0·08150	−0·1184 :
·1	·09947 :	·1333	·1	·09254	·1024 :
·2	·11178	·1129	·2	·10200 :	·0869 :
·3	·12208	·0933	·3	·10995	·0721
·4	·13047	·0747	·4	·11644 :	·0580
4·5	−0·13706	−0·0573	5·5	−0·12157	−0·0447
·6	·14197	·0411	·6	·12541 :	·0323
·7	·14532 :	·0262	·7	·12806 :	·0209
·8	·14725	·0126	·8	·12962	·0104
·9	·14789	−0·0004	·9	·13018	−0·0009
5·0	−0·14737 :	+0·0105	6·0	−0·12983	+0·0076 :
·1	·14584	·0200 :	·1	·12868	·0152 :
·2	·14340 :	·0283 :	·2	·12681 :	·0219
·3	·14020 :	·0355	·3	·12433	·0277
·4	·13635	·0414 :	·4	·12131	·0326
5·5	−0·13195 :	+0·0463	6·5	−0·11783 :	+0·0367
·6	·12712	·0502	·6	·11399	·0401
·7	·12194 :	·0531 :	·7	·10984	·0428
·8	·11651 :	·0553	·8	·10545 :	·0448
·9	·11091	·0567	·9	·10089 :	·0462 :
6·0	−0·10519 :	+0·0574 :	7·0	−0·09622	+0·0472

ν.	$\frac{\partial}{\partial\nu}.J_\nu(7)$.	$\frac{\partial^2}{\partial\nu^2}.J_\nu(7)$.	ν.	$\frac{\partial}{\partial\nu}.J_\nu(8)$.	$\frac{\partial^2}{\partial\nu^2}.J_\nu(8)$.
6·0	−0·07765 :	−0·0948	7·0	−0·07397	−0·0782
·1	·08649 :	·0821	·1	·08126 :	·0678
·2	·09408 :	·0698	·2	·08754	·0577 :
·3	·10047	·0580	·3	·09282 :	·0480 :
·4	·10570 :	·0468	·4	·09717	·0389
6·5	−0·10985 :	−0·0362 :	7·5	−0·10062	−0·0302 :
·6	·11298	·0263 :	·6	·10323 :	·0221
·7	·11515	·0172	·7	·10506	·0145 :
·8	·11644 :	·0088	·8	·10616	·0075 :
·9	·11693	−0·0011	·9	·10659	−0·0011 :
7·0	−0·11668 :	+0·0058 :	8·0	−0·10641	+0·0046 :
·1	·11578 :	·0121	·1	·10568	·0099
·2	·11429 :	·0176	·2	·10445	·0146
·3	·11228 :	·0224 :	·3	·10278	·0187
·4	·10983	·0266	·4	·10072 :	·0223
7·5	−0·10698 :	+0·0301 :	8·5	−0·09834	+0·0254
·6	·10381 :	·0331	·6	·09566 :	·0280 :
·7	·10038	·0355	·7	·09275	·0302
·8	·09673	·0374	·8	·08964	·0319 :
·9	·09291 :	·0388 :	·9	·08637 :	·0333
8·0	−0·08898	+0·0398 :	9·0	−0·08299	+0·0343

ν.	$\frac{\partial}{\partial\nu}.J_\nu(9)$.	$\frac{\partial^2}{\partial\nu^2}.J_\nu(9)$.	ν.	$\frac{\partial}{\partial\nu}.J_\nu(10)$.	$\frac{\partial^2}{\partial\nu^2}.J_\nu(10)$.
8·0	−0·07055 :	−0·0660 :	9·0	−0·06743	−0·0568
·1	·07671 :	·0572	·1	·07273 :	·0493
·2	·08202	·0488 :	·2	·07730	·0421
·3	·08650	·0407 :	·3	·08116 :	·0351 :
·4	·09018 :	·0330 :	·4	·08434 :	·0286
8·5	−0·09312 :	−0·0257 :	9·5	−0·08689	−0·0223
·6	·09535	·0189	·6	·08882 :	·0164 :
·7	·09692	·0125	·7	·09019	·0109 :
·8	·09787	·0066	·8	·09102 :	·0058 :
·9	·09825 :	−0·0011 :	·9	·09137 :	−0·0011 :
9·0	−0·09812	+0·0038	10·0	−0·09126 :	+0·0032
·1	·09751	·0083	·1	·09075	·0071
·2	·09647 :	·0123 :	·2	·08986	·0106 :
·3	·09506	·0159 :	·3	·08863 :	·0138
·4	·09330 :	·0191	·4	·08711 :	·0166
9·5	−0·09125 :	+0·0218	10·5	−0·08533	+0·0190 :
·6	·08895 :	·0241 :	·6	·08331 :	·0211 :
·7	·08643 :	·0261 :	·7	·08110 :	·0229 :
·8	·08373 :	·0277 :	·8	·07873 :	·0244 :
·9	·08089 :	·0290 :	·9	·07622 :	·0257
10·0	−0·07793 :	+0·0300 :	11·0	−0·07360 :	+0·0266 :

ν.	$\frac{\partial}{\partial\nu}.J_\nu(11)$.	$\frac{\partial^2}{\partial\nu^2}.J_\nu(11)$.	ν.	$\frac{\partial}{\partial\nu}.J_\nu(12)$.	$\frac{\partial^2}{\partial\nu^2}.J_\nu(12)$.
10·0	−0·06459	−0·0495 :	11·0	−0·06200 :	−0·0438
·1	·06922	·0430 :	·1	·06609 :	·0380 :
·2	·07321	·0368	·2	·06962 :	·0325 :
·3	·07659	·0308	·3	·07261 :	·0272 :
·4	·07937 :	·0250 :	·4	·07508 :	·0222
10·5	−0·08161	−0·0196	11·5	−0·07706 :	−0·0174
·6	·08331	·0145	·6	·07858	·0129 :
·7	·08451 :	·0097	·7	·07966	·0086 :
·8	·08526	·0052 :	·8	·08032 :	·0047
·9	·08557 :	−0·0011	·9	·08061	−0·0010 :
10·0	−0·08549	+0·0027	12·0	−0·08054 :	+0·0023
·1	·08504 :	·0061 :	·1	·08015 :	·0054
·2	·08427	·0093	·2	·07947	·0082 :
·3	·08319 :	·0121	·3	·07852	·0107 :
·4	·08185 :	·0146	·4	·07732 :	·0130 :
11·5	−0·08028	+0·0168 :	12·5	−0·07592	+0·0150 :
·6	·07850	·0187 :	·6	·07433	·0168
·7	·07654	·0204	·7	·07257	·0183
·8	·07442 :	·0218	·8	·07067	·0196
·9	·07218 :	·0229 :	·9	·06865 :	·0207
12·0	−0·06984 :	+0·0238 :	13·0	−0·06654	+0·0216

ν.	$\frac{\partial}{\partial \nu} . J_\nu$ (13).	$\frac{\partial^2}{\partial \nu^2} . J$ (13).	ν.	$\frac{\partial}{\partial \nu} . J_\nu$(14).	$\frac{\partial^2}{\partial \nu^2} . J_\nu$(14).
12·0	−0·05965	−0·0390 :	13·0	−0·05749	−0·0351 :
·1	·06330	·0340	·1	·06078	·0306
·2	·06645	·0291	·2	·06362	·0262 :
·3	·06912 :	·0244	·3	·06603	·0220
·4	·07133 :	·0199	·4	·06802 :	·0180
12·5	−0·07311	−0·0156 :	13·5	−0·06963	−0·0141 :
·6	·07447	·0116	·6	·07086	·0105 :
·7	·07544	·0078 :	·7	·07174	·0071
·8	·07604 :	·0043	·8	·07229	·0039 :
·9	·07631	−0·0010	·9	·07253 :	−0·0009 :
13·0	−0·07625 :	+0·0020 :	14·0	−0·07249	+0·0018
·1	·07591	·0048	·1	·07218 :	·0043
·2	·07530	·0073 :	·2	·07163 :	·0066 :
·3	·07444 :	·0096 :	·3	·07086 :	·0087 :
·4	·07337 :	·0117	·4	·06989 :	·0106
13·5	−0·07211	+0·0135 :	14·5	−0·06875	+0·0123
·6	·07067 :	·0151 :	·6	·06744	·0138
·7	·06908 :	·0166	·7	·06599 :	·0151
·8	·06736 :	·0178	·8	·06442 :	·0162 :
·9	·06553 :	·0188	·9	·06275	·0172
14·0	−0·06361	+0·0196 :	15·0	−0·06098 :	+0·0180

ν.	$\frac{\partial}{\partial \nu} . J_\nu$ (15).	$\frac{\partial^2}{\partial \nu^2} . J_\nu$ (15).	ν.	$\frac{\partial}{\partial \nu} . J_\nu$ (16).	$\frac{\partial^2}{\partial \nu^2} . J_\nu$(16).
14·0	−0·05551 :	−0·0319	15·0	−0·05369 :	−0·0291
·1	·05849 :	·0277 :	·1	·05641 :	·0253 :
·2	·06107 :	·0238	·2	·05877	·0217 :
·3	·06326	·0200	·3	·06077	·0183
·4	·06507 :	·0163 :	·4	·06243	·0149 :
14·5	−0·06653 :	−0·0129	15·5	−0·06376 :	−0·0118
·6	·06766	·0096	·6	·06479 :	·0088
·7	·06846 :	·0065	·7	·06553 :	·0060
·8	·06896 :	·0036	·8	·06600	·0033 :
·9	·06919	−0·0009	·9	·06621	−0·0009
15·0	−0·06915 :	+0·0016	16·0	−0·06618	+0·0014 :
·1	·06888	·0039	·1	·06593	·0035 :
·2	·06838 :	·0060 :	·2	·06547 :	·0055
·3	·06768 :	·0079 :	·3	·06483 :	·0073
·4	·06680	·0097	·4	·06402 :	·0089
15·5	−0·06575	+0·0112 :	16·5	−0·06306 :	+0·0103 :
·6	·06455 :	·0126 :	·6	·06196 :	·0116 :
·7	·06323	·0138 :	·7	·06074	·0128
·8	·06179	·0149 :	·8	·05941	·0138
·9	·06025	·0158 :	·9	·05798 :	·0146 :
16·0	−0·05862 :	+0·0166	17·0	−0·05648 :	+0·0154

ν.	$\frac{\partial}{\partial \nu}.J_\nu(17)$.	$\frac{\partial^2}{\partial \nu^2}.J(\nu\ 17)$.	ν.	$\frac{\partial}{\partial \nu}.J_\nu(18)$.	$\frac{\partial^2}{\partial \nu^2}.J_\nu(18)$.
16·0	−0·05201 :	−0·0267	17·0	−0·05045 :	−0·0246
·1	·05451	·0233	·1	·05276	·0214 :
·2	·05667 :	·0200	·2	·05475 :	·0184 :
·3	·05851	·0168	·3	·05645 :	·0155
·4	·06004	·0137 :	·4	·05786 :	·0127 :
16·5	−0·06127	−0·0108 :	17·5	−0·05900 :	−0·0100 :
·6	·06221 :	·0081 :	·6	·05988	·0075 :
·7	·06290	·0055 :	·7	·06051 :	·0051 :
·8	·06333	·0031	·8	·06091 :	·0029
·9	·06352 :	−0·0008 :	·9	·06110	−0·0008
17·0	−0·06350 :	+0·0013	18·0	−0·06108	+0·0011 :
·1	·06327 :	·0032 :	·1	·06087	·0030
·2	·06286	·0050 :	·2	·06049	·0046 :
·3	·06227	·0067	·3	·05994 :	·0062
·4	·06152 :	·0082	·4	·05925	·0076
17·5	−0·06063 :	+0·0095 :	18·5	−0·05842 :	+0·0088 :
·6	·05961 :	·0107 :	·6	·05748	·0100
·7	·05848 :	·0118 :	·7	·05643	·0110 :
·8	·05725	·0128	·8	·05528	·0119 :
·9	·05593	·0136	·9	·05405	·0127
18·0	−0·05453	+0·0143 :	19·0	−0·05274 :	+0·0134

ν.	$\frac{\partial}{\partial \nu}.J_\nu(19)$.	$\frac{\partial^2}{\partial \nu^2}.J_\nu(19)$.	ν.	$\frac{\partial}{\partial \nu}.J_\nu(20)$.	$\frac{\partial^2}{\partial \nu^2}.J_\nu(20)$.
18·0	−0·04901	−0·0228	19·0	−0·04766 :	−0·0212
·1	·05114 :	·0199	·1	·04965	·0185
·2	·05299 :	·0171	·2	·05137	·0159
·3	·05457	·0144	·3	·05283 :	·0134
·4	·05588	·0118	·4	·05405 :	·0110
18·5	−0·05693 :	−0·0093 :	19·5	−0·05504 :	−0·0087
·6	·05775 :	·0070	·6	·05580 :	·0065 :
·7	·05834 :	·0048	·7	·05635 :	·0045
·8	·05872	·0027	·8	·05671	·0025 :
·9	·05889	−0·0007 :	·9	·05687	−0·0007 :
19·0	−0·05887 :	+0·0010 :	20·0	−0·05685 :	+0·0010
·1	·05868	·0027 :	·1	·05668	·0025 :
·2	·05832 :	·0043	·2	·05635	·0040
·3	·05782	·0057 :	·3	·05588	·0053 :
·4	·05718	·0071	·4	·05528	·0066
19·5	−0·05641	+0·0082 :	20·5	−0·05456	+0·0077 :
·6	·05553	·0093 :	·6	·05373 :	·0087 :
·7	·05454 :	·0103	·7	·05281 :	·0096 :
·8	·05347 :	·0111 :	·8	·05181	·0104 :
·9	·05232	·0119	·9	·05072 :	·0111 :
20·0	−0·05109 :	+0·0125 :	21·0	−0·04957 :	+0·0118

References.

(1) J. R. Airey, "Tables of Bessel Functions of the Second Kind, Zero and Unit Order, $G_0(x)$, $G_1(x)$," Report of the Math. Tables Comm., British Association, 1913.
—— "Tables of $G_n(x)$," Report, 1914.
(2) P. R. Ansell and R. A. Fisher, "Note on the Numerical Evaluation of a Bessel Function Derivative," Proc. Lond. Math. Soc. vol. xxiv. (1926).
(3) P. Schafheitlin, "Beziehungen zwischen dem Integral-logarithmus und den Besselschen funktionen," *Sitz. Berl. Math. Gesell.* viii. Jahrgang (1909).
(4) J. R. Airey, "Tables of $J_{\frac{1}{3}}(x)$ and $J_{-\frac{1}{3}}(x)$: also Bessel Functions of Half-odd Integral Order, $J_{n+\frac{1}{2}}$, n positive and negative," Report of the Math. Tables Comm., British Association (1925).
——, "Tables of the Exponential, Sine, and Cosine Integrals," Report, 1927, and British Association Math. Tables, vol. i.
(5) J. R. Airey, "Tables of the Bessel Function Derivative $\frac{\partial}{\partial \nu}.J_\nu(x)$; $\nu = \pm\frac{1}{2}$, $\pm\frac{3}{2}$," Report of the Math. Tables Comm., British Association (1928).

XIX. *Devices for ensuring Constancy in the Masses of Precision Weights.* *By* J. J. Manley, *M.A., D.Sc. Oxon.* (*Fellow of Magdalen College, Oxford*) *.

[Plate VIII.]

Introductory.

ATTENTION was, in a former paper †, directed to certain imperfections in the plans usually adopted for storing precision weights. It was shown that weights kept in velvet-lined boxes are sometimes so affected that the acquired films are quite abnormal and also corrosive.

Investigation proved that the exceptional density of these films and their corroding powers were chiefly due to the acid character of the glue used for securing the velvet linings. It was also found that occasionally the black velvet so commonly used is itself directly harmful—this apparently from the want of a complete cleansing following the process of dyeing. Hence the conclusion that the use of dyed velvet should be abandoned. It was also apparent that in constructing boxes intended

* Communicated by the Author.
† Phil. Mag. (7) xvi. pp. 489–504 (Suppl. Aug. 1933).

for the reception of weights some adhesive possessing chemically inert properties should be substituted for the injurious glue. Facts and inferences such as these led to an extension of the research, with the result that we are now able to show that by adopting certain plans the desired constancy in the mass of a precision weight can be maintained. This conclusion was reached by means of the following experiments.

Experiment I.

For one of the experiments described in my former paper use was made of a box of African blackwood having a single cell. The walls of the cell, made for the reception of a 200 grm. weight of gilt brass, were finely tooled and left entirely bare. When the weight had been stored in the closed cell for 13 weeks the film was measured, and found to be $=\cdot 0001_3$ mg. per 1 sq. cm. From this it was concluded that in African blackwood we have for the construction of boxes for precision weights a substance almost ideally perfect. Owing, however, to the bareness of the walls of the cell and the hardness of the wood it was evident that, notwithstanding the smoothness of the walls, frequent withdrawals and replacements would, owing to friction, entail minute but appreciable variations in the mass of the weight. It may be added that certain other experiments had shown that for glass and also for metal cells, the same being either entirely bare or lined with carefully cleansed white woollen felt, the results obtained were comparable to that given above. Seeing, however, that in general the employment either of metal or of glass is impracticable we here confine ourselves to a description of the tests made with the aid of blackwood and boxwood cells. The procedure was therefore as follows.

To begin with, a rectangular strip of rolled electrolytic copper 0·15 mm. thick was prepared and a hole pricked near each extremity of one of the diagonals. The length of the strip was equal to the circumference of the weight to be used and its width the same as the depth of the cell. Secondly, the surfaces and edges were smoothed, polished, and cleaned; then the strip was curved so as to form a slotted cylinder. Thirdly, a thread of pure white silk was drawn through one of the holes, then

knotted and continuously and firmly coiled upon the cylinder after the manner shown in fig. 1. When the metal was almost entirely covered the thread was passed through the second hole *h* and secured. Fourthly, the silk-covered copper cylinder was repeatedly washed with highly purified benzene, then drained and stood upon chemically purified filter-paper; subsequently it was warmed, and so completely dried. The lining thus prepared was at once placed within a cell of African blackwood. Finally, the standard 100 grm. weight of chromium-plated brass chosen for the new test was thoroughly wiped with warm silk, lightly brushed with

Fig. 1.

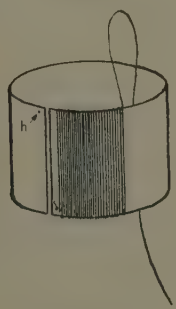

camel's hair, and then transferred to the cell, which was at once closed and set aside.

A period of 72 weeks having elapsed the weight, which had kept its lustre and was apparently unaffected, was lifted, again lightly brushed with camel's hair, and then placed upon the balance, and its value, both before and after wiping with dry and warm silk, measured in terms of another standard 100 grm. weight which was of platinized brass. For the comparison use was made of the various devices and refinements mentioned in my former paper. It was thus found that the film acquired during the storage of the weight amounted to $\cdot 0032_4$ mg. The total area of the weight was 32·1 sq. cm. Hence the weight of the film per 1 sq. cm. was $= \dfrac{\cdot 0032_4}{32 \cdot 1} = \cdot 0001_0$ mg.

This same weight when stored for 11 weeks within an

unlined glass cell acquired a film weighing $\cdot 0022_5$ mg., and this was $= \cdot 0000_7$ mg. per 1 sq. cm. Making due allowance for the difference in the times allotted in the two experiments for storage it will be seen that these two experimental results are mutually confirmatory. We also infer that the films, which are almost entirely negligible and in all probability practically irreducible, represent in large degree the normal gas-grown skins with which under prevailing conditions all solids are clothed.

Experiment II.

For this experiment use was made of a set of precision weights of polished "nichrome." These were stored

Fig. 2.

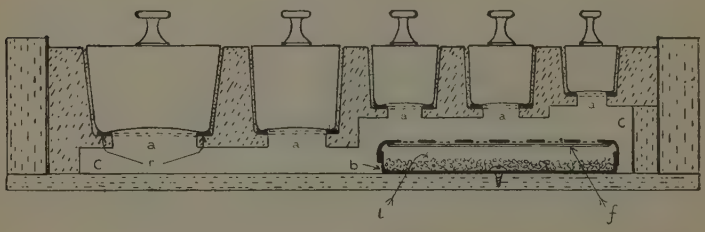

as shown diagrammatically in fig. 2. In the figure the shaded portions represent sections of the case and also of the block in which were cut the cells for the weights; both were of fully seasoned boxwood. The major and more central portions of the floors of the cells were cut away as indicated (a .... a), so as to provide airways to the chamber C, C beneath. Within this chamber, and screwed to its floor, was a shallow tin box, b, containing cocoanut-shell charcoal, l, and having a tightly fitting and freely perforated lid. The inner surface of the lid was covered with a disk of filter-paper, f, the edges of which were attached with shellac. All particles of charcoal were thus retained within the box. Between each weight and the walls of its cell was inserted a silk-covered cylindrical copper envelope, similar in every respect to that already described and used for the 100 grm. weight of the preceding experiment; whilst upon the

perforated floor of each cell was placed a thin flat ring of ivory, *r*, upon which the weight when *in situ* stood. The weights ranged in value from 1 to 100 grm., but our immediate purpose will be served if we confine our attention to the results obtained by experimenting with the largest weight.

For the projected test the weights were prepared in the usual manner (*vide supra*) and then stored in their cells and set aside for 60 weeks.

When measured the film upon the 100 grm. weight was $=\cdot0056$ mg., and this was $=\cdot0001_9$ mg. per 1 sq. cm., a result in agreement with the former value of $\cdot0001_4$ mg. obtained when experimenting with the same weight after it had been stored for 11 weeks within an aluminium cell lined with purified woollen felt. From this it will be seen that by substituting fully aged boxwood for the more costly African blackwood, and by the use of charcoal for the absorption and retention of volatile emanations, our primary object, namely, the discovery of an inexpensive and reliable plan for the storage of precision weights, had now been attained This conclusion was confirmed by the results of a close inspection of the several minor weights of the set. Nothing was revealed to indicate that the condition of these was other than that found for the weight critically and quantitatively examined. Two other experiments, the results of which are informative and important, may now be dealt with.

Experiment III.

The third experiment of the present series was made with a set of plain brass weights of the kind so generally used for quantitative determinations in laboratories devoted to chemistry and physics. For these weights a case similar as to form and equipment to that described and employed for the nichrome weights was constructed. but instead of aged boxwood use was again made of African blackwood. Also, the weights when stored rested not upon ivory rings but upon triangles of polished brass. The weights were prepared as we have already described, and at once introduced into their respective cells ; then the box was closed and set aside for 58 weeks. At the end of that period the film upon the 100 grm. weight was found to be $=\cdot0308$ mg., and this was

$=\cdot 0009_6$ mg. per 1 sq. cm. This result was largely in excess of that expected; also it was for the imposed conditions quite abnormal. On re-wiping the weight with silk an additional total loss $=\cdot 0421$ mg. was noted, and this was $=\cdot 0013$ mg. per 1 sq. cm. Each of these two losses was some five or six times greater than those observed for other brass weights which had been stored under conditions less favourable. We therefore inferred that this particular weight was wanting in hardness, and in consequence was less resistant to the action of rubbing than were those also of plain brass constituting another and independent set. This conclusion was borne out by the fact that in experimenting with the 50 grm. weight of the same set the observed total loss on wiping was also abnormal and $=\cdot 0178$ mg., and this was $=\cdot 0009_4$ mg. per 1 sq. cm. These several exceptional and closely similar losses are of interest, in that they emphasize the necessity for care in the choice of the brass, the hardness of which should be such that any loss producible by gentle rubbing is negligible *. We now describe our fourth and final experiment of this series.

Experiment IV.

The concluding experiment was carried out with a new 100 grm. weight of chromium-plated brass which I had on loan. When idle the weight was stored within a cylindrical case of boxwood having a screw-on lid. The walls of the cell, although bare, were smooth, but the floor was covered with a disk of white woollen felt. The weight, having been duly prepared, was immediately transferred to its newly dusted cell, which was then closed and kept near the balance.

When, after a period of 56 weeks, the weight was inspected its normal brightness was seen to be dimmed by an acquired film. The total mass of this exceptional film was $=\cdot 0175$ mg., and its mass per 1 sq. cm. was $=\cdot 0005_8$ mg. On wiping the weight the film was easily removed and the intrinsic brightness of the chromium surface completely restored. Upon reflexion it was concluded that the observed film was chiefly due to the

* We observe that the objection to the use of a *soft* as distinguished from a *hard* brass entirely disappears when the weights are chromium-plated.

unsuspected presence within the felt disk of volatile matter. Accordingly the disk was removed and repeatedly washed with pure benzene, and this upon evaporation yielded a most distinct oily residue. Hence we infer that oil unavoidably absorbed during the manufacture of the material had not been wholly removed by any final treatment. Possibly no attempt was made to do so. The defect arising from injurious matter originally present in the felt has now probably been successfully met in the following way.

First, with the aid of a lathe, the lower part of the case was removed and a screw-on base in the form of a lid constructed (fig. 3). Secondly, the central portion of the floor of the cell was cut away, and an ample airway thus

Fig. 3.

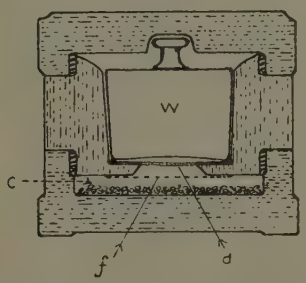

provided to the shallow chamber beneath. Thirdly, a disk of filter-paper, *f*, was placed over the lower opening of the airway, and there secured by means of shellac. Fourthly, cocoanut-shell charcoal, C (previously strongly heated and then cooled), was introduced into the chamber, and the lid-like base, thus charged, screwed on. Finally, the disk of felt, *d*, which had been washed with benzene, was replaced, and, the elaborated case thus made entirely ready for the weight, W ; and this was re-wiped with warm silk and then placed *in situ*.

The plan just described has been but recently completed, and so at the present moment it is impossible to give *direct* proof as to its efficacy. But from the evidence derived from Experiments I. and II. we may confidently conclude that under the newly imposed conditions the weight will now remain quite unimpaired.

Summary.

The object of this research was, as we have already stated, the discovery of a plan for storing precision weights in such a way as to ensure constancy of mass.

From the results yielded by Experiments I. and II., and for which the storage periods were respectively 72 and 60 weeks, it appears that two reliable methods have now been found. Of these that which largely depends upon the absorptive power of charcoal is, in our opinion, to be preferred ; this although the density of the normal film of Experiment I. was slightly less than that of Experiment II. Our preference for the second method is based upon the fact that, given a different specimen of blackwood, even though it be fully aged, the volatile emanations might be exceptionally effective, and thus produce films denser than that resulting from Experiment I. In the presence of highly absorptive charcoal, such as that producible from the shell of the cocoanut, the influence of volatile matter is continuously and apparently completely suppressed ; further, the activity of the charcoal can be by periodic heating indefinitely prolonged.

Concluding Remarks.

Metrologists may be interested to know that the nichrome weights of Experiment II. are now, when idle, stored within the cylindrical case N of aged boxwood shown in fig. 4 (Pl. VIII.). Each and all of the cells for the weights, including those for the fractions in platinum, have airways communicating with a chamber beneath and common to all. The cells are fitted with silk-covered copper cylinders which are identical with that of Experiment I., and upon the floor of each cell is placed an ivory ring as seen in the illustration (Pl. VIII.). The platinum fractional weights rest upon the smooth and bare wood. Por covering these minor weights use is made of a plate F of lacquered aluminium. The base, which carries the perforated tin box M charged with charcoal, is, when in its normal position, securely held by a screw R, which engages a nut situated centrally in M. The lid O of the case is of aluminium 2 mm. thick and lacquered within. Originally it was the bottom of a saucepan. Anyone

skilled in the use of a lathe designed for ornamental work will experience but little difficulty in producing a replica of this highly efficient case.

The Gables,
Littledown Avenue,
Bournemouth.

XX. *The Average and Local Rates of Heat Transfer from the Surface of a Hot Cylinder in a Transverse Stream of Fluid. By* JAMES SMALL, *B.Sc., Ph.D., Carnegie Teaching Fellow, The James Watt Laboratories, The University of Glasgow* *.

IN connexion with some observations on the variation in the local rate of heat transfer from the surface of a cylinder in a cross-stream of fluid, as we pass from

Fig. 1.

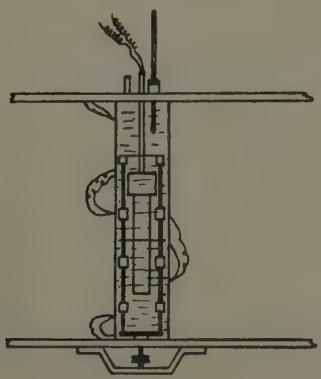

the front of the cylinder to the back, it was first necessary to measure the average rate. The brass cylinder $4\frac{1}{2}$ inches diameter, placed vertically across the 2 ft. square section wind-channel (fig. 1), was filled with a solution of glycerine in water. Fitted within it was a motor-driven stirrer, surrounding an electric immersion heater. The

* Communicated by the Author.

thermal capacity of the apparatus was carefully estimated. By means of copper-constantan thermo-couples set into the surface at various points the temperature of the cylinder was recorded. The thermo-couple leads were taken through the side of the channel to the cold junction and connected to the millivoltmeter through double pole switches, so that each couple was isolated when being read.

A thermometer, introduced from the top, recorded the temperature within the cylinder.

The air-speeds in the wind-channel were measured by means of a carefully calibrated orifice in a plate built into the side of the channel. The secondary indicator used was a special tilting gauge designed by the writer *.

The stirrer was started up, the air-speed adjusted to a steady value, and the heater switched on. The current was arranged so that the temperature of the liquid approached 100° C. When equilibrium was sufficiently established, readings of current, voltage, and temperatures were made at five-minute intervals. In this way it was possible to apply accurately a correction for the heating or cooling of the mass of the apparatus.

A correction was applied for loss of heat from the ends (these being in contact with the top and bottom of the channel) and an allowance made for loss by radiation. It was assumed that the emissibility was 0·06, a figure given by E. Schmidt for polished but slightly tarnished brass †.

A summary of the observations and results is given in Table I., and the values are plotted in figs. 2 and 3. They fit the equation $\frac{Hd}{K\theta} = 2{\cdot}96\left(\frac{Vcd}{K}\right)^{0{\cdot}626}$.

These results show rates of heat transmission considerably higher than those of most other observers. In fig. 4 they are plotted alongside the curve of correlated values given by Fishenden and Saunders. The values obtained are in line with those of Hughes for short cylinders ‡, but the manner in which the cylinder is mounted in the present case does not bring it within the category implied by the term "short cylinder."

* Aero. Res. Comm., R. and M., no. 1430.

† See 'Calculation of Heat Transmission,' Fishenden and Saunders, p. 19.

‡ Phil. Mag. xxxi. p. 118 (1916).

TABLE I.—Water equivalent of tube, glycerine solution, and fittings = 11·11 lb.
Total area of cylindrical surface = 2·445 ft.².

Mean value of $K = 1{\cdot}48 \times 10^{-2} \frac{\text{C.H.U.}}{\text{ft.} \times \text{hr.} \times {}^\circ\text{C.}}$. Mean value of $\frac{c}{K} = 1{\cdot}1 \frac{\text{hr.}}{\text{ft.}^2}$.

Room temp. °C.	Air-speed. ft./sec.	Temp. in glycerine solution. °C.	Rate of heating or cooling. °C./min.	Average temp. of brass tube. °C.	Temp. elevation of surface. θ °C.	Input to heater. amps.	Input to heater. volts.	Input to heater. C.H.U./min.	Correction due to temp. change. C.H.U./min.	Radiation loss. C.H.U./min.	Loss through ends. C.H.U./min.	Fully corrected heat flow. C.H.U./min.	Heat flow per ft.² per min. C.H.U.	H. C.H.U./ft.² × hr. × °C.	$\frac{Hd}{K\theta}$ or $\frac{hd}{K}$	$\frac{Ved}{K}$
19·8	5·0	98·1	+0·08	91·5	71·7	2·41	155·3	11·84	−0·88	0·253	0·486	10·22	4·18	3·498	88·64	7416
18·6	5·1	98·6	−0·02	92·0	73·4	2·32	149·8	11·0	0·22	0·255	0·498	10·47	4·28	3·498	88·64	7564
19·7	10·1	99·6	+0·015	91·5	71·8	2·877	186·5	16·99	−0·17	0·253	0·487	16·08	6·57	5·496	139·27	14980
21·5	14·9	98·2	+0·04	87·9	66·4	3·132	203·0	20·10	−0·44	0·236	0·450	18·97	7·75	6·996	177·28	22100
21·8	20·1	98·3	−0·01	89·4	67·6	3·373	219·3	23·40	0·11	0·242	0·459	22·81	9·34	8·286	209·97	29812
19·4	25·15	99·5	0	89·5	70·1	3·724	239·5	28·20	0	0·243	0·475	27·48	11·23	9·612	243·57	37302
20	29·9	98·8	−0·02	88·6	68·6	3·828	246·9	29·95	0·22	0·288	0·465	29·42	12·04	10·530	266·83	44348
20·9	34·9	93·8	−0·01	83·5	62·6	3·852	249·0	30·35	0·11	0·216	0·425	29·82	12·20	11·694	296·33	51764
20·9	40·0	86·2	+0·01	77·3	56·4	3·852	249·3	30·40	−0·11	0·189	0·382	29·72	12·15	12·930	327·65	59328

The present observations are in striking agreement, however, with the results recently published by Dr. Ezer Griffiths and Mr. Awbery in a paper read recently before the Institution of Mechanical Engineers (Proc. Inst. Mech. Eng. vol. cxxv. p. 319 (1933)).

Variation in the Local Rate of Heat Transfer from the Surface.

Measurements of the rate of heat flow at different points round a cylinder have been made notably by

Fig. 2.

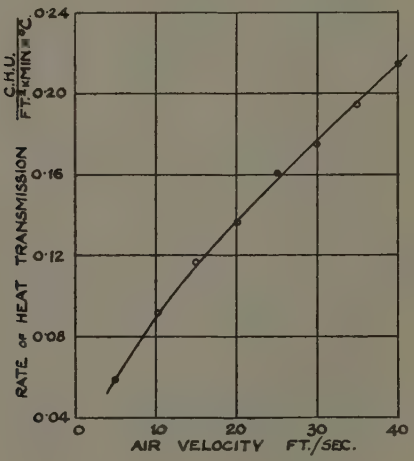

Lohrisch * with his chemical absorption method (making use of the analogy between gaseous diffusion and heat-flow) and by the Americans Paltz and Starr whose results, published by Drew and Ryan †, were obtained by noting the condensation from each of several internal divisions in a pipe supplied with steam.

The results of these workers agree in their general characteristics. They show maximum values of heat transfer at the front and back of the cylinder, and

* *Mitt. Forschungsarbeiten*, p. 322 (1929).
† Amer. Inst. Chem. Engrs. (June 1931).

minimum values on the sides (*i. e.*, in the region of 90° from the front) of the cylinder.

Results have just been published by V. Klein *, who uses a somewhat strange method, but obtains results comparable with those of the above-mentioned workers. He exposes a cylinder of ice to a current of hot air,

Fig. 3.

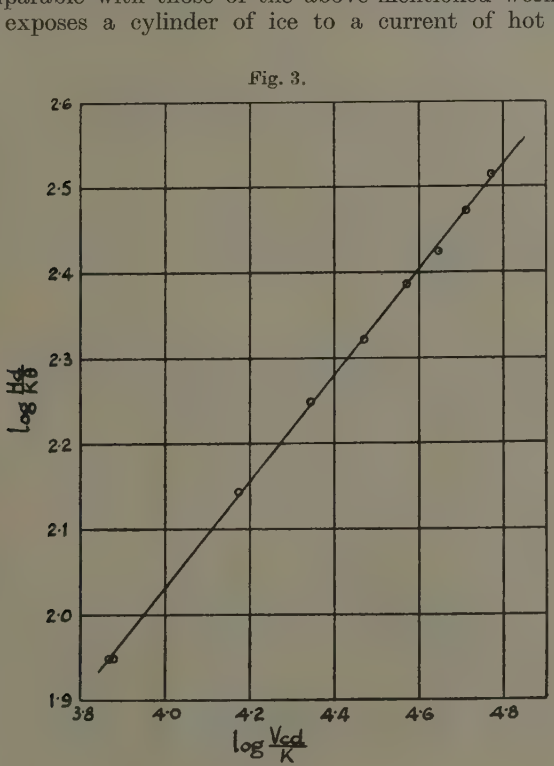

removes it, encases it in plasticine and from the plasticine mould makes a plaster cast from which he examines the amount of the erosion from the ice. This may be open to the criticism that the aerodynamic conditions are affected as the ice alters from its cylindrical shape.

The writer described in 'Engineering' † some time ago observations made with a thermopile indicator

* *Archiv für Wärmewirtschaft* (June 1934).
† 'Engineering' (Nov. 1931).

built into the surface of a cylinder, inside of which, and close to the thermopile, was fitted a small electric heater. These observations were of a rather qualitative nature and were characteristic of the local heating of the surface.

A thoroughly quantitative set of results, also with

Fig. 4.

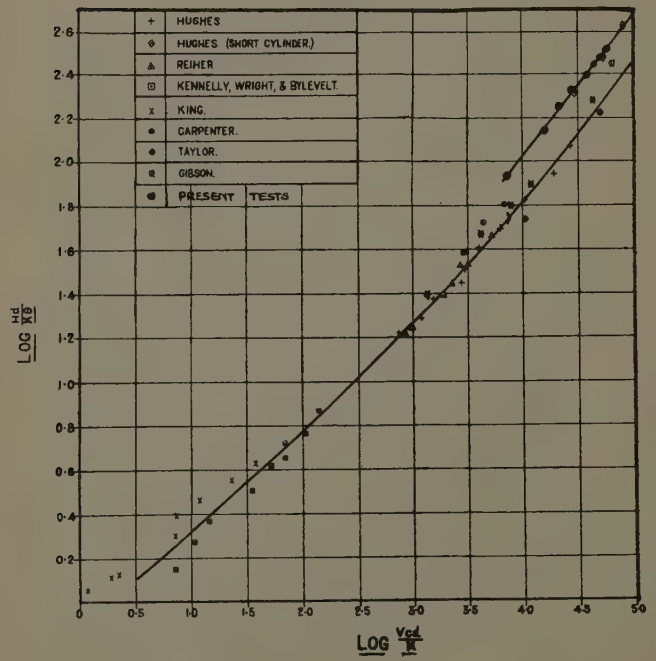

local heating of the surface, was obtained by Fage and Falkner * in the course of an investigation into the relationship between the heat transmission rate and the surface friction. Both these sets of observations with local heating show a minimum rate of heat flow at the front of the cylinder, a maximum in the region of 50 degrees of angle from the front, and, for the rest of the

* Aero. Res. Comm., R. and M., no. 1408.

surface, another minimum near 90 degrees of angle from the front and a maximum value at the back.

With a view to testing thoroughly the characteristics of the distribution of the heat transmission rate round a uniformly heated cylinder, the writer reverted to the method of the surface thermopile. It is shown diagrammatically in fig. 5. A number of thermo-couples of copper-constantan elements are connected in series and aligned along a generator of the cylinder. The outer junctions are finished flush with the surface. The insulating materials used are bakelite and dental cement. The latter has good dielectric properties when it sets and dries. Steam is introduced to the inside of the cylinder, which is so mounted in the wind-channel that it can be rotated to cause the line of thermo-couples to occupy any angular

Fig. 5.

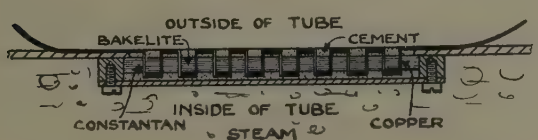

DIAGRAMMATIC SECTION OF THERMOPILE.

position relative to the air-stream. A millivoltmeter connected to the thermopile is read at each position.

It is reasonable to assume that the heat flux through the thermopile is practically symmetrical about a radius of the cylinder and that the drop in temperature between the inner and outer junctions, while not equal to the actual temperature drop in the wall of the tube at the corresponding position, bears a one to one relationship with it, and therefore with the rate of heat flow. The temperature difference between the inner and outer functions is less than 1° F.

The observations on the millivoltmeter are plotted on a base of angle, for each of a number of air-speeds. By integrating the areas under the resulting curves and dividing by the length of the base, the mean millivoltmeter reading at each air-speed is obtained. The logarithms of these readings are plotted on a base of log V and a fair curve drawn through the points. Now, choosing a point

on the curve, a value for V or of $\frac{Vcd}{K}$ is obtainable for a certain millivoltmeter reading. By using the curve in fig. 3, or any similar curve, the corresponding value of $\frac{Hd}{K\theta}$ or $\frac{hd}{K}$ is found. Thus the millivoltmeter scale is converted to a scale of $\frac{Hd}{K\theta}$ or $\frac{hd}{K}$.

Fig. 6.

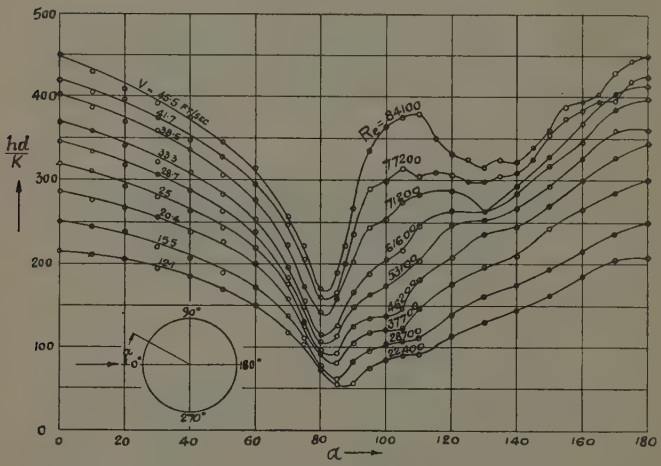

The observations are plotted in this form in fig. 6, for which the curve of fig. 3 has been used to fix the scale.

Since the mean ordinates of the curves represent the average rate of heat flow from the cylinder, the scale having been fixed as above, a test of the validity of the thermopile method consists in plotting the rates obtained from the curves on the same axis as those in fig. 3 obtained directly. The result is shown in fig. 7. The indirectly obtained rates conform closely to the law governing the directly obtained rates.

The curves of the rates of heat transfer round a cylinder obtained from the different sources are plotted together in fig. 8, corresponding to a Reynolds number of 39,600.

Curve A is that obtained by means of the thermopile when the scale of $\frac{Hd}{K\theta}$ is fixed by reference to the directly obtained values plotted in fig. 3. Curve B is a plot of the same readings when the scale of $\frac{Hd}{K\theta}$ is fixed by

Fig. 7.

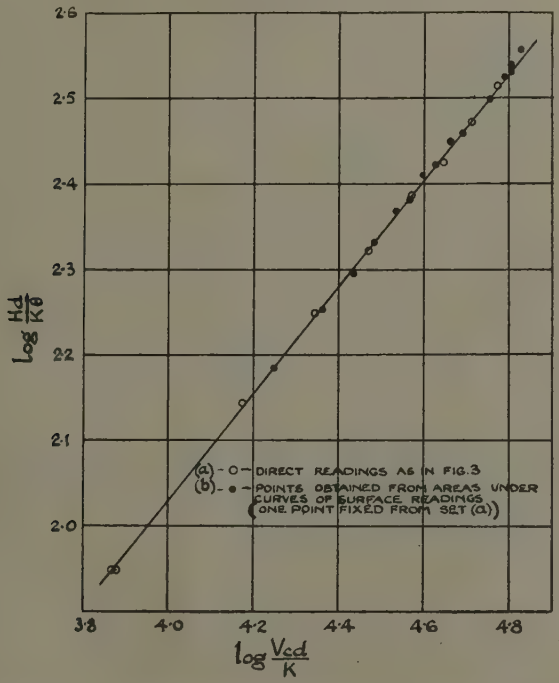

reference to the curve of correlated values given by Fishenden and Saunders.

The close agreement of Curve B in its general characteristics with those of the other observers further supports the validity of the method.

It is suggested that an indicator of the type described above could with advantage be used in the course of investigations into the best spacing in banks of tubes,

such as are to be found in multitubular heaters and coolers.

Fig. 8.

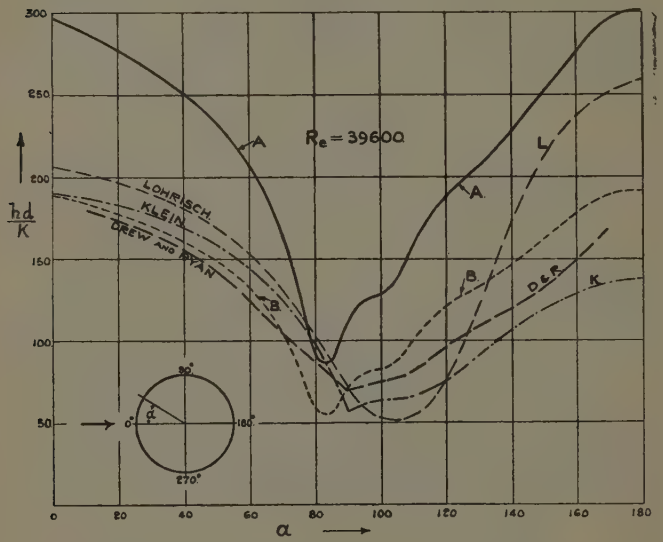

The writer wishes to acknowledge the facilities extended to him by Professors Goudie and Cormack in connexion with the above work.

XXI. *Kinks on Impact Diagrams of Struck Strings.* *By* R. N. Ghosh, *D.Sc.*, *A.Inst.P.*, *and* Haji Ghulam Mohammad, *M.Sc.**

[Plate IX.]

§ 1. Introduction.

ORDINARILY the time-displacement curve of any point of the string during the time the hammer is in contact with the string, *i. e.*, the impact curve, is a

* Communicated by the Authors.

smooth damped harmonic curve; but under certain circumstances small or big kinks of discontinuous nature are found superposed upon the damped harmonic curve. The present note is meant to indicate that Kaufmann's theory when slightly extended is sufficient to explain the kinks[1] in the impact diagrams[2] (1) of any point on the shorter portion of the string between the striking point and the nearer end, (2) their absence at the striking point, or (3) on the longer portion of the string. When the length of the smaller portion is increased to such an extent that the impact wave reflected from the farther end on the longer side reaches the striking point, large kinks begin to appear on this side also, and upon them are found superimposed smaller kinks that filter through the striking point from the smaller portion of the string. The period of vibration of the kinks of each kind is the same as the free vibration period[3] of that portion of the string. In the present note such cases have been studied when one portion of the string on one side of the striking point is small and the other portion is large. Gradually the former is increased and the latter decreased. The phenomenon that takes place is described in section 2, while in section 3 a theoretical explanation has been put forward based on Kaufmann's assumption. The agreement between the curves obtained by photographic methods and those drawn from the formulæ developed in section 3 is remarkable. We shall briefly describe the experimental arrangements and results in section 2, and develop our formulæ in section 3, and in section 4 we shall compare the experimental results with theory.

§ 2. Experiments.

Photography of Time-displacement Diagrams during Impact.

A simple method for obtaining the time-displacement diagrams is to use photographic method, as was done by Kaufmann. For this purpose a vertical steel wire was kept stretched between two bridges, and was struck at various points by a felt hammer. A slit in a wooden plank allowed the shadow of a point on the string to be observed when the point was strongly illuminated by arc light. The velocity of impact of the felt hammer was

kept constant by an arrangement described in Phil. Mag. vol. vii. p. 346 (1929). By adjusting the position of the slit any desired point of the struck string could be photographed during the time the hammer is in contact with the string ; in this arrangement it was possible to obtain the shadowgraph of any point by means of a vertically falling photographic plate.

Shadowgraphs were obtained of points lying on both sides of the point struck by the hammer as well as the striking point itself. It was, however, found that when the duration of contact is nearly the same as the free vibration period of the whole string this arrangement was not suitable, and a horizontal arrangement was made. A steel wire 140 cm. long was kept stretched over two bridges, and it was struck by an elastic hammer dropped down from a given height upon the string by an electromagnetic arrangement. The shadowgraph was taken by a horizontally sliding photographic plate released by another electromagnet actuated by the same current as the former one, so that when the current was switched off both fell simultaneously. In this arrangement, however, the shadowgraph of the point struck by the hammer could not be obtained. Putting on electrically maintained tuning-fork near the point to be photographed, *i. e.*, near the slit, a time record was also obtained from which the duration of contact of the hammer with the string, and also the number of kinks per second, could be determined.

A large number of curves showing the displacement of the point struck during impact was obtained by Kaufmann for different values of the distance of the striking point from the nearer end (α), and for different points on the string. Kaufmann obtained one impact curve in which a large number of kinks were superimposed upon the main curve. We have also included a large number of cases as described below.

Figs. 1, 2, and 3 (Pl. IX.) show the impact diagrams for a string 100 cm. in length struck at a given distance α from the nearer end for points of observation β measured from the same end, (1) less than α, (2) equal to α, and (3) greater than α respectively. It will be observed that in case (1) a large number of kinks are superposed over the main impact curve, while in (2) and (3) they are not present. It has already been pointed out that the period

of vibration of the kinks is equal to $\tau = \frac{2\alpha}{c}$ (4). These discontinuous changes of velocity are confined to the smaller portion of the string, and no traces of such phenomena are observed on the striking point or on the other side. This is the case so long as no reflected wave from the farther end reaches the striking point. And in the case when the wave reflected from the farther end reaches the striking point, *i. e.*, when the duration of impact is large, kinks begin to appear and modify the impact diagram in a manner which depends upon the total duration of impact. Three such special cases are shown in figs. 4, 5, and 6 (Pl. IX.). The legend for each is noted below.

TABLE I.

Number of Kinks per Second.

Fig. (Pl. IX.)	ϕ.	α.	M.	N (obs.).	N (cal.).
7.....	$1{\cdot}5\times10^{-2}$	43	5	270	274
8.....	$1{\cdot}8\times10^{-2}$	43	10	276	274
9.....	$2{\cdot}6\times10^{-2}$	43	20·5	264	274
10.....	$2{\cdot}4\times10^{-2}$	72	20·5	156	163
11.....	$1{\cdot}6\times10^{-2}$	96	20·5	125	122

Period of vibration of the whole string =·0108 sec., length=140 cm., mass=2·603 grm.

For fig. 4 (Pl. IX.) $\alpha=16$ cm., $\beta=63$ cm., $\frac{T}{\phi}=1{\cdot}27$, M=7·0 grm., and K=69·65.

For fig. 5 (Pl. IX.) $\alpha=30{\cdot}7$ cm., $\beta=106$ cm., $\frac{T}{\phi}=0{\cdot}70$, M=13·5 grm., and K=37.

For fig. 6 (Pl. IX.) $\alpha=30{\cdot}7$ cm., $\beta=69$ cm. $\frac{T}{\phi}=0{\cdot}83$, M=7·0 grm., and K=37.

Figs 7, 8, 9, 10, and 11 (Pl. IX.) show the kinks in the case of the same string when the velocity of impact was 104 cm.; the values of other constants are given in Table I.

It will be observed from the last two columns of Table I. that the number of kinks per second is equal to the number of free vibration of that portion. Further, on careful examination of the figures 1, 10, and 11 it will be found that upon the larger kinks are superposed smaller ones; an explanation of these results will be given in section 4.

§ 3. Theory.

Now let us examine how far Kaufmann's theory, as extended for elastic hammers, can account for the above results. Kaufmann assumes that the shorter portion of the string between the hammer and the nearer end remains straight. This, of course, is not rigorously true from the beginning of the impact; after a few periods $\tau = \frac{2\alpha}{c}$, Kaufmann's assumption will be practically true[5] for small values of α, when

$$\frac{\tan K\alpha}{K\alpha} \doteq 1, \quad K = \frac{2\pi}{\lambda}.$$

Experiments show that up to $\alpha/l = \frac{1}{6}$, Kaufmann's assumption holds good, while the results from the above assumption are quite simple and can be put to practical use readily. In the case of the elastic hammers we divide the total duration of impact into two parts[6], viz.:—(1) *the time during which the hammer is in contact with the string without imparting any displacement to the latter*, and (2) *the interval during which the string is displaced from the equilibrium position, and disturbances travel on both sides of the string.* This mode of dividing the total duration of impact into two parts is in agreement with our own experimental results. Recently Messrs. Ghosh and Kar[7] have also done the same thing in the case of very soft hammers and low velocity of impact. Let us call the first part the Helmholtz regime, while the second one will be called the Kaufmann regime.

Helmholtz Regime.

In this interval the compressional force is entirely due to the compression of the hammer felt, and therefore the equation of motion of the hammer is given by

$$M\frac{d^2\xi}{dt^2}=-p \quad . \quad . \quad . \quad . \quad . \quad . \quad (1)$$

and $$\xi=1-e^{-p/\mu}, \quad . \quad . \quad . \quad . \quad . \quad . \quad (2)$$

where ξ=compression of the felt,

μ=elastic strength of the same,

and M=effective mass of the hammer.

For very small compression (2) reduces to

$$p=\mu\xi, \quad . \quad . \quad (3) \text{ (Hooke's law)},$$

while for large values of ξ higher powers may be retained, and the solution obtained (see appendix, (1)). Making use of (1) and (3) we obtain

$$\xi=\frac{V_0}{n}\sin nt, \quad . \quad . \quad . \quad . \quad . \quad (4)$$

where $n^2=\frac{\mu}{M}$ and V_0 is the initial velocity of impact of the hammer. Equation (4) is known as Helmholtz law of pressure. The state of affairs represented by (4) continues, till at a certain time, t_1, a wave

$$y_2=f_1(ct'-x+a) \quad . \quad . \quad . \quad . \quad . \quad . \quad (5)$$

starts on the longer side of the string, while on the shorter portion a distribution of velocity given by

$$\dot{y}=\dot{y}_0\frac{x}{a} \quad . \quad . \quad . \quad . \quad . \quad . \quad . \quad (6)$$

takes place *without any displacement over that portion*, where $\dot{y}_0$ is the velocity of the striking point at time t_1 and α has the same meaning as before, and x is the abscissa of any point on the string measured from the nearer end as origin. The time t_1 marks the end of Helmholtz regime and the beginning of Kaufmann regime. And this happens when the compressional force between the hammer and the string reaches a definite value such that this equals the transverse component of tensions due to displacements on both sides of the striking point. The transverse component of tensions is given by

$$T_0\left\{\left(\frac{dy}{dx}\right)_1-\left(\frac{dy}{dx}\right)_2\right\}; \quad . \quad . \quad . \quad . \quad (7)$$

T_0=tension of the string.

Hence by (3), (4), and (7) we find the compressional force p to be given by

$$p=\frac{\mu V_0}{n}\sin nt_1=\frac{T_0}{c}\dot{y}_0;$$

since $$\dot{y}_0=\dot{\xi} \quad \text{at} \quad t=t_1,$$

we get $$\tan nt_1=\left(\frac{T}{\mu}\cdot\frac{\rho}{M}\right)^{\frac{1}{2}}; \quad . \quad . \quad . \quad . \quad . \quad (8)$$

thus the time t_1 is determinate. *Further, a distribution of velocity represented by* (6) *has been shown by Sir C. V. Raman*[8] *to be equivalent to two discontinuous velocity waves travelling backwards and forwards along the string and giving rise to free vibrations similar to those of the bowed string, which can be written down as*

$$y=\Sigma P_r \sin\frac{r\pi x}{\alpha}\cdot\sin\frac{r\pi ct'}{\alpha}, \quad . \quad . \quad . \quad . \quad (9)$$

where r is any integer, c is the transverse wave velocity in the string, and t' is the time measured from the instant t_1. The velocity of any point on the string is

$$\dot{y}=\Sigma P_r\frac{r\pi c}{\alpha}\cdot\sin\frac{r\pi x}{\alpha}, \quad \text{at } t'=0,$$

and $\dot{y}$ is given by (6);

hence $$P_r=-\frac{2V_1(-1)^r}{c\pi^2}\cdot\frac{1}{r^2}, \quad . \quad . \quad . \quad . \quad (10)$$

where

$$V_1=V_0\cos nt_1=V_0\Big/\left(1+\frac{T}{\mu}\frac{\rho}{M}\right)^{\frac{1}{2}}.$$

Kaufmann Regime.

During this interval the total displacement of the hammer is given by

$$\xi=y_0+\xi \quad . \quad . \quad . \quad . \quad . \quad . \quad . \quad (11)$$

and $$y_1=\frac{y_0 x}{\alpha} \quad . \quad . \quad . \quad . \quad . \quad . \quad (12)$$

over the smaller segment of the string, while the wave represented by (5) travels forward in the positive direction of x-axis. This equation of motion of the hammer is now

$$M\frac{d^2\xi}{dt^2}=-p. \quad . \quad . \quad . \quad . \quad . \quad . \quad (13)$$

Substituting the values of y_1 and y_2 in (7), and making use of (3), we obtain the equation of motion of the striking [9] point:

$$\frac{MT_0}{\mu c}\ddot{y}_0+M\left(1+\frac{T_0}{\mu\alpha}\right)\ddot{y}+\frac{T_0}{c}\dot{y}_0+\frac{T_0}{\alpha}y=$$

$$\Sigma T_0 P_r \frac{\gamma\pi}{\alpha}(-1)^r \sin\frac{r\pi ct'}{\alpha}\left\{\frac{r^2\pi^2 T_0 M}{a.\mu\rho a}-1\right\}. \quad (14)$$

Neglecting the small term in $\ddot{y}$ we get the solution

$$y_0=\frac{V_1}{q}e^{-\frac{k}{2}t'}\sin qt'-\frac{2a^2V_1\rho}{c\pi^2M}\Sigma\frac{1}{r^3}\sin\frac{r\pi ct'}{a}, \quad . \quad . \quad (15)$$

and the compressional force [10] at any time t' is given by

$$p=V_1\rho c\left[e^{-\frac{k}{2}t'}\sin qt'\left(\frac{c}{a}-\frac{k}{2}\right)+e^{-\frac{k}{2}t'}\cos qt'\right.$$

$$\left.+\frac{2}{\pi}\left(1-\frac{T_0}{\mu\alpha}\right)\Sigma\frac{1}{r}\sin\frac{r\pi ct'}{\alpha}\right], \quad . \quad . \quad (16)$$

and the displacement over the smaller portion of the string is given by

$$y_x=y_0\frac{x}{a}+\Sigma P_r\sin\frac{r\pi ct'}{\alpha}.\sin\frac{r\pi x}{\alpha}. \quad . \quad . \quad . \quad (17)$$

The second term produces the discontinuities which are found to be superposed over the displacement y_0 produced by the hammer during Kaufmann regime.

To determine the time-displacement curve during impact when the duration of contact is large we have to consider (1) the incident wave $y_2=f_1(ct'+\alpha-x)$, (2) the reflected wave from the farther end, and (3) the reflexion from the impinging hammer. Now

$$y_2=\frac{V_1}{q}e^{-\frac{k}{2c}(ct'-x+\alpha)}\sin\frac{q}{c}(ct'-x+\alpha). \quad . \quad . \quad (18)$$

This wave is reflected from the farther end as

$$y_r=-\frac{V_1}{q}fe^{-\frac{k}{2c}(ct'+x-\alpha-2b)}\sin\frac{q}{c}(ct'+x-\alpha-2b), \quad (19)$$

where b is the distance of the striking point from the

farther end and f the coefficient of reflexion from that end. When this wave arrives at the striking point at $t'=\frac{2b}{c}$ it gives rise to a new wave $f_2(ct'-x+\alpha)$ towards the positive direction of x-axis, and produces a new displacement

$$y_1=f_3(ct')_{\alpha}^{x}$$

over the shorter segment of the string. At $x=\alpha$ the displacements on both sides of the striking point should be continuous; hence

$$f_3(ct')=f_2(ct')-f_1(ct'-2b)$$

and

$$y_0=f_1(ct')+f_2(ct')-f_1(ct'-2b)$$

for $t'>\frac{2b}{c}$. The compressional force p is now

$$p=T_0\left\{\frac{f_1(ct')}{\alpha}+\frac{f_2(ct')}{\alpha}-\frac{f_1(ct'-2b)}{\alpha}+\frac{\dot{f}_1(ct')}{c}+\frac{\dot{f}_2(ct')}{c}+\frac{\dot{f}_1(ct'-2b)}{c}\right\}.$$

Remembering that

$$f_1(ct'-2b)=-\frac{V_1 f}{q}e^{-\frac{k}{2}(t'-\tau)}\sin q(t'-\tau),$$

where $\tau=\frac{2b}{c}$ and $\dot{f}_1(ct'-2b)$ is equal to

$$\dot{f}_1(ct'-2b)=-V_1 R f e^{-\frac{k}{2}(t'-\tau)}\cos\{q(t'-\tau)+\phi\}, \quad . \quad (20)$$

where $\tan\phi=\frac{k}{2q}$ and $R^2=1+k^2/4q^2$.

Substituting the value of the compressional force, f_1, f_2, etc. in (14), we find the particular value of $f_2(ct)$, viz. :

$$f_2(ct')=-\frac{fKV_1Re^{-\frac{k}{2}(t'-\tau)}}{q}.t'\sin\{q(t'-\tau)+\phi\},$$

and the complete value of $f_2(ct')$ is

$$f_2(ct')=Ae^{-\frac{k}{2}(t'-\tau)}\sin q(t'-\tau)+Be^{-\frac{k}{2}(t'-\tau)}\cos q(t'-\tau)-\frac{KV_1Rft'}{q}e^{-\frac{k}{2}(t'-\tau)}\sin\{q(t'-\tau)+\phi\}. \quad . \quad (21)$$

At $t'=\tau$ the velocity and displacement should both be the same as calculated from the formulæ which hold good before the arrival of the reflected wave. Hence at $t'=\frac{2b}{c}=\tau$

$$f_1(ct')+f_2(ct')-f_1(ct'-2b)=f_1(ct),$$
$$\dot{f}_1(ct)+\dot{f}(ct')-\dot{f}(ct'-2b)=\dot{f}_1(ct),$$

i. e., $f_2(ct)=f_1(0)$ and $\dot{f}_2(ct)=\dot{f}_1(0)$.

Hence $$B=\frac{k^2V_1f\tau}{2q^2}.$$

Now
$$f_2(ct)=Aqe^{-\frac{k}{2}(t'-\tau)}R\cos\{q(t'-\tau)+\phi\}$$
$$-BRqe^{-\frac{k}{2}(t'-\tau)}\sin\{q(t'-\tau)+\phi\}$$
$$-fkV_1t'R^2e^{-\frac{k}{2}(t'-\tau)}\cos\{q(t'-\tau)+2\phi\}$$
$$-f\frac{kV_1R}{q}e^{-\frac{k}{2}(t'-\tau)}\sin\{q(t'-\tau)+\phi\}.$$

Since $\dot{f}_1(0)=V_1f$, we find

$$fV_1=Aq-\frac{Bk}{2}-\frac{fk^2V_1}{4q^2}-fkV_1\tau R^2\cos^2\phi.$$

Therefore $f_2(ct')$ is given by

$$f_2(ct')=\frac{V_1f}{q}e^{-\frac{k}{2}(t'-\tau)}\Big[\sin q(t'-\tau)\Big\{1+\frac{k^3\tau}{4q^2}+\frac{k^2}{4q^2}+k\tau R^2\cos^2\phi\Big\}$$
$$+\frac{k^2\tau}{2q}\cos q(t'-\tau)-kRt\sin\{q(t'-\tau)+\phi\}\Big],$$

or

$$f_2(ct')=\frac{fV_1e^{-\frac{k}{2}(t'-\tau)}}{q}\Big[\sin q(t'-\tau)\Big\{1-k(t'-\tau)+\frac{k^2}{4q^2}(1+k\tau)\Big\}$$
$$+\cos q(t'-\tau).\frac{k^2}{2q}(\tau-t')\Big]. \quad . \quad . \quad . \quad . \quad . \quad (22)$$

§4. Comparison of Experimental Results with Theory.

The Helmholtz interval for felt hammers is very short in comparison to the total duration of impact ; for instance, in the case of a hammer

$$M=6{\cdot}6 \text{ grm.}, \quad \rho={\cdot}019,$$

$$\frac{T_0}{\mu}={\cdot}2, \quad c=2{\cdot}41\times10^4 \text{ cm./sec.},$$

we find from (8) that

$$t_1={\cdot}83\times10^{-5} \text{ sec.},$$

while the total duration of impact, ϕ, is $1{\cdot}2\times10^{-2}$ sec.

$$\left[\frac{T}{\phi}={\cdot}9,\ T_0=1{\cdot}10\times10^7 \text{ dynes}\right].$$

In Table II. the variation of t_1 with different values of $\frac{T_0}{\mu}$ is shown.

Table II.

Mass of hammer 6 grm.		Mass of hammer 12 grm.	
T_0/μ.	t_1 sec.	T_0/μ.	t_1 sec.
0·2	$\cdot83\times10^{-5}$	0·2	$\cdot83\times10^{-5}$
2·0	$\cdot82\times10^{-4}$	2·0	$\cdot83\times10^{-4}$
20·0	$\cdot90\times10^{-3}$	20·0	$\cdot82\times10^{-3}$
200·0	$\cdot71\times10^{-2}$	200·0	$\cdot77\times10^{-2}$

It is seen from the table that for felt hammers the interval t_1 is very short and *practically independent of the hammer mass for small values of* M. This is true for small values of $\frac{T_0}{\mu}$; for large values of $\frac{T_0}{\mu}$, viz., of the order of 20 or more, the hammer mass does control the interval t_1. Further, for small values of compression, t_1 is independent of the velocity of impact of the hammer which experiments with felt [11] hammers show to be true. For soft and heavy hammers Messrs. Ghosh and Kar have pointed out that the compression is large, and in that case this interval is dependent upon the initial velocity of impact.

When t_1 is an appreciable fraction of the duration of impact, then the total duration of impact, ϕ is $\phi_0 + 2t_1$, since the hammer takes an equal interval at the end of Kaufmann regime before it leaves the string.

The compressional force p starts from a zero value and rises to a value p_1 at $t=t_1$, and then during Kaufmann's regime it follows the graph shown in fig. 12, calculated from (16). It will be observed that the compressional

Fig. 12.

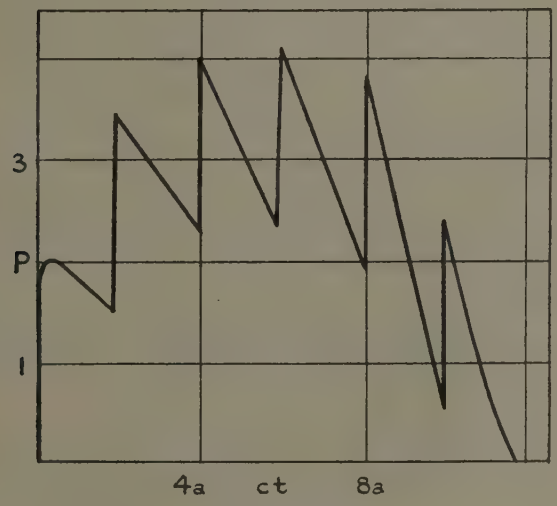

force fluctuates at regular intervals τ, 2τ, 3τ, 4τ, etc. where

$$\tau = \frac{2\alpha}{c} . \quad . \quad . \quad . \quad . \quad . \quad . \quad . \quad (23)$$

Such pressure variations were found experimentally by George [12] with the help of an oscillograph. It will be recalled that it is the initial velocity distribution which really is the cause of the pressure fluctuations.

The kinks referred to in § 2 are really free vibrations superposed over the Kaufmann displacement. Experiments and theory both agree that the free vibration period is equal to τ. Table I. expresses the experimental results. Further, the nature of the kinks is the same as

predicted by theory, viz., of bowed string type (*vide* formula (18)).

Most remarkable is the confirmation of the time-displacement curve during impact, when the total duration of impact is large so that the initial wave after reflexion from the farther end reaches the point of observation. With the aid of the formula (22) the displacement at any time t' at a place x is given by

$$y_2 = \frac{V_1}{q} e^{-\frac{k}{2c}(ct'-x+a)} \sin\frac{q}{c}(ct'-x+\alpha) \text{ (initial wave)}$$

$$-\frac{V_1 f}{q} e^{-\frac{k}{2c}(ct'+x-a-2b)} \sin\frac{q}{c}(ct'+x-\alpha-2b) \text{ (reflected wave)}$$

$$+\frac{V_1 f}{q} e^{-\frac{k}{2c}(ct'-x+a-2b)} \sin\frac{q}{c}(ct'-x+\alpha-2b)\{1-k(t'-\tau)\}$$

$$-\frac{k^2 f V_1}{2q^2} e^{-\frac{k}{2c}(ct-x+a-2b)} (t'-\tau).\cos\frac{q}{c}(ct'-x+\alpha-2b)$$

$$\text{for } t'>2b/c. \quad \ldots\ldots\ldots\ldots\ldots\ldots \quad (24)$$

For the striking point $x=\alpha$ the displacement is given by

$$y_0 = \frac{V_1}{q}\left[e^{-\frac{k}{2}t'} \sin qt' - fe^{-\frac{k}{2}(t'-\tau)} \sin q(t'-\tau)\right.$$

$$+fe^{-\frac{k}{2}(t'-\tau)} \sin q(t'-\tau)\{1-k(t'-\tau)\}$$

$$\left.-\frac{k^2 f}{2q}(t'-\tau)e^{-\frac{k}{2}(t'-\tau)} \cos q(t'-\tau)\right].$$

This is almost the same as found by Das[13], but it should be interpreted in a slightly different manner. Putting the above in the following way, and neglecting $\frac{k^2 f}{2q}$ term, we get

$$y_0 = \frac{V_1}{q}\left[e^{-\frac{k}{2}t'} \sin qt' - \frac{T_0}{Mc}(t'-\tau)e^{-\frac{k}{2}(t'-\tau)} \sin q(t'-\tau)\right];$$

the second term is the displacement due to the striking point not behaving like a nodal point.

Again, $f_3(ct)$, the part which is transmitted across the striking point, is given by the same term. The second term can also be written as

$$-\frac{T_0}{Mc}e^{-\frac{k}{2}(t'-\tau)}\sin q(t'-\tau)\,\Sigma\frac{\tau}{\pi r}\sin\frac{r\pi ct'}{b},$$

where $\tau=\frac{2b}{c}$. And this formula shows clearly that for large values of b there is a small fraction which is transmitted across the striking point, *i. e.*, the hammer, and the displacement amplitude is a function of the free vibrations of the portion of the string.

We have seen that there is no trace of the kinks across the hammer on account of free vibrations on the smaller segment of the string. With regard to these vibrations the hammer behaves like a nodal point, as shown by the formula (17). Neither is there any kink at the striking point. Both these observations agree with (17). Now as α increases very minute kinks begin to appear on the longer side of the string (fig. 11, Pl. IX.) which are superposed on larger kinks due to reflexions from the farther end of the string. Thus for large values of α *some free vibrations are transmitted across the hammer.* In fact the transmitted part is

$$A=\frac{c\rho}{M}(t'-\tau),\quad \text{put } t'=\left(\tau+\frac{\tau}{4}\right);$$

$$\therefore A=\frac{c\rho}{M}\frac{\tau}{4}=\frac{c\rho}{M}\cdot\frac{2b}{c4}=\frac{b\rho}{2M}\cdot\quad\ldots\ldots\quad(25)$$

Let $\rho=\cdot091$, $b=100$, $M=12$ grams, then $A=\cdot38$; while for $M=20$, A reduces to $A=\cdot22$.

Thus the fraction transmitted decreases with the increase of hammer mass.

Again, let us keep M constant, viz., $M=12$ grams, but change b; then

$$A=\cdot2 \quad \text{for} \quad b=50 \text{ cm.}$$

and

$$A=\cdot1 \quad \text{for} \quad b=25 \text{ cm.}$$

From this discussion we come to this conclusion, that the striking point during the time the hammer is in contact with the string does not behave like a nodal point for waves on either part of the string. A small fraction is

always transmitted across the same point, and the reflected part diminishes by the same amount. This fraction is negligibly small when α is small or when the hammer mass is large. As α increases the fraction increases and begins to produce vibrations which appear as kinks on the other side. This is shown, as said before, by the figs. 9, 10, and 11 (Pl. IX.).

The time-displacement curves are drawn with the aid of the formula (24), and are shown graphically in figs. 13, 14, and 15 respectively for different cases of α and β. Fig. 13 refers to a point of observation $\beta=63$ cm. ; $\alpha=16$ cm., $\frac{T}{\phi}=1{\cdot}27$; $l=140$ cm. ; $T=0{\cdot}0108$ sec. ; mass of hammer $M=7{\cdot}0$ grams ; $k=69{\cdot}65$; and $f={\cdot}7$.

Fig. 13.

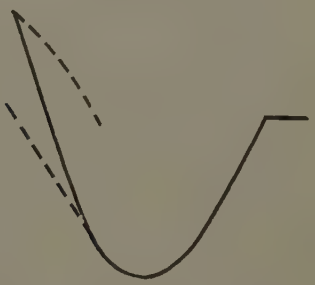

In this case the reflected wave from the farther end reaches the point of observation, while the wave reflected from the striking point is not able to reach the point of observation during the time the hammer is in contact with the string. Taking the period of vibration of the string proportional to $2l$ we find ϕ will be proportional to

$$\phi \propto 1{\cdot}57\,l, \quad i.e., \quad 219{\cdot}8 \text{ cm.},$$

or

$$(2\times77+47+18{\cdot}8).$$

Thus the initial wave, after crossing the pointof observation, is reflected from the farther end and the striking point, and travels a distance of 18·8 cm. from the striking point when the impact is over at the point of observation.

Fig. 14 refers to a case when the length, tension ($1{\cdot}1\times10^7$ dynes), etc. remain the same, but the striking distance α and the distance of the point of observation are 30·7 cm.

and 106 cm. respectively. M=13·5 grams, k=37, and $\frac{T}{\phi}$=·7. Thus in this case the duration of impact is greater than the period of vibration of the string. Hence the initial wave passes through the point of observation, is reflected from (1) the farther end, (2) the striking point, and (3) second time from the farther end. This last reflected wave crosses the point of observation, and is a second time reflected from the striking point, which part, however, does not reach the point of observation during the time the hammer is found to be in contact with the string at the same point. Thus we have four waves

Fig. 14.

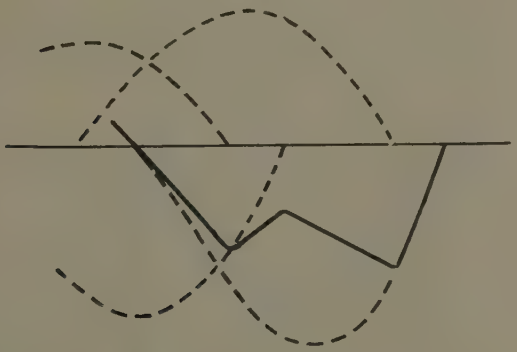

simultaneously present at the point of observation corresponding to each of these parts. The diagram for each wave has been drawn on the assumption that the coefficient of reflexion from the farther end is ·7, as before.

Fig. 15, α=30·7, β=69, $\frac{T}{\phi}$=·83, and other quantities are the same as before. In this case only three waves are simultaneously present at the point of observation, viz., (1) the initial wave, (2) the reflected wave, and (3) the wave reflected from the striking point. Coefficient of reflexion =·7, as before.

A comparison of these curves with those actually obtained by photographic method will show a remarkable agreement (Pl. IX. figs. 7, 8, and 9).

Conclusion.

From these results it is evident that, in spite of the weak point at the initial stages of impact, Kaufmann's theory leads to formulæ which are confirmed in a striking manner for small values of α—the case of practical importance. In the present note we have tried to present one aspect of the problem of struck strings, viz., the presence of small discontinuous impulses in the smaller segment of the string and their absence on the longer side of the string in the case when ϕ is less than the period of vibration of the string. When, however, the duration of impact is nearly equal to the period of vibration of the string the initial

Fig. 15.

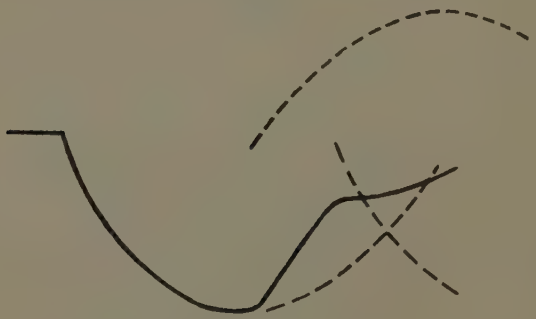

wave, after reflexion from the farther end, reaches the striking point, from which place it is again partly reflected, giving rise to a large kink in the time-displacement diagram of any point of the string on the same side. The manner in which the changes take place in the diagrams is amply verified by Kaufmann's theory when reflexions are taken into consideration (*vide* figs. 13, 14, and 15).

Another point to which attention has been drawn is the reflexion from the striking point. For waves on the shorter segment the above point, when the hammer is in contact with the string, behaves like a nodal point, *i. e.*, waves are completely reflected. For large values of the portion of the string between the hammer and the nearer end there is a transmitted part, the magnitude of which depends (1) upon the mass of the hammer, and (2) upon the length of the portion.

Appendix.

Assume $\xi = 1 - e^{-p/\mu}$ . . . (a general law).

Equation of motion of the hammer

$$M\ddot{\xi} = -p$$

$$\ddot{\xi} = n^2 \log (1-\xi), \qquad (1)$$

where $$n^2 = \frac{\mu}{M},$$

$$\dot{\xi}^2 - V_0^2 = 2n^2 [\xi \log (1-\xi) - \xi - \log (1-\xi)]. \qquad (2)$$

V_0 = initial velocity of the hammer.

$$\dot{\xi}^2 = V_0^2 - n^2\left(\xi^2 + \frac{\xi^3}{3} + \frac{\xi^4}{6} + \ldots\right), \qquad (3)$$

$$\dot{\xi} = V_0 \left\{ 1 - \frac{n^2}{V_0^2}\left(\xi^2 + \frac{\xi^3}{3} + \frac{\xi^4}{6} + \ldots\right)\right\}^{\frac{1}{2}}. \qquad (4)$$

Now $$\frac{n^2}{V_0^2}\xi^2 < 1,$$

hence $$\frac{d\xi}{V_0\left\{1 - \frac{n^2}{V_0^2}\left(\xi^2 + \frac{\xi^3}{3} + \frac{\xi^4}{6} + \ldots\right)\right\}^{\frac{1}{2}}} = dt.$$

Put $\frac{n}{V_0}\xi = x$, and expand and then integrate,

$$nt = \left\{\sin^{-1}x + \frac{V_0}{n}\cdot\frac{1}{24}x^4 + \frac{V_0^2}{n^2}\frac{x^5}{60} + \ldots\right\}, \qquad (15)$$

which reduces to (4) when x^4, x^5 terms are left out. Formula (5) is tentatively put forward for soft hammers.

References.

(1) *Ann. der Phys.* Bd. liv. (1895).
(2) Phil. Mag. xlvii. p. 1142 (1924).
(3) *Loc. cit.*
(4) *Loc. cit.*
(5) *Loc. cit.*
(6) *Loc. cit.*
(7) Phil. Mag. xvii. p. 521 (1934).
(8) Proc. Indian Association for the Cultivation of Science, ii. p. 42 (1916).
(9) Phil. Mag. xlvii. p. 1142 (1924).
(10) *Loc. cit.*
(11) Phil. Mag. xvii. p. 521 (1934).
(12) Proc. Roy. Soc. cviii. p. 284 (1925).
(13) Proc. Indian Assoc. vii. p. 13 (1921).

XXII. *Tribo- and Photo-electric Effects for Palladium.* *By* P. A. Mainstone, *M.Sc., F.Inst.P., Lecturer in Physics, University College of North Wales* *.

In a previous communication [1] the author examined the effect of moderate heat treatment on the tribo-electric charges developed on the surfaces of aluminium, nickel, and palladium. It was shown that in all cases the normal negative charge was greatly diminished on heating, although under certain conditions a considerable recovery took place on subsequent cooling. After heating in hydrogen, the charges on aluminium and palladium were found in certain cases to be reversed in sign, and an explanation in terms of the occluded hydrogen was looked for. A paper by Krüger and Ehmer [2], in which the photo-electric emission from Pd–Ag alloys appeared to be directly related to the amount of hydrogen occluded, suggested that a relation between the tribo- and photo-effects might be expected.

Later experiments on the photo-electric effect, however, have not altogether confirmed the results of Krüger and Ehmer. Thus, Schniedermann [3] finds that in the case of Pd–Ag alloys the photo-electric effect is a maximum with 40 per cent. Ag, while the amount of occluded hydrogen decreases linearly with percentage increase of silver. The conditions in the two researches were not identical, however. Krüger and Ehmer used the solubility figures of Sieverts and Metz [4] (taken at three different temperatures up to 317° C.), but measured the photo-electric effect with the specimens in an atmosphere of hydrogen and heated to about 180° C. Schniedermann, on the other hand, measured the solubility at ordinary temperature, using each specimen as the cathode of a voltameter in which hydrogen was liberated.

Experimental.

The apparatus of the previous experiments was used, with the frictional chamber modified to allow a beam from a mercury arc to be reflected vertically downwards on to the insulated palladium surface. For this purpose a quartz reflecting prism was used, and a short brass

* Communicated by Prof. E. A. Owen, M.A.,D.Sc.

tube projecting from the top of the chamber above the level of water in the cooling trough was closed by a quartz plate, thus allowing the beam to pass through. A grid was mounted at a distance of about 2 cm. above the palladium surfaces, and maintained at a potential of 200 volts.

In the previous experiments with palladium the gas pressure was reduced by means of a " Hyvac " oil pump, and was not generally taken below 0·1 mm. An oil-diffusion pump was now added to the apparatus, and this gave a lowest pressure which, although not given with great accuracy on the McLeod gauge available, certainly did not exceed 0·00025 mm. The vacuum was much improved by coating the whole of the exterior of the brass chamber with an impervious varnish. Sealing-wax varnish was found to be excellent, but inside the water cooling troughs it quickly became porous, and was replaced by a " tacky " mixture of picein wax and benzene. This, although slow in drying, was much more durable.

Very low gas pressures were read on a Pirani gauge, while for higher pressures up to atmospheric a metal Bourdon gauge was used. (This was also coated with sealing-wax varnish.) Later a glass Bourdon gauge, with a pressure range of several millimetres, was added to the apparatus.

Frictional and Photo-electric Isotherms.

The frictional isotherm (at room-temperature) on a freshly polished surface has been fully discussed in previous papers. The apparatus now enabled the photo-electric isotherm to be obtained at the same time. Except at low pressures, the photo-electric emission was very small, and in order to measure it on the same electroscope as the tribo effect, it was necessary to disconnect the large capacity (about 1500 cm) normally used. A screened contact was arranged so that the large capacity could be connected or disconnected at will.

Figures for the two effects in air and in hydrogen are given in Tables I. and II., the figures indicating electroscope deflexion. (One eye-piece division represented 0·6 volt, the relation between potential and deflexion being approximately linear.)

In both cases the photo effect shows a strong maximum at a pressure of about 0·5 mm. but falls off again at the lowest pressure. The tribo effect, on the other hand,

TABLE I.

Air.

Pressure.	Tribo effect.	Photo effect.	
		As observed.	Divs. per sec. (large capacity).
30 cm.	−5·5	4 divs. in 20 sec. (small capacity)*	0·003
20 ,,	−5·0	3·5 ,, ,,	0·003
9 ,,	−4·5	5 ,, ,,	0·004
5 ,,	−4·0	7 ,, ,,	0·006
2 mm. (?) †	−5·5	11 divs. in 10 sec.	0·018
1 ,,	−11·0	21 ,, ,,	0·035
0·5 ,,	−13·0	3 divs. in 20 sec. (large capacity)	0·15
0·1 ,,	−15·0	3 ,, ,,	0·15
0·00025 mm.	−12·5	18·5 divs. in 10 sec. (small capacity)	0·031

* 1 div. with large capacity = 60 divs. with small capacity.
† Pressure outside range of Pirani gauge.

TABLE II.

Hydrogen.

Pressure.	Tribo effect.	Photo effect.	
		As observed.	Divs. per sec. (large capacity).
30 cm.	−3·5	5 divs. in 20 secs. (small capacity).	0·004
20 ,, ...	−3·0	5 ,, ,,	0·004
10 ,, ...	−2·5	6·5 ,, ,,	0·005
5 ,, ...	−3·0	10 ,, ,,	0·008
1 mm. (?)	−4·0	4·5 divs. in 20 secs. (large capacity).	0·22
0·5 mm.	−5·0	6 ,, ,,	0·30
0·1 ,, ...	−6·0	1·5 ,, ,,	0·075
0·00025 mm, ...	−6·0	20 divs. in 10 secs. (small capacity).	0·033

remains approximately constant within this range. Since in the earlier experiments (with brass, silver, and steel) large increases in the tribo effect were always observed

at the lowest pressure, the isotherms at low pressures were at a later stage in the work re-examined. It has always been found difficult to maintain a perfect co-planar adjustment of the insulated and earthed surfaces after a large number of to-and-fro rubs and after long periods of heating, and any variation of this adjustment obviously reduces the possibility of reliable readings. The results of an extended series of readings, in which the effects of occlusion and de-gassing are represented, are shown later in this paper (Table VIII.).

The values of the tribo charges recorded above are steady values obtained after a large number of rubs. The photo emission did not vary appreciably with the number of rubs, although the initial emission at any given pressure was generally slightly greater than any subsequent one. The light beam was prevented from falling upon the surfaces during actual rubbing, but during the short periods of illumination (generally only a few minutes at a time) there were indications of the usual fatigue effects. Although the point has not been examined systematically, it seems unlikely that such very gentle rubbing could affect the surfaces sufficiently to cause a marked change in the photo sensitivity.

Effect of De-Gassing at Low Pressure.

The effect of prolonged de-gassing on the photo-emission has been very exhaustively studied by other investigators. The case of palladium has been dealt with by DuBridge and Roehr [5], who have found that the sensitivity, and hence also the threshold wave-length, increases in the first stages of de-gassing, but diminishes again as de-gassing proceeds. In their experiments the de-gassing proceeded for long periods at temperatures which in some cases exceeded 1000° C. Nothing comparable with this was possible with the author's apparatus, but the typical effect of a short period of de-gassing at 300° C. is shown below :—

Freshly polished surfaces.

Tribo effect at lowest pressure = −17.
(0·00025 mm.).

Photo effect at lowest pressure = 25 divs. in 10 secs.
(small capacity).
= 0·042 div. per sec.
(large capacity).

Surfaces after de-gassing for 2 hours at 300° C.

Tribo effect at lowest pressure = — 13.

Photo „ „ „ = 10 divs. in 20 secs. (large capacity).
= 0·50 div. per sec. (large capacity).

A large increase in the photo-emission is apparent, while the tribo effect is but little changed.

Effect of prolonged Heating in Hydrogen.

The first heating in hydrogen (to about 350° C.) gave a considerable reduction in the tribo charge, which, however, still remained negative in sign. The photo

TABLE III.

Temperature of heating 300° C.

Period.	Pressure during heating.	Subsequent max. tribo effect.	Subsequent max. photo effect.	Subsequent photo effect at lowest pressure.
	cm.		Divs. in 10 secs. (large capacity).	Divs. in 20 secs. (large capacity).
1.....	5	—29	23	4
2.....	5	—15	27	4
3.....	10	—7	22	4·5
4.....	10	—5·5	20	5
5.....	20	—5	22	6
6.....	20	—4	22	5
7.....	30	—3·5	24	6

effect observed at the lowest pressure was also slightly less than before heating.

In the previous experiments hydrogen was generally admitted to a pressure of about half an atmosphere, the temperature and time of heating being varied By means of the Bourdon gauge smaller measured quantities could now be admitted, and the following table shows the *maximum* tribo and photo effects (tribo effect at 0·00025 mm,, photo effect at 0·5 mm.), also the photo effect at the lowest pressure, after successive periods of heating of 1 hour each.

The surfaces were not de-gassed between successive heating processes, although some gas probably came off during pumping at ordinary temperature.

While the photo effect shows little change, the tribo effect becomes progressively less, although it does not actually change its sign, even after 7 hours' heating. This effect is quite contrary to that previously found, when a very brief heating at 300° C,. or even at 250° C., sufficed to show a positive charge.

In the earlier experiments the pressure was not taken below about 0·1 mm,, and the apparatus was never entirely free from small air leaks. In the present experiments freedom from air leaks was much more carefully ensured, hence the conditions in the two cases were not the same. Following the results of Table III., the surfaces were de-gassed and re-polished, after which they were heated for two hours in *air* at 1 mm. pressure and 350° C. On cooling, a small positive charge appeared at low pressure (0·1 mm.). This result was confirmed

TABLE IV.

Initial pressure *.	Conditions of heating.	Subsequent maximum tribo effect.
1 mm.	30 mins. at 300° C.	−7·0
1 ,, ...	2 hrs. at 300° C.	−3·5
2 ,, ...	2 hrs. at 350° C.	+6·0

in a second observation after the surfaces had been re-polished. Hence the appearance of positive charge seems to depend on the presence of a small amount of air (or oxygen) and not on hydrogen at all.

The effect of heating in oxygen is shown in Table IV., the three processes following in succession without de-gassing or re-polishing.

Hence the effect of *oxygen* in producing positive charge appears to be proved. Heating in nitrogen produced no change after a period of three hours.

Measurement of amount of Hydrogen occluded.

In order to measure changes of pressure within the apparatus of the order of a few millimetres, a glass Bourdon gauge was added. The gauge is similar in principle

* During each period of heating a reduction of pressure took place due to oxidation of the copper heater.

to the ordinary metal gauge, the small change of curvature of the thin-walled glass being magnified by means of a long pointer. The gauge is sealed into a cylindrical enclosure, the movement of the pointer recording the difference of pressure between this enclosure and the interior of the gauge. By means of a tap the two pressures can be equalized when desired. In the present experiments the interior of the gauge was connected to the main apparatus. The pointer was observed through a low power telescope provided with an eyepiece scale, the deflexion being about 7 divisions per 1 mm. pressure difference.

The volume of the apparatus was determined by admitting a known small volume of gas at atmospheric pressure from the voltameter and measuring the pressure increase on a McLeod gauge. The volume was found to be 3·9 litres, so that a pressure diminution of 1 mm. represented an absorption of 5·1 c.c. at atmospheric pressure. The mass of both palladium specimens was 37 grams.

When an appreciable amount of hydrogen was admitted to the apparatus the increase of pressure due to heating in the experimental chamber caused a much greater deflexion of the pointer than that due to occlusion. The outer enclosure of the gauge, containing gas at the same pressure as that initially in the main apparatus, was wrapped round with a few turns of wire carrying the same current as the heater in the chamber itself. By this means the pressure increases due to heating on the two sides of the gauge could be made approximately equal, a separate calibration giving the movement of the pointer due to heating alone, the palladium being removed from the heater. With the palladium present the movement of the pointer due to occlusion was in the opposite direction to that due to heating, and the pressure diminution due to occlusion was known. Even so, the deflexion for a given temperature was not quite reproducible when, as in the first readings, the gas pressure was about 30 cm. Readings were taken when, after the comparatively rapid deflexion of the pointer due to heating, its movement (in the opposite direction) represented successive diminutions in pressure of 1 mm. This "apparent" occlusion was no doubt considerably less than the real. The results are recorded in Table V. After each heating the chamber was cooled and the gas pumped off (*a*)

to 0·5 mm. in order to give the maximum photo effect, (*b*) to the lowest pressure to give the maximum tribo effect.

While the tribo effect shows no appreciable variation the photo effect increases, apparently to a maximum when the metal becomes saturated with gas.

On de-gassing without removal of the liberated gas the pressure rose by about 11 mm., and the amount of gas originally occluded was beyond doubt considerably greater than that indicated in the following table. The subsequent deflexions at the lowest pressure were :— Tribo −28, photo 0·125 div. per second (large capacity).

TABLE V.

State of palladium	Max. tribo effect.	Photo effect.	
		Maximum.	At lowest pressure.
		divs. in 20 secs. (large capacity).	div. per sec. (large capacity).
Re-polished and de-gassed	−25	5·5	0·030
Occlusion represented by 1 mm. pressure diminution (apparent).	−27	9	0·048
Further 1 mm. diminution.	−21	14·5	0·063
„ „ „	−29	18	0·10
Further heating but no further pressure diminution.	−27	17	0·10
After de-gassing	−28	.....	0·125

It is noteworthy that the photo effect is not diminished by removal of the occluded gas.

The readings were repeated with a much smaller initial pressure of hydrogen (3 cm.). The effective pressure change due to heating to 250° C. was now approximately 1 mm. The readings were taken in a similar manner to those of Table V., a pressure diminution of 1 mm. due to occlusion just cancelling the pressure increase due to heating. The results as at first obtained were quite different from those of Table V. The tribo effect showed a considerable diminution as occlusion proceeded, while the photo effect changed but little. The surfaces were de-gassed and re-polished, and the drying agent (phosphorus pentoxide), which was affected by oil vapour from the

pumps, was replenished. The subsequent results are shown in Table VI.

The general trend of these results is the same as that of Table V., and it is reasonable to assume that they may be accepted in preference to those previously discarded. The initial tribo effect is much larger than before, but this is doubtless due partly to the possibility of different states of polish of the palladium in the two cases, and partly to the difficulty already referred to of maintaining a perfect co-planar adjustment of the insulated and earthed surfaces. It has never been found possible to reproduce with any certainty the same charge on a given

TABLE VI.

State of palladium	Max. tribo effect.	Photo effect.	
		Maximum.	At lowest pressure.
Re-polished and de-gassed.	approx. 50	Divs. in 20 secs. (large capacity). 6	Div. per sec. (large capacity). 0·020
Occlusion represented by 1 mm. pressure diminution.	,,	7	0·045
Further 1 mm. diminution.	,,	26	0·125
,, ,, ...	,,	20	0·087
,, ½ ,, (saturation).	,,	32	0·15
After 2 hours' de-gassing. .	,,	—	0·097

surface after re-polish ng. In the present case the charge was somewhat too large for exact measurement, but throughout the series there was no appreciable change. The photo emission, starting at about the same value as before, rises to a somewhat higher value at saturation, in spite of the fact that less hydrogen than before was absorbed. After de-gassing, both effects were approximately the same as in Table V.

Further Examination of Reversal of Sign of Charge.

In a series of papers [6] Finch and Stimson have examined the electrical condition of various metal surfaces on heating in different gases to temperatures up to 850° C. Under certain conditions they found that a given surface

could be "normalized" such that its potential in each gas at a particular temperature was exactly reproducible. Thus at 500° C. a platinum surface gave potentials of −1·19, +0·20, and 0·00 volt *in vacuo*, hydrogen and oxygen respectively. In the present experiments it appeared possible that after the reversal of the sign of the charge due to oxygen, the original negative charge might be in part restored by heating in hydrogen or *in vacuo*. This, however, was not found to be the case. After several hours heating in hydrogen, mostly at about 300° C., no definite change in the tribo effect could be established.

TABLE VII.

Duration of heating in oxygen.	Initial pressure of oxygen.	Tribo effect.	Photo effect.
	mm.		Div. per sec. (large capacity).
None (freshly polished surfaces) . .	. .	−39	0·175
30 minutes	1	−46	0·15
Further 30 minutes	1	−45	0·05
,, ,, ,, ...	1	−50	0·05
,, ,, ,, ...	1	over 50	0·08
,, ,, ,, ...	1	,,	0·05
,, 60 ,, ...	2	−17*	0·05
,, ,, ,, ...	2	−4*	0·03
,, ,, ,, ...	2	+10*	0·02
,, 90 ,, ...	2	+14*	0·02
,, 60 ,, ...	2	+15	0·01

* In these readings the tribo charge had not become quite steady after a considerable number of rubs.

It may be, of course, that if heating to a much higher temperature were possible the effect of the oxygen might be removed, as in the case of the normalization referred to above.

Progressive Changes due to Oxygen.

The effects of successive short periods of heating in oxygen are recorded in Table VII. The temperature of heating was about 300° C. throughout, and the readings (on subsequent cooling) were in every case taken at the lowest pressure. During each period of heating the gas

pressure fell considerably, due mainly to the oxidation of the copper former on which the heating coil was wound.

The progressive changes in both effects are very clearly shown. On subsequent de-gassing for 3 hours at 300° C. the tribo effect at the lowest pressure was +15, and the photo effect 0·04 div. per sec. Thus, while de-gassing appears to have no effect on the tribo charge, the photo sensitivity is increased.

Re-examination of Isotherms at Low Pressures.

The variations in both the tribo and photo effects at low pressures are so marked that it is important to examine to what extent, if any, they are influenced by the gas content of the metal. In the early experiments with other metals [7] a sharp increase in the frictional charge at very low pressures was always observed, and it was suggested that these charges are due to actual contact of the metal and glass surfaces, which under these conditions may be assumed to be reasonably free from adsorbed gas layers. It is, however, possible that at such pressures some gas may pass from the interior to the surface and remain adsorbed there for an appreciable time. It is, of course, not to be expected that the amount of such gas would equal that adsorbed at ordinary pressure. Further, the amount of gas should depend largely upon the initial gas content of the metal, *e. g.*, the behaviour of palladium when containing occluded hydrogen should be different from that of the metal in a de-gassed condition.

The result of an examination of this point is shown in Table VIII. Before each set of readings dry hydrogen was admitted to a pressure of about 4 cm. and the tribo and photo effects observed at the three pressures indicated. It is clear that no definite change in the tribo effect at low pressures can be established, and it would appear that the original explanation of the effect must still be regarded as reasonable.

Discussion.

In view of the lack of confirmatory work in this field by other investigators, any adequate discussion still remains difficult. Certain points, however, may be said to be definitely established. Thus there is a definite increase in the photo-electric sensitivity due to occluded

hydrogen, although it is not clear why subsequent degassing leaves the sensitivity practically unchanged. More important is the establishment of the true cause of the reversal of sign of the frictional charge. The failure to remove the positive charge produced by oxygen points to a chemical change in the nature of the surface, although on examination the surface when in this condition showed little signs of oxidation. In the work of Finch and Stimson the case of palladium does not yet appear to have been dealt with, but platinum [8] normalized at 500° C. showed exactly zero potential in oxygen, while the *in vacuo* potential was negative and the hydrogen potential

TABLE VIII.

State of surfaces.	Pressure 4 cm.		Pressure 0·5 mm.		Pressure 0·00025 mm.	
	Tribo effect.	Photo effect.	Tribo effect.	Photo effect.	Tribo effect.	Photo effect.
		div. per sec.		div. per sec.	exceeding	div. per sec.
Freshly polished	−4	0·002	−50	0·073	−50	0·007
De-gassed for 1 hour at 300° C.	−4·5	0·022	−37	0·70	−45	0·050
Heated in hydrogen for 2 hours at 275° C.	−2	0·012	−50	1·2	−50	0·095
De-gassed for 2 hours at 300° C.	−3	0·027	−50	1·2	−50	0·086
Further de-gassed for 2½ hours at 300° C.	−2·5	0·035	−40	1·7	−43	0·095

positive. After normalization at 850° C., however, the surface showed a small positive potential in oxygen over the range 150–620° C. The extension of the temperature range in the present experiments would be interesting, and it is hoped to construct a new form of chamber to make this possible.

The behaviour of surfaces of metallic oxides might be expected to supply useful information in this connexion. Before the commencement of the experiments described here, the frictional charges produced on a natural face of haematite, Fe_2O_3, were investigated. The crystal was cast in aluminium, and fixed in the frictional chamber in the usual manner. It was sufficiently conducting to allow the surface charge to pass through to the electroscope. The charges were comparatively small,

but were negative in all cases. The crystal was subjected to the same moderate heat treatment as in the present experiments, and was also heated in hydrogen. The variation of the charge with gas pressure was much the same as in the case of a polished metallic surface. Further experiments with crystalline oxides are necessary, although it is difficult to obtain specimens with natural faces large enough for this purpose.

Summary.

1. The frictional and photo-electric isotherms for palladium in both air and hydrogen have been examined. Whilst the frictional charge is a minimum at a moderately low pressure, the photo-electric sensitivity is a maximum at about the same pressure.

2. The effect of de-gassing at 300° C. is very small in the case of the frictional charge, but the photo sensitivity is much increased thereby.

3. Prolonged heating in hydrogen fails to reverse the sign of the frictional charge when sufficient care is taken to prevent small air leaks. The reversal is definitely traced to the presence of oxygen, and when once produced cannot be destroyed by heating at 300° C. either *in vacuo* or in hydrogen.

4. The photo sensitivity shows a marked increase due to occluded hydrogen, reaching a maximum when the saturation point is reached. The sensitivity is not diminished by subsequent removal of the occluded gas.

5. The form of the frictional isotherm at low pressures is approximately the same whether the metal contains occluded gas or is in a de-gassed condition.

It is a pleasure to record my indebtedness to Prof. E. A. Owen for laboratory facilities, as well as for his continued help and advice.

References.

(1) Phil. Mag. xvi. pp. 1083–1096 (December 1933).
(2) *Zeits. f. Physik*, xiv. (1), pp. 1–5 (1923).
(3) *Ann. d. Physik*, (7), pp. 761–779 (June 1932).
(4) *Zeits. f. anorg. Chem.* xcii. p. 329 (1915).
(5) Phys. Rev. xxxix. pp. 99–107 (1932).
(6) Proc. Roy. Soc. A, cxvi. pp. 379–400 (1927) and later papers.
(7) Phil. Mag. viii. pp. 733–749 (November 1929).
(8) Proc. Roy. Soc. A, cxxiv. pp. 356–365 (June 1929).

Bangor.
September 1934.

XXIII. *Crystal Orientation in Tooth Enamel.* By J. Thewlis, *M.Sc., Physics Department, National Physical Laboratory, Teddington, Middlesex* *.

[Plates X.–XII.]

PRELIMINARY work by the author has shown that the enamel of teeth is largely composed of preferentially oriented crystallites of apatite †. The present paper gives the results of detailed work on the nature of this orientation in dog's teeth and in human teeth ‡.

1. *The Type of Orientation.*

The teeth examined were in the form of longitudinal sections, of thickness about 0·2 to 0·3 mm., and a fine beam of X-rays was passed through that part of the section which was to be examined. The beam was at right angles to the section and a photographic plate was set up parallel to the section. A molybdenum target was employed.

The enamel photographs resembled very strongly the type of photograph obtained from a cold-worked metal and it was clear that they were due to preferential orientation. A typical photograph is given in fig. 1 (Pl. X.), and examination shows that in all probability the line AB is parallel to a fibre-axis. The problem at once arises as to whether the orientation is analogous to that which is found in the case of a cold-rolled metal or to that which is found in the case of a cold-drawn wire. In the first case we should expect to find directions corresponding to the rolling direction, normal direction, and cross direction. In the second case we should have only one fibre-axis, corresponding to the direction of drawing. This problem was settled by setting up a tooth section so that it could be rotated about the direction corresponding to AB, and taking a series of X-ray photographs of the same portion of enamel with the section in different positions about the axis. The same pattern was obtained

* Communicated by Dr. G. W. C. Kaye, O.B.E., M.A.

† Brit. Dental. Journ. liii. p. 655 (1932); Brit. J. of Radiology, v. p. 353 (1932).

‡ A paper dealing with the dental aspect of the investigation with reference to human teeth was published in the Brit. Dental Journal, lvii. p. 457 (1934).

each time. This indicates that there is random orientation with respect to all directions except one, namely, that corresponding to AB. Hence the orientation is analogous to that found for a cold-drawn metal wire. If the orientation had been analogous to that obtained in the case of a rolled metal the X-ray patterns would have been different for each position of the section.

Having determined that the preferential orientation in tooth enamel is such that there is only one axis of preferential orientation, two problems remain to be cleared up. The first of these is the determination of the crystallographic nature of this axis, and the second is the determination of its relationship to the tooth itself.

2. *The Crystallographic Nature of the Fibre-axis.*

In the case of theoretically perfect preferential orientation and with an accurately parallel X-ray beam the crystallographic plane at right angles to the fibre-axis would not give rise to any X-ray reflexion. In practice, since the preferential orientation is never perfect and the X-ray beam is divergent, it is always found that this plane does in fact give rise to marked reflexions which, of course, lie on the line corresponding to the fibre-axis.

If we look at fig. 1 (Pl. X.) we see that on the line AB there are reflexions due to two planes. These reflexions are marked S_1 and S_2, and calculation shows that they are due to the (002) and (004) planes of apatite respectively. Hence it appears probable that the fibre-axis is at right angles to the (001) plane, *i.e.*, that it is the [001] direction. This can be tested by calculation. Assuming that the fibre-axis is the [001] direction of apatite we can calculate the positions on the photographic plate of the reflexions due to the various planes. The angle measured on the photographic plate, between the line corresponding to the fibre-axis and a line joining the central spot and the (*hkl*) reflexion, is given by

$$\cos \nu = \frac{\cos \phi}{\cos \theta},$$

where ν is the measured angle, θ is the Bragg angle of reflexion, and ϕ is the angle between the fibre-axis and the normal to the plane (*hkl*).

Now apatite is a hexagonal crystal, and in the hexagonal system the angle ϕ, between the normals to two planes (hkl) and (pqr), is given by

$$\cos\phi = \frac{hp+kq+\frac{1}{2}(hq+pk)+\frac{3a^2}{4c^2}\cdot lr}{\sqrt{\left\{\left(h^2+k^2+hk+\frac{3a^2}{4c^2}\cdot l^2\right)\left(p^2+q^2+pq+\frac{3a^2}{4c^2}\cdot r^2\right)\right\}}},$$

where a is the length of the side of the unit-cell and c is the height.

If the fibre-axis is the [001] direction, then (pqr) becomes (001), and we have

$$\cos\phi = \frac{l}{\sqrt{\left\{\frac{4c^2}{3a^2}(h^2+k^2+hk)+l^2\right\}}}.$$

Several kinds of apatite exist, and it is not known which is present in tooth enamel, although it is hoped that the question will be settled in the near future. However, the small differences in the lattice sizes of the various kinds of apatite are not sufficient to matter for the present purpose, which is that of identifying the various planes whose reflexions are observed and calculating the values of ϕ and ν for them. Consequently the values of the lattice constants of fluor-apatite given by St. Náray-Szabó * have been employed; these are $a=9{\cdot}37$ Å. and $c=6{\cdot}88$ Å.

Table I. gives a comparison of the observed and calculated values of ν for the various reflecting planes assuming the fibre-axis to be the [001] direction. It will be seen that a very satisfactory agreement is obtained; hence it seems fairly certain that the fibre-axis in tooth enamel coincides with the [001] direction of apatite.

In many of the X-ray photographs of human tooth enamel it was observed that a double orientation was present. Two positions of the fibre-axis occurred, inclined to each other at an angle of about 30°. Fig. 2 (Pl. X.) is a reproduction of such a photograph. It will be seen that there are now two sets of reflexions. It will also be noticed that one set of reflexions is stronger than the other. Hence more of the crystallites are oriented about

* St. Náray-Szabó, *Z. f. Krist.* lxxv. p. 387 (1930).

one fibre-axis than are oriented about the other. These fibre-axes will be referred to as (i.) and (ii.), (i.) being the fibre-axis which corresponds to the strong set of reflexions. In many photographs the presence of fibre-axis (ii.) is shown merely by an extension to one side of the spots corresponding to fibre-axis (i.). This is due to overlapping on account of imperfection of orientation. A photograph showing this effect is given in fig. 3 (Pl. XI.).

TABLE I.

Plane.	ν observed.	ν calculated.
002	0°	0° *
120.210	90	90
121.211	66	65·7
112	33	35·6
300	90	90
130.310	90	90
222	55	55
123.213	31	35·2
140.410	90	90
004	0	0 *
133.313	45	44·1

* See the beginning of this section.

3. *The Relationship between the Fibre-axes and the Tooth.*

It has been found that the line AB of fig. 1 (Pl. X.) corresponds to a fibre-axis, and that this axis is the [001] direction of apatite. We are now faced with the problem of the determination of the position of the fibre-axis with respect to the tooth. Since the fibre-axis is parallel to the line AB, it follows that it lies in the plane of the tooth section. The problem, then, is to determine the position which the fibre-axis occupies in this plane.

In order to do this an X-ray camera was constructed as shown in fig. 4. It consists of slits S_1 and S_2, a tooth-holder and a photographic plate. The slits are made from a lead-antimony alloy. One of them, S_1, is carried by a thick brass plate and is of circular cross-section, $\frac{1}{2}$ mm. in diameter. This opens out into a cylindrical chamber C. into which the brass tooth-holder, carrying the second slit S_2, fits tightly. The slit S_2 is also of circular

cross-section, $\frac{1}{2}$ mm. in diameter. The screw K is to ensure that the tooth-holder goes back into the same position each time. The tooth section is held in contact with the tooth-holder by plasticine.

When an X-ray photograph has been taken the tooth-holder, with the tooth still attached, is removed from the camera and a beam of light is passed through the slit S_2, thereby illuminating the circular portion of the tooth section which has been examined by X-rays. An ordinary photograph of the tooth-holder and tooth is then taken,

Fig. 4.

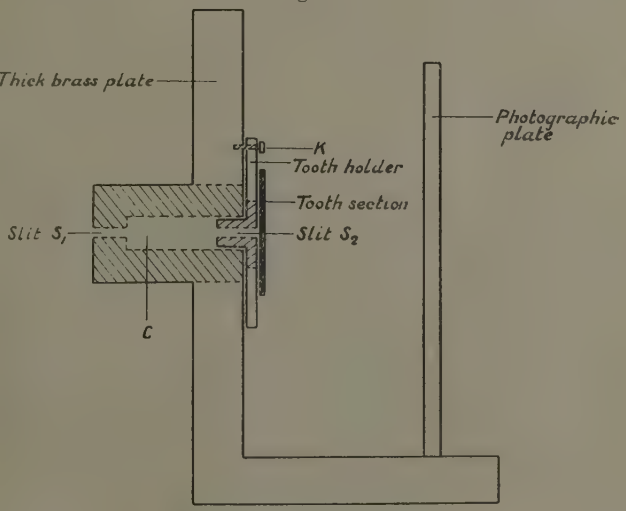

X-ray camera. (Not to scale.)

showing this disk of light on the tooth. Such a photograph is shown in fig. 5 (Pl. XI.).

Now the tooth-holder is so fixed to the brass plate that its edges are parallel to those of the photographic plate. Hence the angle which a line such as AB on fig. 1 (Pl. X.) makes with the edge of the photographic plate is the angle which the fibre-axis makes with the corresponding edge of the tooth-holder. Therefore the relationship between the fibre-axis and the tooth section can be obtained at once.

By this method it was found for photographs of human teeth showing a single fibre-axis that this axis always made an angle of about 20° with the normal to the edge of the section. Moreover the fibre-axis was always inclined towards the tip of the tooth.

When photographs showing two fibre-axes were examined it was found that fibre-axis (i.) was the same as the one described above, *i. e.*, it made an angle of 20° with the normal to the edge of the section. Fibre-axis (ii.), as already mentioned, makes an angle of about 30° with fibre-axis (i.). It is inclined to the latter axis in a direction away from the tip of the tooth. Fig. 6 (Pl. XII.) shows the relationship of these fibre-axes to the tooth section.

In the case of dog's teeth it was found that the fibre-axis was always normal to the edge of the tooth section. No double orientation was observed.

The X-ray photographs of some portions of the teeth examined differed from those discussed above in two ways. Fig. 7 (Pl. XII.) is an example of this type of photograph. It will be noticed that one of the (002) reflexions (marked A_1 on the photograph) is stronger than the other (A_2), and the corresponding (004) reflexions (B_1 and B_2) also differ in intensity in the same way. Also in the case of planes for which ν is not 90° the value of ν for the upper pair of reflexions is different from that for the lower pair. This is precisely what we should expect to find if the fibre-axis were not at right angles to the X-ray beam, *i. e.*, if the fibre-axis were not in the plane of the tooth section.

It is clear that the effect of tilting the fibre-axis with respect to the X-ray beam would be to increase the intensity of one of the (002) reflexions at the expense of that of the other, and similarly for the (004) reflexions. The alteration of ν in such a case has been worked out by Polanyi *, and corresponds with that observed. The value of ν is increased in that half of the photograph which corresponds to a tilting of the fibre-axis towards the X-ray beam, and is decreased in that half which corresponds to a tilting of the fibre-axis away from the X-ray beam. Hence it may be concluded that photographs such as that shown in fig. 7 (Pl. XII.) are due to the fibre-axis being tilted out of the plane of the tooth section.

* M. Polanyi, *Zeit. f. Phys.* vii. p. 149 (1921).

4. *Summary.*

X-ray examination has shown that the apatite crystallites of which tooth enamel is largely composed are preferentially oriented so as to have the [001] direction in common, *i. e.*, the [001] direction is the fibre-axis.

In a section of a human tooth the fibre-axis is inclined towards the tip of the tooth at an angle of about 20° to the normal to the edge of the section, and lies in the plane of the section. Sometimes a second position of the fibre-axis is also found. This second fibre-axis makes an angle of about 30° with the first and is inclined away from the tip of the tooth. In general more of the crystallites are oriented about the first fibre-axis than about the second.

In a section of a dog's tooth the fibre-axis is normal to the edge of the section and lies in the plane of the section. No double orientation is observed.

In some cases it is found that the fibre-axes are tilted out of the plane of the tooth section.

The above work forms part of an investigation carried out on behalf of the Dental Disease Committee of the Medical Research Council, to which the author is indebted for permission to publish.

The author wishes to express his indebtedness to Dr. E. Wilfred Fish, who supplied the tooth sections, to Dr. G. W. C. Kaye and Dr. G. Shearer for their interest, and to Messrs. H. F. Cook and J. A. G. Smith for their assistance in the experimental work.

XXIV. *On the Theoretical Determination of Earth Resistance from Surface Potential Measurements.* *By* A. F. Stevenson, *M.A., Ph.D., Department of Applied Mathematics, University of Toronto* *.

§1. *Introduction.*

THE problem of determining earth resistance from surface potential measurements with a single point electrode is of practical importance in geophysical prospecting. For this reason much effort has been

* Communicated by the Author.

devoted to the calculation of surface potentials from an assumed conductivity variation, the case usually considered being that in which the conductivity is some simple function of the depth (in particular that of the "layer-earth") *, but little attention has been paid to a direct attack on the converse problem.

In a recent paper of the same title † the author has given a general theory of the determination of surface potentials when the conductivity is an arbitrarily assigned function of position (not necessarily of depth only) and of the converse problem, it being shown that the latter problem is in general indeterminate, but may be rendered determinate in various ways, in particular by postulating that the conductivity is a function of depth only. In its practical application the method is only tractable in the latter case, and then only approximately. Another method for this case, which is exact under certain conditions—not always realisable in practice—has been given by Slichter ‡ and Langer §. Both these methods express the conductivity as a power series in the depth, and this is not very satisfactory from the practical point of view, as it is the detection of regions where there is a rapid change, or discontinuity, in the conductivity which is of importance.

In the present paper another method is given in which both the conductivity (being a function of depth only) and the surface potential are expressed as Fourier series. A Fourier series is better adapted to expressing a rapidly varying function than a power series, and it is thought the method might be of practical use, at least in certain cases. It is hoped in a future paper to carry out the further numerical calculations necessary for the actual application of the method, and also to test it out by applying it to some cases where the answer is known in advance ||; in the present paper only the method is presented. Attention is also briefly called to the possibility of applying a variational method (well known in other connexions) to such problems.

* See, for instance, L. V. King, Proc. Roy. Soc. A, cxxxix. p. 237 (1933); Phil. Trans. A, ccxxxiii. p. 327 (1934); M. Muskat, 'Physics,' v. p. 129 (1933); L. B. Slichter, Physics, iv. p. 307 (1933).

† A. F. Stevenson, 'Physics,' v. p. 114 (1934). Referred to as Paper I.

‡ L. B. Slichter, *loc. cit.*

§ R. E. Langer, Bull. Am. Math. Soc. xxxix. p. 814 (1933).

|| One such simple case was used for testing the Slichter-Langer method and the author's previous method in Paper I.

§2. *The Fourier Series Method.*

Choosing the electrode at the earth's surface as origin of cylindrical coordinates (r, z), z being the depth, let $\sigma(z)$ be the conductivity and ϕ the potential. Then ϕ satisfies the equation

$$\frac{\partial}{\partial r}\left(r\sigma\frac{\partial\phi}{\partial r}\right)+\frac{\partial}{\partial z}\left(r\sigma\frac{\partial\phi}{\partial z}\right)=0 \quad . \quad . \quad . \quad . \quad (1)$$

subject to the conditions

(*a*) $\phi\rightarrow\dfrac{C}{\rho}$ as $\rho\rightarrow 0$, where $\rho=(r^2+z^2)^{\frac{1}{2}}$ is the distance from the electrode, and $C=I/2\pi\sigma_0$, I being the current and $\sigma_0=\sigma(0)$ the conductivity at the surface.

(*b*) $\phi\rightarrow\dfrac{C'}{\rho}$ as $\rho\rightarrow\infty$, where C′ is a constant (not necessarily equal to C) *.

(*c*) $\dfrac{\partial\phi}{\partial z}=0$ when $z=0$.

In order to remove the singularity at the origin implied by condition (*a*), we put

$$\phi=C\left(\frac{1}{\rho}+V\right). \quad . \quad . \quad . \quad . \quad . \quad . \quad (2)$$

Then V satisfies

$$r\sigma\left(\frac{\partial^2V}{\partial r^2}+\frac{\partial^2V}{\partial z^2}\right)+\sigma\frac{\partial V}{\partial r}+r\sigma'\frac{\partial V}{\partial z}-\frac{rz}{(r^2+z^2)^{3/2}}\sigma'=0, \quad (3)$$

where $\sigma'=\dfrac{d\sigma}{dz}$. The boundary conditions are now

(*a*′) $\rho V\rightarrow o$ as $\rho\rightarrow 0$.

(*b*′) V vanishes to order $1/\rho$ or higher at infinity.

(*c*′) $\dfrac{\partial V}{\partial z}=0$ when $z=0$.

It can be shown that if the first and second derivatives of σ vanish at the origin, V and its first derivatives remain finite and continuous there (this therefore replacing condition (*a*′)) †. We shall suppose this to be the case. It is a reasonable approximation to make, in any case.

* This is not always so, the precise condition depending on the behaviour of σ at infinity, but it is sufficiently general for our purpose.

† This follows from an extension of the argument used to establish the validity of the method used in Paper I.

In order to use Fourier series, we shall now suppose that we may, to a sufficient approximation, confine ourselves to the cylinder of radius R and height H defined by

$$0 \leq r < R, \quad 0 \leq z \leq H, \quad . \quad . \quad . \quad . \quad . \quad . \quad (4)$$

and that V and its first derivatives vanish at the boundaries of the cylinder, while σ' vanishes when $z=H$. Since $V \to 0$ as r or $z \to \infty$, the conditions on V may be approximated to by making R and H sufficiently large. Moreover, the condition imposed on σ is not unduly restrictive, particularly since really only a finite portion of the medium is accessible to observation.

Under these circumstances, we may assume for σ and V, Fourier cosine series of the form

$$\sigma = \sum_{n=-\infty}^{\infty}{}' b_n \cos \frac{n\pi z}{H}, \quad . \quad . \quad . \quad . \quad . \quad . \quad (5)$$

$$V = \sum_{i,j=-\infty}^{\infty}{}' a_{ij} \cos \frac{i\pi z}{H} \cos \frac{j\pi r}{R}, \quad . \quad . \quad . \quad . \quad (6)$$

all boundary conditions being then fulfilled. The summations are taken from $-\infty$ to ∞, rather than 0 to ∞, simply for subsequent convenience; we suppose all summations taken in this way in what follows unless the contrary is stated. We may, without loss of generality, suppose that b_n is an even function of n, and a_{ij} an even function of both i and j. Under our assumptions, it will be permissible to differentiate these series term by term *twice* *; this is essential for what follows. The surface potential, or rather that portion of it defined by (2), V_s say, is given by

$$V_s = V(r, 0) = \sum_j \alpha_j \cos \frac{j\pi r}{R}, \quad . \quad . \quad . \quad . \quad (7)$$

where

$$\alpha_j = \Sigma a_{ij} \quad . \quad . \quad . \quad . \quad . \quad . \quad . \quad (8)$$

Substitute (5) and (6) in (3), multiply by $\cos \frac{k\pi z}{H} \cos \frac{l\pi r}{R}$,

* For instance σ, defined as an even function of z in the interval $-H \leq z \leq H$ possesses a continuous derivative, and the values of the function, and of its derivative, at the ends of the interval are equal. It is then permissible to differentiate (5) twice term by term. Similarly for (6). We suppose throughout that σ is a continuous function and possesses a continuous derivative.

and integrate over the region defined by (4). We obtain, after evaluation of the integrals with respect to z as far as possible, and simplification, the set of equations

$$\sum_{i,j}\{F(i,j,l)(b_{k+i}+b_{k-i})+G(i,j,l)[(k+i)b_{k+i}-(k-i)b_{k-i}]\}a_{ij} = \sum_{n} K(k,l,n)b_n. \quad (k,l=0,\pm1,\pm2,\ldots) \quad (9)$$

where

$$F(i,j,l)=\pi^2 H\left(\frac{i^2}{H^2}+\frac{j^2}{R^2}\right)\int_0^R r\cos\frac{j\pi r}{R}\cos\frac{l\pi r}{R}\,dr + \frac{\pi H}{R}j\int_0^R \sin\frac{j\pi r}{R}\cos\frac{l\pi r}{R}\,dr \quad \ldots \quad (10)$$

$$G(i,j,l)=-4\frac{i\pi^2}{H^2}\int_0^R r\cos\frac{j\pi r}{R}\cos\frac{l\pi r}{R}\,dr.$$

$$K(k,l,n)=\frac{2n\pi}{H}\int_0^R dr\int_0^H dz \times\frac{rz}{(r^2+z^2)^{3/2}}\sin\frac{n\pi z}{H}\cos\frac{k\pi z}{H}\cos\frac{l\pi r}{R}. \quad (11)$$

If we regard the conductivity as assigned, equations (9) are an infinite set of linear equations for the determination of the a_{ij}, and hence V, in terms of the b's. The converse problem of determining conductivity from surface potential requires a solution for the b's in terms of the α's through elimination of the a_{ij} between equations (8) and (9). Fortunately, it is possible to perform this elimination in a form which leaves a set of linear equations between the b's and the α's. For this purpose we need merely sum equations (9) with respect to k (from $-\infty$ to ∞). Since

$$\sum_k b_{k+i}=\sum_k b_{k-i}=\sum_k b_k=\sigma_0, \text{ from (5)},$$

and

$$\sum_k (k+i)b_{k+i}=\sum_k (k-i)b_{k-i}=\sum_k kb_k=0,$$

on account of the even character of the b_k, we obtain in this manner

$$\sigma_0\sum_{i,j}F(i,j,l)a_{ij}=\sum_{n,k}K(k,l,n)b_n, \ (l=0,\pm1,\ldots). \quad (11')$$

But from (10)

$$\sum_{i,j}F(i,j,l)a_{ij}=\sum_j[L(j,l)(\sum_i a_{ij})+M(j,l)(\sum_i i^2a_{ij})], \quad (12)$$

where
$$\left.\begin{aligned} \mathrm{L}(j,l) &= \frac{\pi^2\mathrm{H}}{\mathrm{R}^2} j^2 \int_0^{\mathrm{R}} r \cos\frac{j\pi r}{\mathrm{R}} \cos\frac{l\pi r}{\mathrm{R}}\, dr \\ &\quad + \frac{\pi\mathrm{H}}{\mathrm{R}} j \int_0^{\mathrm{R}} \sin\frac{j\pi r}{\mathrm{R}} \cos\frac{l\pi r}{\mathrm{R}}\, dr \\ \text{and} \quad \mathrm{M}(j,l) &= \frac{\pi^2}{\mathrm{H}} \int_0^{\mathrm{R}} r \cos\frac{j\pi r}{\mathrm{R}} \cos\frac{l\pi r}{\mathrm{R}}\, dr \end{aligned}\right\} \quad . \quad . \quad (13)$$

Now from (3), putting $z=0$ and using $\left(\frac{\partial \mathrm{V}}{\partial z}\right)_{z=0}=0$, we have

$$r\sigma_0 \frac{d^2\mathrm{V}_s}{dr^2} + r\sigma_0 \left(\frac{\partial^2 \mathrm{V}}{\partial z^2}\right)_{z=0} + \sigma_0 \frac{d\mathrm{V}_s}{dr} = 0$$

or
$$\left(\frac{\partial^2 \mathrm{V}}{\partial z^2}\right)_{z=0} + \frac{d^2\mathrm{V}_s}{dr^2} + \frac{1}{r}\frac{d\mathrm{V}_s}{dr} = 0. \quad . \quad . \quad . \quad (14)$$

But from (6),

$$\left(\frac{\partial^2 \mathrm{V}}{\partial z^2}\right)_{z=0} = -\frac{\pi^2}{\mathrm{H}^2} \sum_j \left(\sum_i i^2 a_{ij}\right) \cos\frac{j\pi r}{\mathrm{R}} \quad . \quad . \quad (14')$$

and from (7),

$$\frac{d^2\mathrm{V}_s}{dr^2} = -\frac{\pi^2}{\mathrm{R}^2} \sum_j j^2 \alpha_j \cos\frac{j\pi r}{\mathrm{R}} \quad . \quad . \quad . \quad (14'')$$

and
$$\frac{1}{r}\frac{d\mathrm{V}_s}{dr} = -\frac{\pi}{\mathrm{R}} \sum_j j\alpha_j \frac{1}{r} \sin\frac{j\pi r}{\mathrm{R}}.$$

Expanding $\frac{1}{r}\sin\frac{j\pi r}{\mathrm{R}}$ in a cosine series, we have

$$\frac{1}{r}\sin\frac{j\pi r}{\mathrm{R}} = \frac{\pi}{\mathrm{R}} \sum_t c_{jt} \cos\frac{t\pi r}{\mathrm{R}}$$

where
$$\left.\begin{aligned} c_{jt} &= \frac{1}{\pi}\int_{(t-j)\pi}^{(t+j)\pi} \frac{\sin x}{x}\, dx, \quad t \neq 0 \\ &= \frac{1}{\pi}\int_0^{j\pi} \frac{\sin x}{x}\, dx, \quad t=0, \end{aligned}\right\} \quad . \quad . \quad . \quad (15)$$

so that
$$\frac{1}{r}\frac{d\mathrm{V}_s}{dr} = -\frac{\pi^2}{\mathrm{R}^2} \sum_{j,t} j\alpha_j c_{jt} \cos\frac{t\pi r}{\mathrm{R}}$$
$$= -\frac{\pi^2}{\mathrm{R}^2} \sum_{j,t} t\alpha_t c_{tj} \cos\frac{j\pi r}{\mathrm{R}}. \quad . \quad . \quad (15')$$

Substituting the series (14'), (14''), and (15') in (14), and equating to zero the coefficient of $\cos \frac{j\pi r}{R}$, we obtain *

$$\sum_i i^2 a_{ij} = \sum_t f_{tj} \alpha_t, \quad \ldots \quad (16)$$

where $$f_{tj} = -\frac{H^2}{R^2}(tc_{tj} + t^2 \delta_{tj}), \quad \ldots \quad (17)$$

δ_{tj} being the usual Kronecker delta.

Substituting (16) and (8) in (12), we obtain

$$\sum_{i,j} F(i, j, l) a_{ij} = \sum_j [L(j, l)\alpha_j + M(j, l) \sum_t f_{tj}\alpha_t]$$
$$= \sum_j [L(j, l) + \sum_t M(t, l) f_{jt}]\alpha_j,$$

whence from (11')

$$\sum_j P(j, l)\alpha_j = \sum_{n,k} K(k, l, n) b'_n, \ (l = 0, \pm 1, \ldots), \quad (18)$$

where $$P(j, l) = \sigma_0 L(j, l) + \sigma_0 \sum_t M(t, l) f_{jt}. \quad \ldots \quad (19)$$

Equations (18) are now a set of linear equations to determine the b's in terms of the α's (or *vice versa*), and contain the solution of the problem. The quantities P and K are independent of any particular problem except in so far as they depend on R and H ; they are defined by equations (19), (13), (17), (15), and (11).

It will now be seen that all summations can be taken from 0 to ∞ instead of from $-\infty$ to ∞, the latter device having served its purpose, and, further, that we can confine ourselves to $l > 0$ in (18), the equations with negative l being merely a repetition of those with positive l. Moreover, the integrals in (13) are easily evaluated. Effecting these and certain minor simplifications, and changing the notation somewhat, our final result for the determination of conductivity from surface potential can be stated as follows :—

If V_s is defined from the surface potential ϕ_s by $\phi_s = C_1\left(\frac{1}{r} + V_s\right)$, $(C_1 = I/2\pi\sigma_0)$, and V_s expanded in the

* We may note that the series $\sum_i i^2 a_{ij}$ is convergent on account of our assumption that the series (6) may be differentiated twice term by term.

form $$V_s = \frac{1}{H}\sum_{i=0}^{\infty} \alpha_i \cos\frac{i\pi r}{R}, \quad (0 \leq r \leq R) \quad . \quad . \quad . \quad (20)$$

then the conductivity σ is given by

$$\frac{\sigma}{\sigma_0} = \sum_{i=0}^{\infty} b_i \cos\frac{i\pi z}{H}, \quad (0 \leq z \leq H) \quad . \quad . \quad . \quad (21)$$

where the b's are given in terms of the α's by the set of equations

$$\left.\begin{aligned} &\sum_{j=1}^{\infty} A\left(i, j\,;\ \frac{H}{R}\right) b_j = \sum_{j=1}^{\infty} B(i, j)\alpha_j, \ (i=0, 1, 2, \ldots), \\ &\sum_{j=0}^{\infty} b_j = 1, \end{aligned}\right\} \quad . \quad (22)$$

where

$$A\left(i, j\,;\ \frac{H}{R}\right) = \frac{j\pi}{4H}\sum_{k=-\infty}^{\infty} J\left(i, j, k\,;\ \frac{H}{R}\right),$$

$$J\left(i, j, k\,;\ \frac{H}{R}\right) = \int_0^H dz \int_0^R dr \cdot \frac{rz}{(r^2+z^2)^{3/2}} \sin\frac{j\pi z}{H} \cos\frac{k\pi z}{H} \cos\frac{i\pi r}{R},$$

$$B(i, j) = C(i, j) + \sum_{k=0}^{\infty} D(i, k)E(k, j),$$

$$C(i, j) = -\frac{i^2 j^2}{(i^2-j^2)^2}, \quad \text{if} \quad (i-j) \text{ is odd}$$

$$= \frac{\pi^2}{16} i^2, \quad \text{if} \quad i=j\neq 0$$

$$= 0, \text{ otherwise}$$

$$D(i, k) = \frac{i^2+k^2}{(i^2-k^2)^2}, \quad \text{if} \quad (i-k) \text{ is odd}, \ k\neq 0$$

$$= \frac{1}{2i^2}, \quad \text{if} \quad k=0\neq i$$

$$= \frac{\pi^2}{8}, \quad \text{if} \quad i=k$$

$$= 0, \quad \text{otherwise}$$

$$E(k, j) = j^2\delta_{jk} + \frac{j}{2\pi}\int_{(k-j)\pi}^{(k+j)\pi} \frac{\sin x}{x} dx.$$

The coefficients A, ... E defined above are dimensionless quantities independent of any particular problem, which can be calculated once and for all, except A, which depends also on the ratio $\frac{H}{R}$.

The practical procedure would be as follows :—First, the numbers H and R must be fixed, R being determined from the extent of the surface potential measurements, and an estimate of H being then made ; failing other indication, H could be taken equal to R. Next, from the observed values of ϕ_s, and hence V_s, as a function of r, a certain number of the Fourier coefficients α in (20) would be calculated numerically. Then a certain number of terms and equations in the set (22) would be used to solve for the Fourier coefficients b. The conductivity is then immediately given by (21).

Only an approximate answer can, of course, be expected on account of the conditions imposed at the boundaries of the cylinder defined by (4) which are not strictly accurate, and because only a finite number of terms in the Fourier series can be taken in practice. With a reasonable number of terms in the Fourier series this procedure should not involve too great an amount of labour, and this method has the advantage that one uses the surface potential directly, whereas in both the Slichter-Langer method and the method of paper I. another function must first be calculated from the surface potential by numerical integration.

The coefficients C, D, E above, and hence B, can be calculated and tabulated without difficulty. The only one that presents any difficulty is A. It does not appear possible to evaluate the integral J in finite terms ; without too great an error, however, the limits for r and z can be taken to be infinite, in which case an evaluation is possible, though the resulting expression for A is rather complicated. We shall go no further into the matter here, however, as it is intended to give the numerical calculations in a subsequent paper.

§ 3. *Variational Method.*

We now wish to call attention briefly to the possibility of applying a variational method to the solution of current-flow problems. The differential equation (1) is equivalent to the variational problem *

* In the general case where σ is a general function of position, the variational problem is $\delta\int\sigma\left[\left(\frac{\partial\phi}{\partial x}\right)^2+\left(\frac{\partial\phi}{\partial y}\right)^2+\left(\frac{\partial\phi}{\partial z}\right)^2\right]d\tau=0$, where $d\tau$ is an element of volume and the integral is extended over the half-space $z>0$.

$$\delta\int_0^\infty\int r\sigma\left[\left(\frac{\partial\phi}{\partial r}\right)^2+\left(\frac{\partial\phi}{\partial z}\right)^2\right]dr\,dz=0$$

with the same boundary conditions on ϕ, while the associated equation (3) is equivalent to the variational problem

$$\delta\int_0^\infty\int\left\{r\sigma\left[\left(\frac{\partial V}{\partial r}\right)^2+\left(\frac{\partial V}{\partial z}\right)^2\right]+\frac{2rz}{(r^2+z^2)^{3/2}}\sigma' V\right\}dr\,dz=0.$$

We may then choose any appropriate expressions for σ and V (or ϕ) which contain arbitrary parameters, and which fulfil (or approximately fulfil) the boundary conditions. The minimising of the resultant integral then determines the best possible solution for V of the postulated type, σ being regarded as assigned.

A large range of choice appears then to be opened up, but the difficulty lies in choosing appropriate expressions for σ and V which render the evaluation and minimising of the integral sufficiently simple. It seems worth while, however, to call attention to the possibility, particularly as it might be applied to the more general case where σ is not a function of depth only. If Fourier series of the form (5) and (6) are chosen, and the problem restricted to the cylinder defined by (4), precisely the same results are obtained by the variational method as by the more straightforward method used above.

XXV. *Notices respecting New Books.*

Mathematical Problems of Radiative Equilibrium. By E. Hopf. [Pp. 1–105+i–viii.] (Cambridge Tracts in Mathematics and Mathematical Physics No. 31.) (Cambridge University Press, 1934. Price 6*s.* net.)

THE flow of radiation in a stellar atmosphere, controlled as it is by the coefficients of emission, of absorption, and of scattering of the material forming the atmosphere, presents a mathematical problem bristling with difficulties. As yet only two simplified cases have been dealt with: either the atmosphere is supposed to be such that scattering alone occurs in it or it is assumed to be of grey material in which absorption alone takes place. The equations governing the flow of radiation are integral equations whose solutions have

hitherto only been found in separate memoirs. The theory and the results so far obtained are here collected and extended so that the book contains the mathematical equipment necessary for a study of the outer layers of a star. Dr. Hopf has rendered a great service to astrophysicists, but it is difficult to avoid a feeling of disappointment that so little care appears to have been given to method of presentation, to style, and even to grammar, in the writing of this book.

The Hardness of Metals and its Measurement. By Hugh O'Neill, D.Sc., M.Met. [Pp. 292, figs. 119.] (Chapman & Hall. Price 25*s.* net.)

This volume may be regarded as a successful attempt to coordinate the vast amount of information which has been published during the last thirty years on this important subject. With this object in view, the author has found it necessary to interpret hardness in its widest sense, including, for example, observations on the deformation of metals by tension and compression as well as by indentation. Such a wide interpretation of hardness makes this work a comprehensive study of the subject and cannot fail to be of value to the physicist and engineer, as well as to the metallurgist, for whom it was primarily prepared.

In an introductory essay the author briefly discusses the various aspects of the problems of hardness in its relation to certain physical properties.

The first two chapters, which treat the subject from a rather academic standpoint, deal with the principles upon which static tests operate. This is followed by a detailed study of the static ball test in which attention is directed to Meyer's work and its significance in showing how different hardness values for indentations of varying angularity are bound up with what the author terms " hardenability " of the material.

In contrast to these first chapters the third deals with details of practice, containing brief descriptions of popular testing machines accompanied by a consideration of the requirements of an ideal testing machine.

The subjects dealt with in the succeeding chapters include hardness and its relation to deformation and strainhardening, the crystallinity of metals and its bearing upon hardness. The sklerometer and its applications are described in this section ; alloying and heat treatment as related to hardness ; hardness tests on soft metals and hot metals, in which the dynamic test is considered in comparison with the static test ; and also the preparation and examination of the hardness test specimen. The subjects included in the final chapter are of great industrial importance, *e. g.*, abrasion, " machinability,"

and cutting-hardness. In this section consideration is given to wear testing machines, also lathe, drilling, and sawing tests for " machinability."

An appendix is included in which formulæ for the approximate conversion of hardness scales appear, and also a comprehensive bibliography containing references to more than four hundred publications.

The author, already well known for his own contributions to the study of this subject, has exercised much care and discrimination in preparing this monograph.

The book is well illustrated, and can be recommended with confidence.

The Fundamentals of Chemical Thermodynamics.—Part II. Thermodynamical Functions and their Applications. By J. A. V. Butler. [Pp. ix+271.] (Macmillan, 1934. Price 8*s.* 6*d.*)

It is probably the experience of most teachers of physical chemistry that the thermodynamical treatment of chemical problems does not make a strong appeal to the majority of students of chemistry. This would seem to be due in part to the limited acquaintance which these students have made with thermodynamics as a branch of physics, and in part to the difficulty of visualising the thermodynamic functions which are now almost universally employed. Under these circumstances it is essential that the presentation of the subject should not only be clear and precise, but should also be made as attractive as possible. In this respect the author, who is, of course, a recognised expert, has been remarkably successful, and the more advanced student who has covered the ground represented by Part I. should have no difficulty in understanding the developments and applications which are described and discussed in Part II.

The greater part of the book is devoted to the consideration of the properties of solutions, but other chapters deal with gas reactions, the third law, phase potential differences, thermodynamics of surfaces, and general criteria of equilibrium and stability. In most cases the discussion of the particular subject is fairly complete, and, apart from its use as a text-book, Part II. may be regarded as a review of recent progress in the application of thermodynamics to chemical problems. In both capacities it is a book which can be very warmly recommended.

[*The Editors do not hold themselves responsible for the views expressed by their correspondents.*]

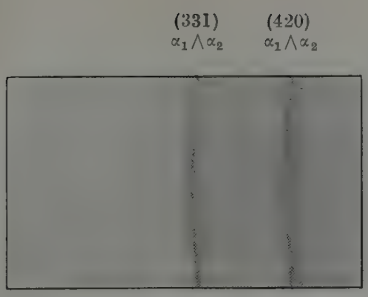

(*a*) 119 Brinell.

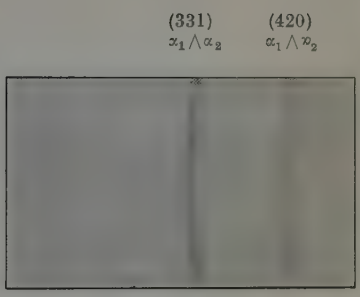

(*b*) 128 Brinell.

(*c*) 132 Brinell.

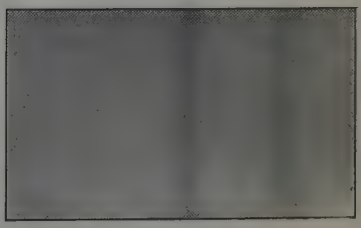

(*d*) 146 Brinell.

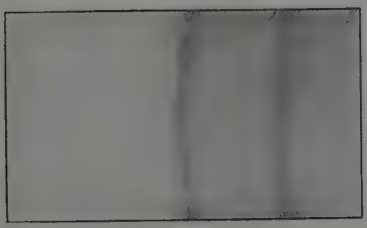

(*e*) 147 Brinell.

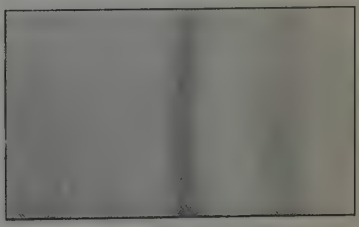

(*f*) 186 Brinell.

(331) and (420) diffraction lines of α-brass of different hardness values.

FIG. 4.

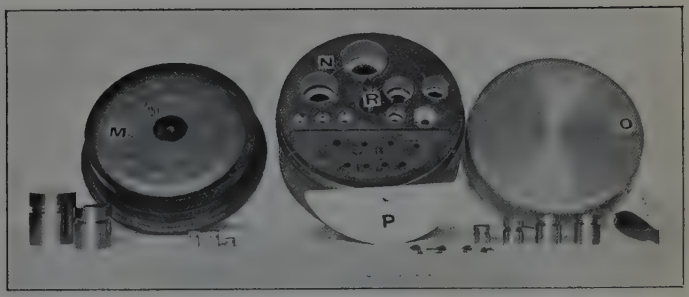

Figs.

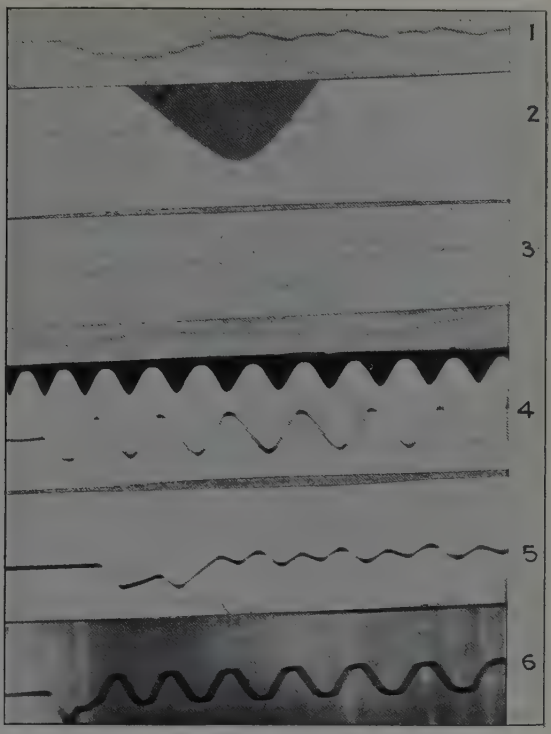

Figs.

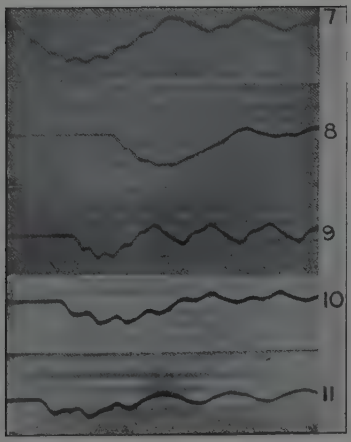

Kinks on impact diagrams of struck strings.

FIG. 1.

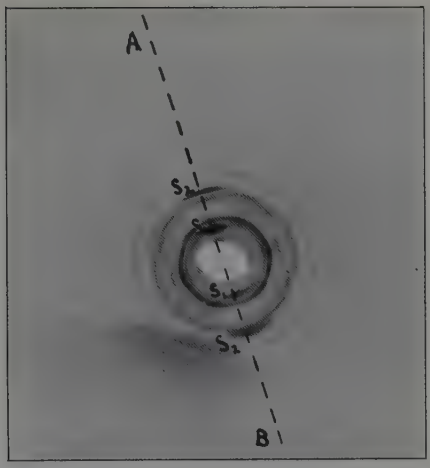

Enamel. Showing preferential orientation.

FIG. 2.

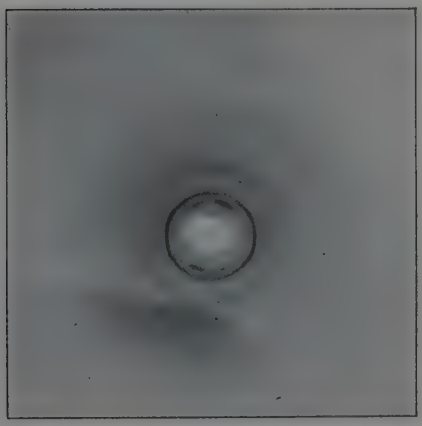

Enamel. Showing doublo orientation.

FIG. 3.

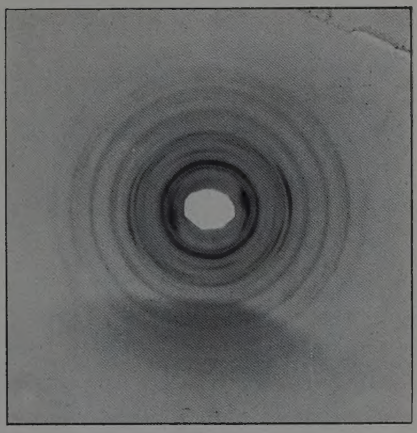

Enamel. Showing overlapping double orientation.

FIG. 5.

Tooth section and holder.
The spot of light shows where the X-ray beam strikes the tooth.

Fig. 6.

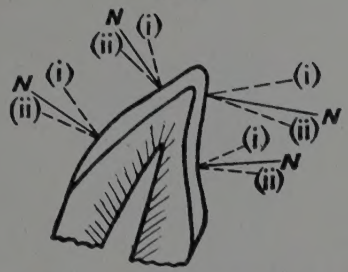

Showing the nature of the enamel orientation.
N = normal ; (i) = fibre-axis (i) ; (ii) = fibre-axis (ii).

Fig. 7.

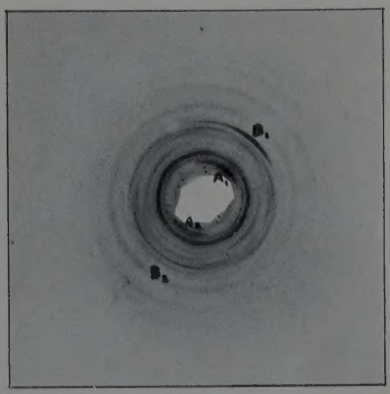

Enamel. Showing fibre-axis tilt.